

AD-A069 171

LOCKHEED-CALIFORNIA CO BURBANK

F/G 1/3

SUMMARY OF RESULTS FOR A TWIN-ENGINE, LOW-WING AIRPLANE SUBSTRU--ETC(U)

JAN 79 G WITTLIN

DOT-FA75WA-3707

UNCLASSIFIED

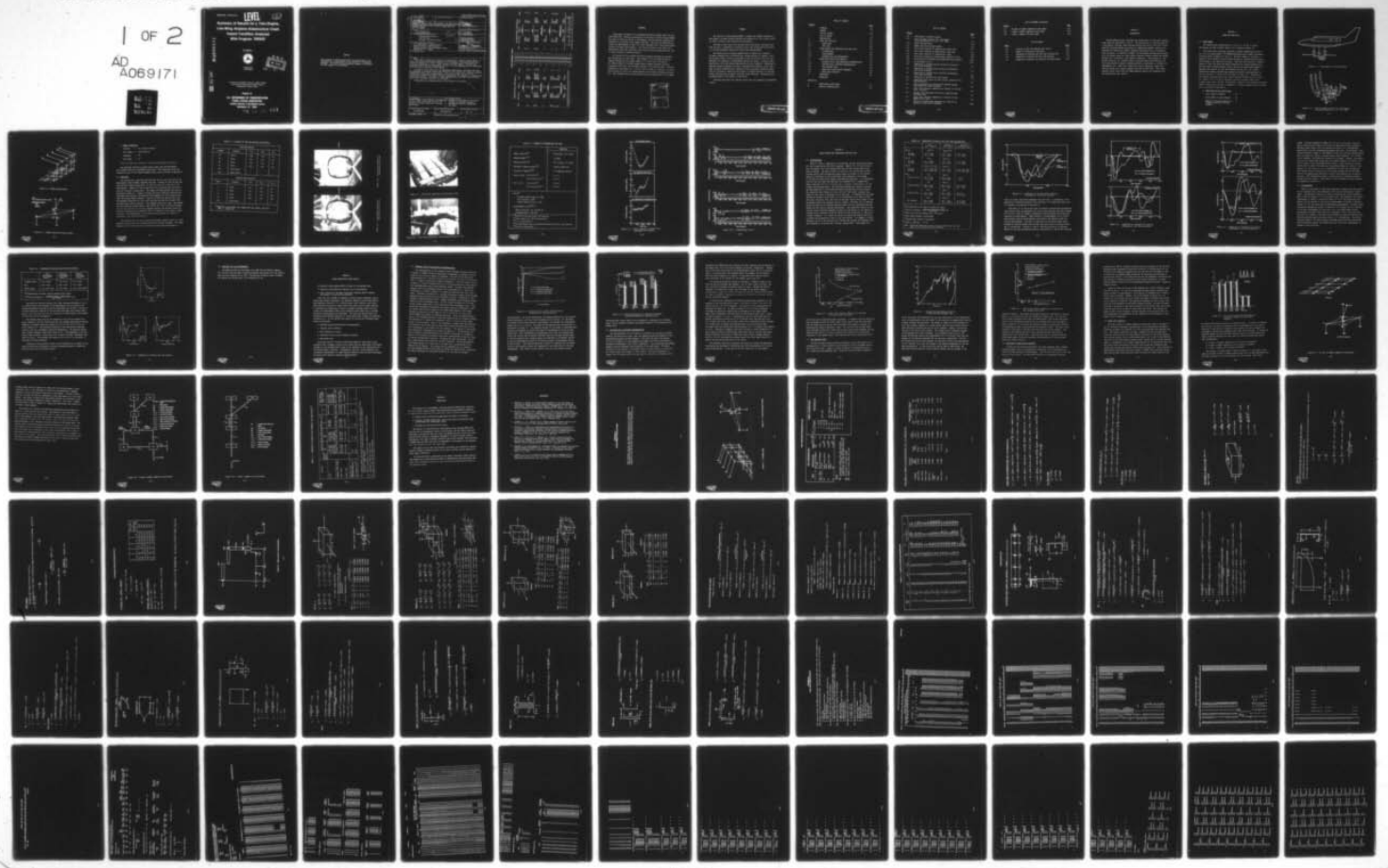
LR-28869

FAA-RD-79-13

NL

1 OF 2

AD A069171



REPORT NO: FAA-RD-79-13

LEVEL

**Summary of Results for a Twin-Engine,
Low-Wing Airplane Substructure Crash
Impact Condition Analyzed
With Program 'KRASH'**

AD A069171

Gil Wittlin



January 1979
Final Report

DDC
RECEIVED
MAY 30 1979
C

DDC FILE COPY

Document is available to the U.S. public through
the National Technical Information Service,
Springfield, Virginia 22161.

Prepared for

**U.S. DEPARTMENT OF TRANSPORTATION
FEDERAL AVIATION ADMINISTRATION
Systems Research & Development Service
Washington, D.C. 20590**

79 05 24 011

NOTICE

This document is disseminated under the sponsorship of the Department of Transportation in the interest of information exchange. The United States Government assumes no liability for its contents or use thereof.

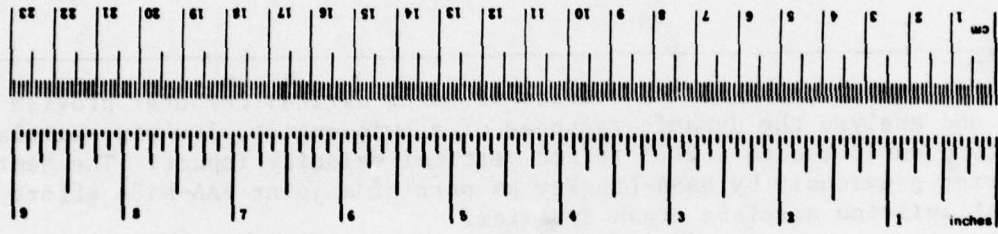
1. Report No. 18 FAA-RD-79-13	2. Government Accession No.	3. Recipient's Catalog No. 14	
4. Title and Subtitle 6 SUMMARY OF RESULTS FOR A TWIN-ENGINE, LOW-WING AIRPLANE SUBSTRUCTURE CRASH IMPACT CONDITION ANALYZED WITH PROGRAM 'KRASH'		5. Report Date Jan 1978 1979	
7. Author(s) 10 Gil Wittlin		6. Performing Organization Code L	
9. Performing Organization Name and Address Lockheed California Co. P.O. Box 551 Burbank, California 91520		8. Performing Organization Report No. 12 LR-28869	10. Work Unit No. (TRAIS) 121 P.A.
12. Sponsoring Agency Name and Address U.S. Department of Transportation Federal Aviation Administration Systems Research and Development Service Washington, D.C. 20590		11. Contract or Grant No. 15 DOT-FA75WA-3707	
15. Supplementary Notes		13. Type of Report and Period Covered 9 Final <i>rept.</i> Jul 1978 ← Jan 1979 1979	
16. Abstract <p>This report contains the results of using digital computer program KRASH to model and analyze the dynamic response of a twin-engine, low-wing airplane substructure subjected to a 27.5 ft/sec vertical velocity impact. The test was performed previously by NASA-Langley as part of a joint FAA-NASA effort concerning general aviation airplane crash dynamics.</p> <p>Included in this report are the math model description, pertinent test data, a comparison of analysis versus test results and the results of a limited parameter sensitivity study using program KRASH. Floor and occupant pelvis vertical acceleration responses obtained from test measurement are compared to corresponding analytical results. The effect of model representation and input data selection variations on dynamic behavior are evaluated.</p> <p>Conclusions are presented based on the results of the effort.</p>			
17. Key Words Program KRASH, Crash dynamics, Mathematical Models, Light Fixed-Wing Aircraft, Sub-Structure, Dynamic Responses, Parameter Sensitivity		18. Distribution Statement Document is available to the public through the National Technical Information Service, Springfield Va. 22151	
19. Security Classif. (of this report) Unclassified	20. Security Classif. (of this page) Unclassified	21. No. of Pages 121	22. Price -

209 970 *mt*

METRIC CONVERSION FACTORS

Symbol	What You Know	Multiply by	To Find	Symbol
LENGTH				
in	inches	2.54	centimeters	cm
ft	feet	30.48	centimeters	cm
yd	yards	0.9144	meters	m
mi	miles	1.60934	kilometers	km
AREA				
sq in	square inches	6.4516	square centimeters	cm ²
sq ft	square feet	0.092903	square meters	m ²
sq yd	square yards	0.836127	square meters	m ²
sq mi	square miles	2.59978	square kilometers	km ²
acres	acres	0.404686	hectares	ha
MASS (weight)				
oz	ounces	28.3495	grams	g
lb	pounds	453.592	kilograms	kg
	short tons (2000 lb)	0.907185	tonnes	t
VOLUME				
teaspoon	teaspoons	5	milliliters	ml
fluid ounce	fluid ounces	29.5735	milliliters	ml
cup	cup	236.588	milliliters	ml
quart	quarts	946.353	liters	l
gallon	gallons	3.78541	liters	l
qt	quarts	0.946353	liters	l
gal	gallons	3.78541	liters	l
ft ³	cubic feet	0.0283168	cubic meters	m ³
yd ³	cubic yards	0.764555	cubic meters	m ³
TEMPERATURE (exact)				
°F	Fahrenheit temperature	5/9 (after subtracting 32)	Celsius temperature	°C

Symbol	What You Know	Multiply by	To Find	Symbol
LENGTH				
mm	millimeters	0.0393701	inches	in
cm	centimeters	0.393701	inches	in
m	meters	3.28084	feet	ft
km	kilometers	0.621371	miles	mi
AREA				
cm ²	square centimeters	0.155001	square inches	in ²
m ²	square meters	1.19599	square yards	yd ²
ha	square kilometers	0.386102	square miles	mi ²
hectare (10,000 m ²)	hectares (10,000 m ²)	2.47105	acres	acres
MASS (weight)				
g	grams	0.0352335	ounces	oz
kg	kilograms	2.20462	pounds	lb
t	tonnes (1000 kg)	1.10231	short tons	short tons
VOLUME				
ml	milliliters	0.033814	fluid ounces	fl oz
l	liters	1.05669	quarts	qt
l	liters	0.264172	gallons	gal
m ³	cubic meters	35.2335	cubic feet	ft ³
m ³	cubic meters	1.35168	cubic yards	yd ³
TEMPERATURE (exact)				
°C	Celsius temperature	9/5 (then add 32)	Fahrenheit temperature	°F



*1 in = 2.54 exactly. For other exact conversions and more detailed tables, see NBS Misc. Publ. 286, Units of Weights and Measures, Price \$2.25, SO Catalog No. C13.10.286.

FOREWORD

This report, prepared by the Lockheed-California Company under Contract DOT-FA75WA-3707, contains a description of the effort in which program KRASH was used to model and analyze a twin-engine, low-wing airplane substructure subjected to a vertical crash impact condition. The test was performed previously by NASA-Langley as part of a joint FAA-NASA effort concerning general aviation airplane crash dynamics. The work discussed in this report was administered under the direction of the Federal Aviation Administration with H. Spicer acting as Technical Monitor.

Gil Wittlin of the Lockheed-California Company performed the analysis and correlation with test data. Bill LaBarge of the Lockheed-California Company assisted in the initial phases of the math model development. Dr. Robert Hayduk of the NASA-Langley Impact Dynamics Research Facility coordinated the effort and provided structure, test and film data. The data presented in this report are a partial input to NASA for purposes of evaluating the state of the art in light-airplane crash dynamics modeling and analysis. The Lockheed effort was performed under the supervision of J.E. Wignot.

ACCESSION for	
NTIS	Write Section <input checked="" type="checkbox"/>
DDC	Brief Section <input type="checkbox"/>
MANAGEMENT	<input type="checkbox"/>
JUSTIFICATION	
BY	
DISTRIBUTION/AVAILABILITY CODES	
D. 1	OFFICIAL
A	

SUMMARY

The results of using program KRASH to analyze the dynamic response of a twin-engine, low-wing airplane substructure subjected to a 27.5 ft/sec vertical impact velocity crash condition are presented.

Included in this report are the math model description, pertinent data from the test, a comparison of analysis versus test results and the results of a limited parameter sensitivity study using program KRASH.

The substructure is modeled symmetrically in KRASH with 32 masses, 57 member elements and 44 nonlinear beam element degrees of freedom. Floor and occupant pelvis vertical acceleration responses obtained from test measurements are compared to corresponding analytical results. Occupant chest, substructure roof, and window-ledge motions are also compared. Variations in external spring (crushable structure) load-deflection behavior, seat stiffness, occupant representation, analytical filter frequency cutoff and model size are included to ascertain their effect on dynamic behavior for the particular substructure and impact condition being evaluated. Conclusions are presented based on the results of the effort.

Pertinent math model and computer output data are presented in Appendices A and B.



TABLE OF CONTENTS

<u>Section</u>		<u>Page</u>
	FOREWORD	111
	SUMMARY	v
	LIST OF FIGURES	viii
	LIST OF TABLES	ix
1	INTRODUCTION	1-1
2	MODEL AND TEST DATA	2-1
2.1	KRASH MODEL	2-1
2.2	TEST DATA	2-5
3	KRASH RESULTS AND COMPARISON WITH TEST DATA	3-1
3.1	ACCELERATIONS	3-1
3.2	DISPLACEMENTS	3-6
3.3	COMPUTER COST AND PERFORMANCES	3-9
4	KRASH SENSITIVITY STUDY RESULTS	4-1
4.1	EXTERNAL SPRING LOAD-DEFLECTION REPRESENTATION	4-2
4.2	OCCUPANT AXIAL STIFFNESS REPRESENTATION	4-4
4.3	SEAT MAXIMUM FORCE	4-6
4.4	ANALYTICAL FILTER CUTOFF FREQUENCY	4-8
4.5	MODEL SIZE VARIATION	4-9
5	CONCLUSIONS	5-1
	REFERENCES	
 Appendices		
A	KRASH MODEL CALCULATIONS	A-1
B	ANALYSIS COMPUTER PRINT	B-1



LIST OF FIGURES

<u>Figure</u>		<u>Page</u>
2-1	Twin-engine, low-wing airplane.	2-2
2-2	Lower fuselage structure for twin-engine, low-wing airplane (F.S. 135 - F.S. 181).	2-2
2-3	KRASH fuselage model.	2-3
2-4	KRASH floor-seat-occupant model.	2-3
2-5	Post-crash condition of substructure, front view	2-7
2-6	Post-crash condition of substructure, rear view	2-7
2-7	Post-crash condition of substructure, floor	2-8
2-8	Post-crash condition of substructure, partial of roof	2-8
2-9	Motion histories obtained from high-speed film analysis.	2-10
2-10	Accelerometer traces.	2-11
3-1	Comparison of occupant pelvis vertical acceleration, test versus analysis.	3-3
3-2	Comparison of fuselage floor vertical acceleration, test versus analysis.	3-4
3-3	Comparison of fuselage floor vertical acceleration, test versus analysis.	3-5
3-4	Comparison of analysis and test motions.	3-8
4-1	Normalized force versus external spring load-deflection characteristics.	4-3
4-2	Peak acceleration as a function of external spring load-deflection characteristics.	4-4
4-3	Lower torso (pelvis) response as a function of occupant axial stiffness.	4-6
4-4	Typical force-deflection curve for a light-aircraft passenger seat.	4-7
4-5	Lower torso (pelvis) response as a function of seat maximum force level.	4-8
4-6	Floor and occupant peak responses as a function of analysis filter cutoff frequency.	4-10

LIST OF FIGURES (Continued)

<u>Figure</u>		<u>Page</u>
4-7	16 mass, 32 member symmetrical math model	4-11
4-8	6 mass, 8 member symmetrical math model	4-13
4-9	5 mass, 5 member full math model	4-14

LIST OF TABLES

<u>Table</u>		<u>Page</u>
2-1	Location of Test and Analysis Data Points	2-6
2-2	Summary of Substructure Test Data	2-9
3-1	Comparison of Analysis and Test Peak Accelerations	3-2
3-2	Comparison of Analysis and Test Peak Motions	3-7
4-1	Comparison of Results for Different Size Math Models	4-15

SECTION 1

INTRODUCTION

Program KRASH has been validated with several sets of full-scale aircraft crash test data (References 1 and 2). The availability of crash test data for a twin-engine, low-wing, light-airplane substructure and an additional impact condition provided another opportunity to demonstrate KRASH's capability to represent the significant dynamic response characteristics of a survivable crash condition. In addition to KRASH, the twin-engine airplane substructure is to be modeled using two other digital computer programs, DYCAST and ACTION, designed for a structural crash dynamics evaluation. The modeling of a particular structure for a defined impact condition using three different current crash dynamics computer programs provides an opportunity to compare the requirements for: model size, input data, ease of modeling, output data, analysis versus test results, machine costs and machine time. This report concerns itself solely with the KRASH modeling results and comparison with the substructure test results.



SECTION 2
MODEL AND TEST DATA

2.1 KRASH MODEL

The substructure representing F.S. 135 to F.S. 181 for a typical twin-engine low-wing airplane (Figure 2-1) is shown in Figure 2-2.

The substructure including occupants is modeled symmetrically (about B.L. 0.0) in program KRASH. The KRASH substructure and occupant representations are shown in Figures 2-3 and 2-4. The floor masses at locations 2 through 6 and 8 through 12 have external springs to represent ground contact and crushing of the underside structure. Only half the structure is shown in Figure 2-3 since the model and impact conditions are treated symmetrically. The dash lines jutting laterally from 14 and 18 are tension-only members to represent the lateral tie rods (see Figures 2-5 and 2-6). For clarity, tension-only members representing occupant seat belts connecting mass 5 to mass 30 and mass 11 to mass 30 are not shown in Figure 2-4. Compression-only members representing the seat cushion and pan connect mass 30 to mass 29. Masses 29, 30, 31 and 32 represent the seat, occupant lower torso, occupant upper torso, and DRI, respectively. Details of the modeling including sample calculations are shown in Appendix A. Computer program input and output data are provided in Appendix B.

● KRASH Substructure model size:

Total number of masses	-	32
Total number of beam elements	-	57
Number of nonlinear degrees of freedom associated with beam elements	-	44

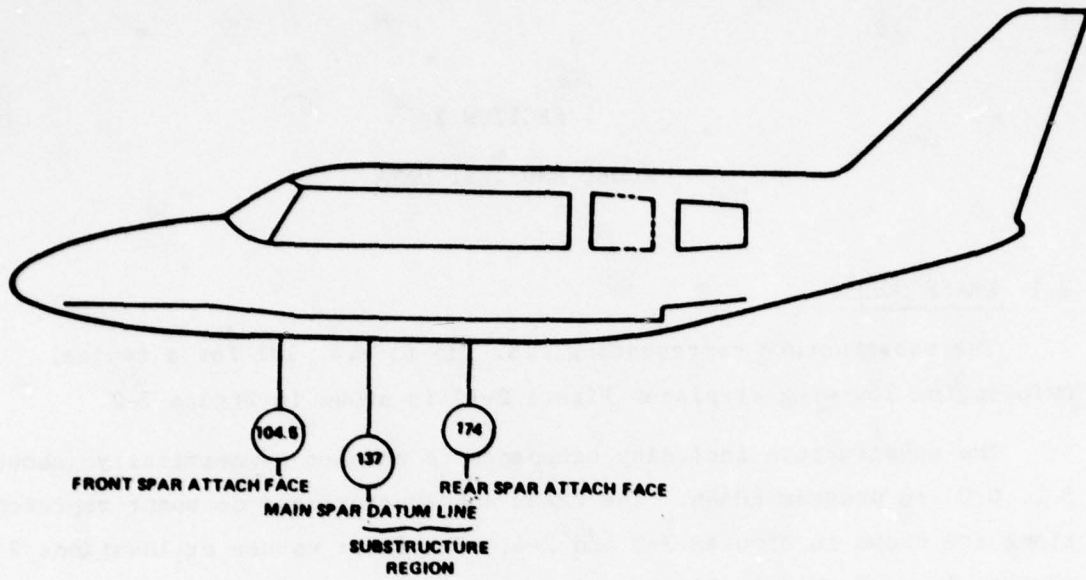


Figure 2-1. - Twin-engine, low-wing airplane.

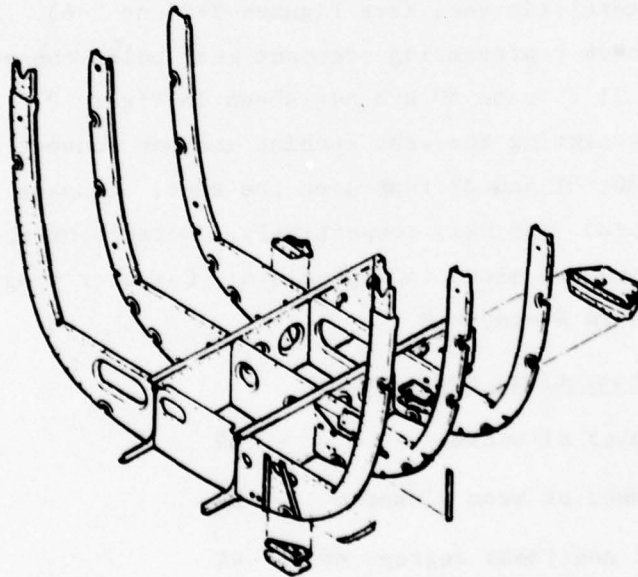


Figure 2-2. - Lower fuselage structure for twin-engine, low-wing airplane (F.S. 135 - F.S. 181).

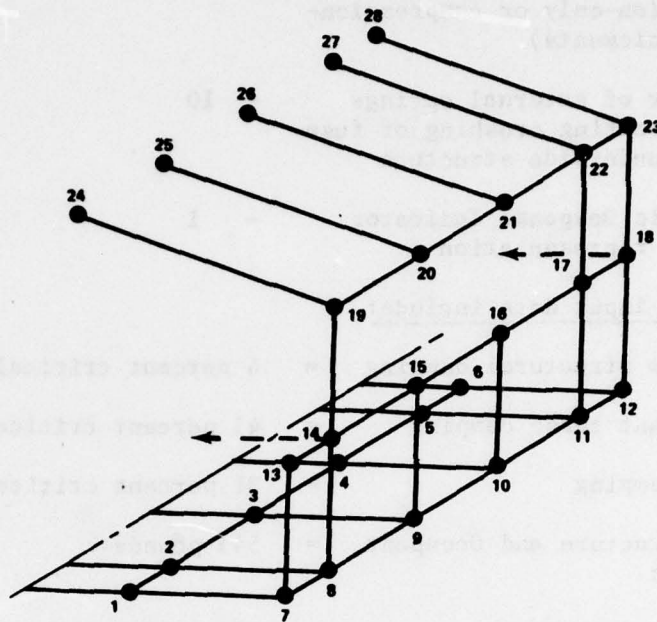


Figure 2-3. - KRASH fuselage model.

NOTE:

29, 1 REPRESENTS MASS 29, NODE 1

MEMBERS NOT SHOWN

- 5-30
- 11-30
- 29,5-30,1

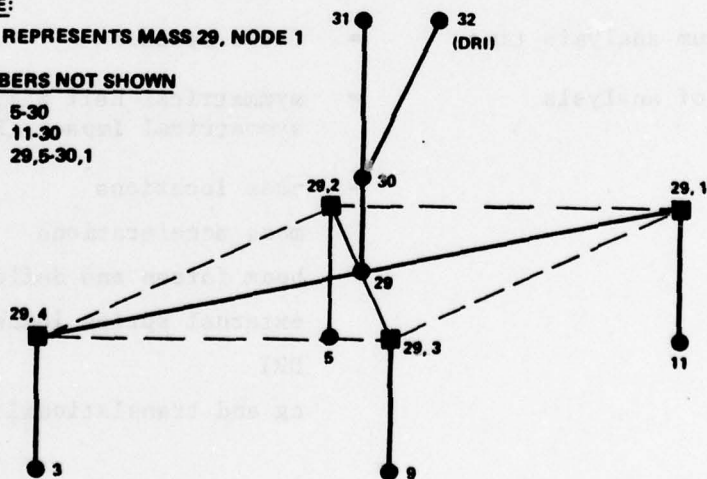


Figure 2-4. - KRASH floor-seat-occupant model.

● Impact conditions

Velocity	=	27.5 ft/sec vertical
Pitch angle	=	3/4° pitch-up
Yaw-angle	=	0°
Roll angle	=	0°

Table 2-1 shows the location of the test and analysis data points.

The nonlinear deflection values used as input into the KRASH model were obtained directly from KRASH calculations. The deflection values are contained as part of the 'Model Parameter Data' print, provided in Appendix B.

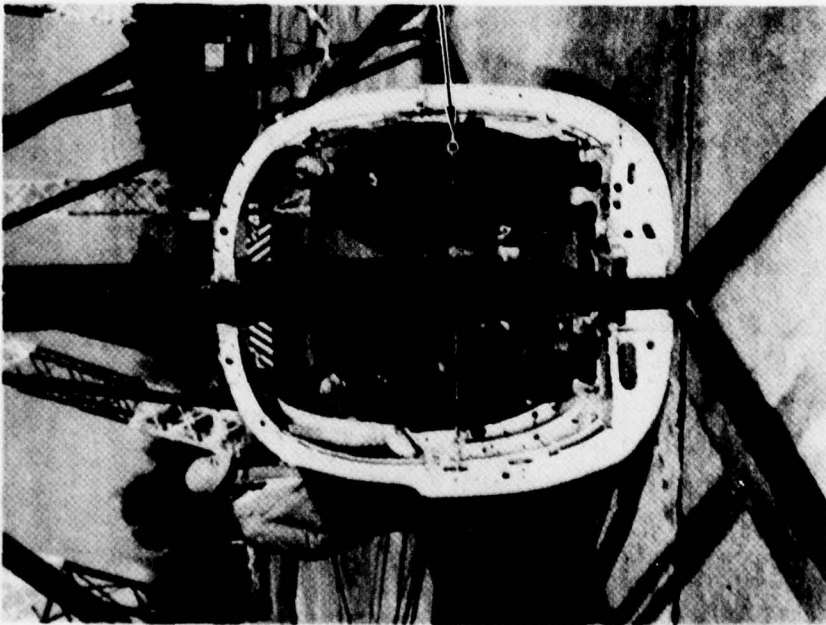
2.2 TEST DATA

The substructure crash test data and film analyses were provided by the NASA-Langley Impact Dynamics Research Facility. Figures 2-5 and 2-6 show the front and rear views, respectively, of the post-crash test condition of the substructure. Figures 2-7 and 2-8 show the floor structure and a portion of the roof structure, respectively. The summary of NASA-provided test data is presented in Table 2-2. Figure 2-9 shows the motion histories obtained from high-speed film analysis, performed by NASA-Langley, for the occupant chest, roof, and window-ledge locations. Figure 2-10 shows the reduced test data accelerometer histories for four floor locations and the two occupant (left and right side) pelvis locations. The channels record D.C. data. The reduced data are obtained by NASA using a least-square fit (LSF) filtering technique. All the test data are for vertical response channels and motions since this direction represents the predominant mode of response for this type of impact condition. Correspondingly, all correlation with analysis is limited to responses in the vertical direction.

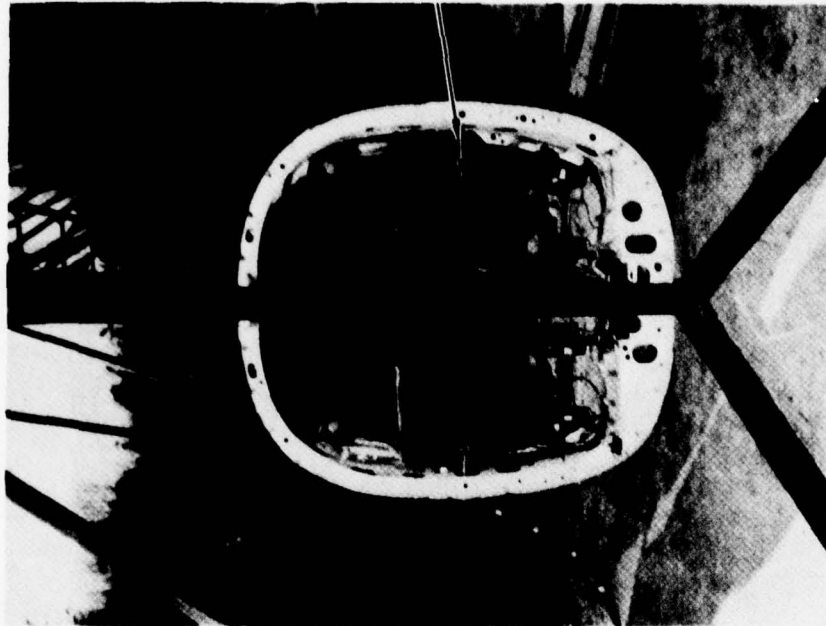
The substructure test was previously performed by NASA as part of a joint general aviation crash test program initiated by the FAA and NASA. The impact dynamics test facility and test procedures are described in Reference 3.

TABLE 2-1. - LOCATION OF TEST AND ANALYSIS DATA POINTS

Test Data Points				
Channel	Location	F.S.	W.L.	B.L.
A1	Floor	140.	-16.	6L
A2	Floor	151.	-16.	24L
B2	Floor	151.	-16.	6L
D1	Floor	162.	-16.	24L
D9	Left Pelvic	-	-	-
D10	Right Pelvic	-	-	-
Analysis Data Points ^(a)				
Mass	Location	F.S.	W.L.	B.L.
2	Floor	140.	-16.	6L
3	Floor	151.	-16.	6L
9	Floor	151.	-16.	20L
10	Floor	163.	-16.	20L
30	Lower Torso	-	-	-
^(a) Analysis is performed with symmetrical half model, thus left side = right side.				



TIE ROD



TIE ROD

Figure 2-5. - Post-crash condition of substructure, front view

Figure 2-6. - Post-crash condition of substructure, rear view

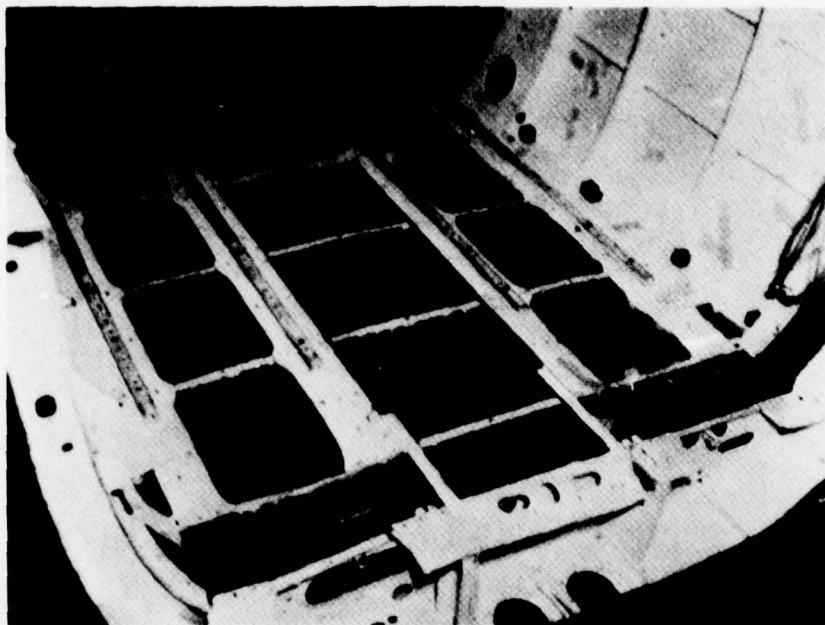


Figure 2-7. - Post-crash condition of substructure, floor



Figure 2-8. - Post-crash condition of substructure, partial of roof

TABLE 2-2. - SUMMARY OF SUBSTRUCTURE TEST DATA

	Magnitude
Impact velocity ^(a)	330 in/sec; 27.5 ft/sec
Rebound height ^(a)	5 inches
Rebound velocity ^(a)	62.1 in/sec; 5.2 ft/sec
Duration of ground contact ^(a)	0.058 ± 0.0015 sec.
Attitude at impact ^{(a)(d)}	0.75 degrees pitch-up
Window ledge: peak motion ^(a)	1.64 in.
final deflection ^(e)	0.65 in.
Roof center: peak motion ^(a)	3.65 in.
final deflection ^(e)	0.99 in.
<p>Plots^(a)</p> <ul style="list-style-type: none"> - Occupant chest motion vs. time - Roof motion vs. time - Window-ledge motion vs. time <p>Accelerometer traces^{(b)(c)}</p> <p>Floor structure - A1, A2, B2, D1</p> <p>Occupant pelvis - D9, D10</p>	
<p>(a) Obtained from high speed film analysis</p> <p>(b) Least Square Fit (LSF) filtered data</p> <p>(c) D.C. Accelerometers</p> <p>(d) No significant roll or yaw motion obtained from the film analysis</p> <p>(e) Post-test measurement</p>	

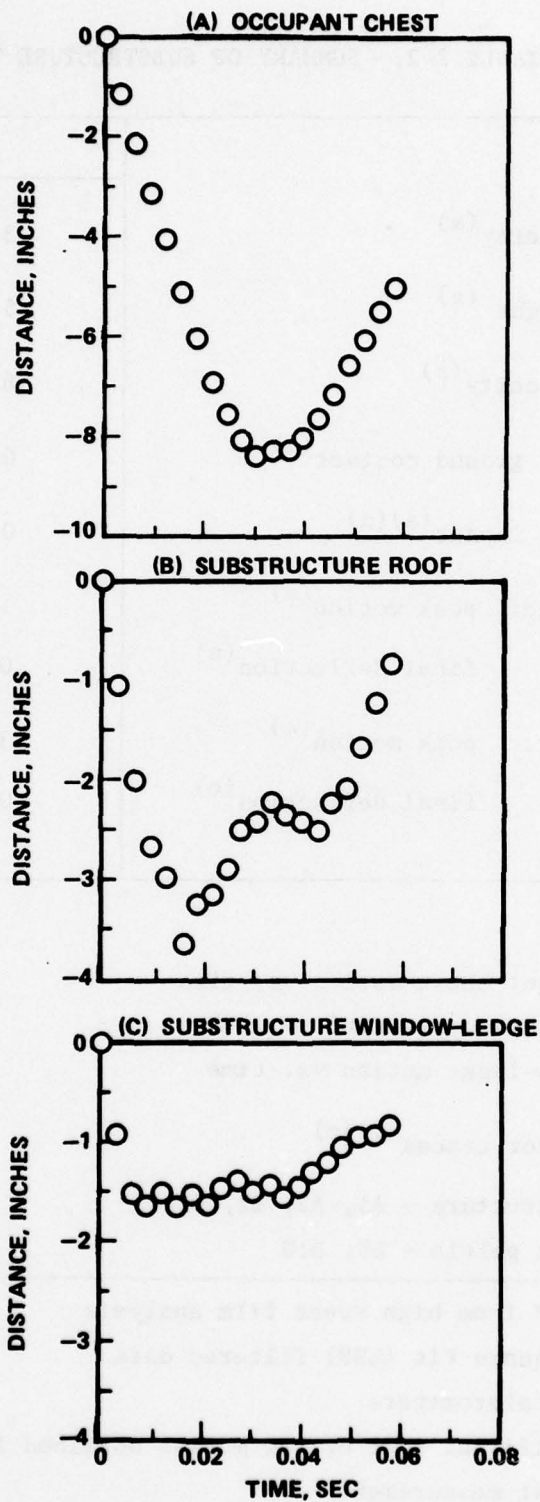


Figure 2-9. - Motion histories obtained from high-speed film analysis



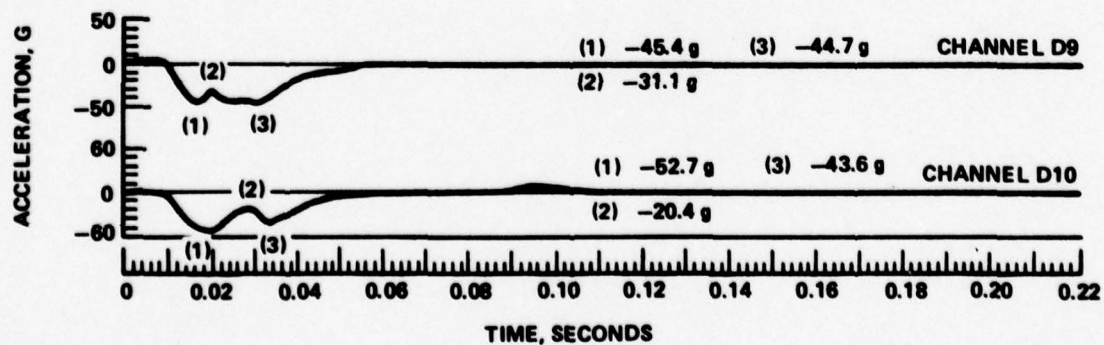
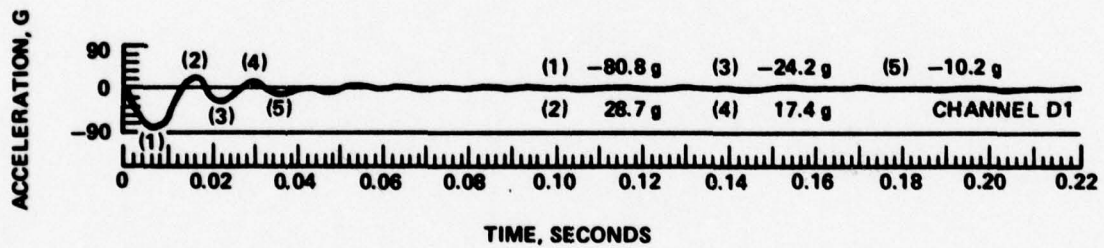
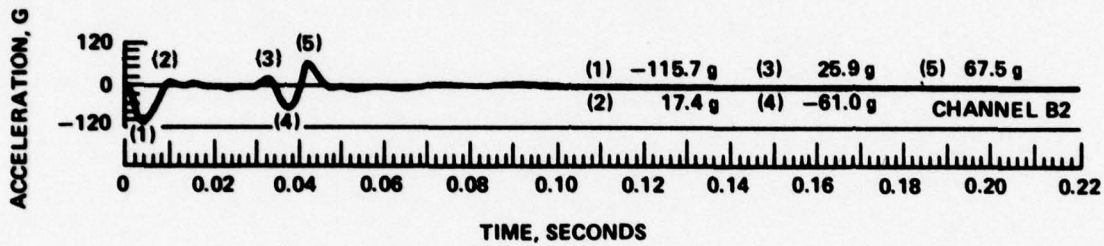
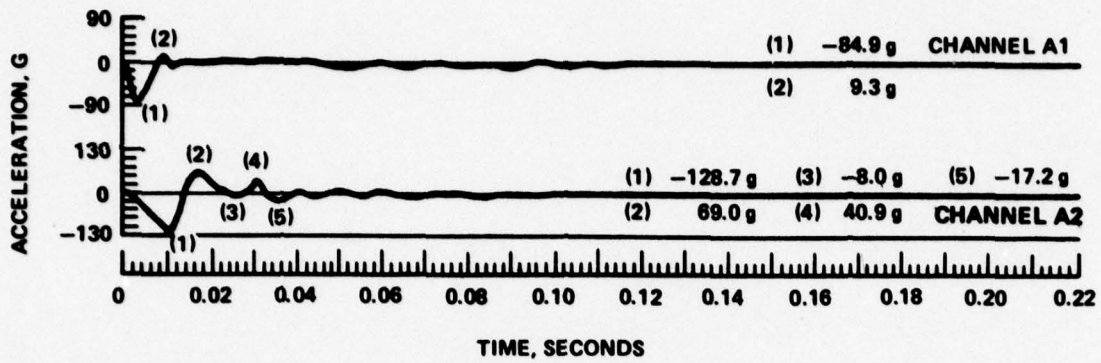


Figure 2-10. - Accelerometer traces

SECTION 3

KRASH RESULTS AND COMPARISON WITH TEST DATA

3.1 ACCELERATIONS

Table 3-1 shows a comparison of the analysis and test peak accelerations for the occupant pelvis and floor responses. Figures 3-1, 3-2 and 3-3 present the analysis and test response histories for the occupant pelvis and floor locations. The data in Table 3-1 show that the analytically obtained occupant pelvis peak accelerations agree within 19 percent for the initial peak and 6.8 percent for the second peak, when compared to the average of the left and right side occupant test measured responses. It is noteworthy that the left and right side measured test responses for a "symmetrical" impact condition differ by 16 percent and 2.5 percent, respectively, for the primary and secondary peaks. The difference between test results is nearly the same magnitude as the difference between the analysis and test results. The analytical data (Figure 3-1) show the same "camel hump" response phenomenon as that which is exhibited in the test data. In addition the two peaks obtained by analysis occur within 4 to 6 milliseconds of the time at which they occur during the test. The test and analysis results show a decay to zero acceleration after the secondary peak is reached. The decay rate is approximately the same for the analysis and test data, with the analytical data preceding the test data by several milliseconds. The analytical results for the occupant pelvis response presented in Table 3-1 and Figure 3-1 are based on a low-pass filter frequency cutoff of 100 Hz as noted in Section 2. The use of a higher frequency cutoff value will result in analytical results which will be higher and consequently closer to the test results. For example, a 150 Hz frequency cutoff in the analysis will increase the primary and secondary occupant response by 5 percent and 2 percent, respectively. This change will

TABLE 3-1. COMPARISON OF ANALYSIS AND TEST PEAK ACCELERATIONS

	Test Accel (Time) (a)	Analysis Accel (Time) (a)	Percent (b) Differences (Time)
Pelvis	(D9) (d)	(Mass 30) (e)	
1st Peak	-45.4 (.018)	-39.7 (.017)	-12.6 (.001)
2nd Peak	-44.7 (.030)	-41.1 (.026)	- 8.1 (.004)
Pelvis	(D10)	(Mass 30)	
1st Peak	-52.7 (.020)	-39.7 (.017)	-24.7 (.003)
2nd Peak	-43.6 (.032)	-41.1 (.026)	- 5.7 (.006)
Pelvis	(Avg. of D9 & D10)	(Mass 30)	
1st Peak	-49.0 (.018-.020)	-39.7 (.017)	-19.0 (.001-.003)
2nd Peak	-44.1 (.030-.032)	-41.1 (.026)	- 6.8 (.004-.006)
Floor	(A1)	(Mass 2)	
Forward Inboard	-84.9 (.004) 9.3 (.010)	-89.0 (.004) 43.9 (.028)	4.8 (0) (c)
	(A2)	(Mass 9)	
Forward Outboard	-128.7 (.010) 69.0 (.018)	-101.0 (.011) 61.8 (.025)	-21.5 (.001) -10.4 (.007)
	(B2)	(Mass 3)	
Forward Inboard	-115.7 (.004) 25.9 (.032)	-90.7 (.004) 34.9 (.026)	-21.6 (0) 34.0 (.006)
	(D1)	(Mass 10)	
Aft Outboard	-80.8 (.008) 28.7 (.017)	-99.2 (.007) 37.1 (.018) (f)	22.8 (.001) 29.3 (.002)

a) Accelerations in G's, time in seconds after impact

b) Percent difference = $\left(\frac{\text{analysis value} - \text{test value}}{\text{test value}} \right) \times 100$

c) Test trace shows no response after .012 seconds

d) Test channel numbers in parenthesis

e) Analysis mass numbers in parenthesis

f) Peak at .026 msec = 53.7 g

NOTE: Difference between test results for right (D10) versus left (D9) side \approx 16.1% (1st peak) and 2.5% (2nd peak).



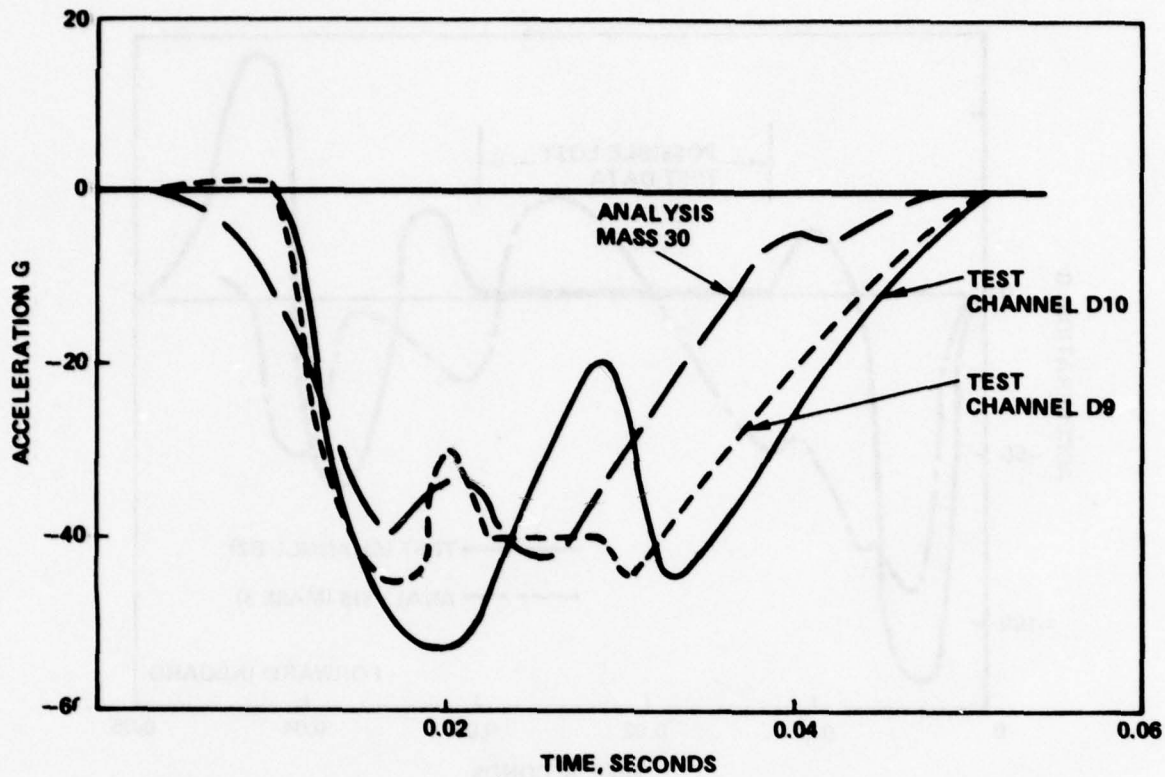


Figure 3-1. - Comparison of occupant pelvis vertical acceleration, test versus analysis.

result in closer correlation agreement with test data. A discussion of the sensitivity of analysis results to the selection of an analytical filter cut-off frequency is discussed in Section 4.4.

From Table 3-1 it can be seen that the analysis initial peak acceleration values agree within approximately ± 22 percent with measured test data obtained from the four floor dc channel accelerometer locations which were chosen for comparison by NASA-Langley. NASA considers dc accelerometers to be overall more reliable than ac accelerometers, particularly the behavior after the initial peak response. The time of occurrence of the initial peak values obtained by analysis agrees with the test data peak value occurrences within one (1) millisecond. Figures 3-2 and 3-3 show the similarity in response shapes for the test and analysis results, particularly in the initial response

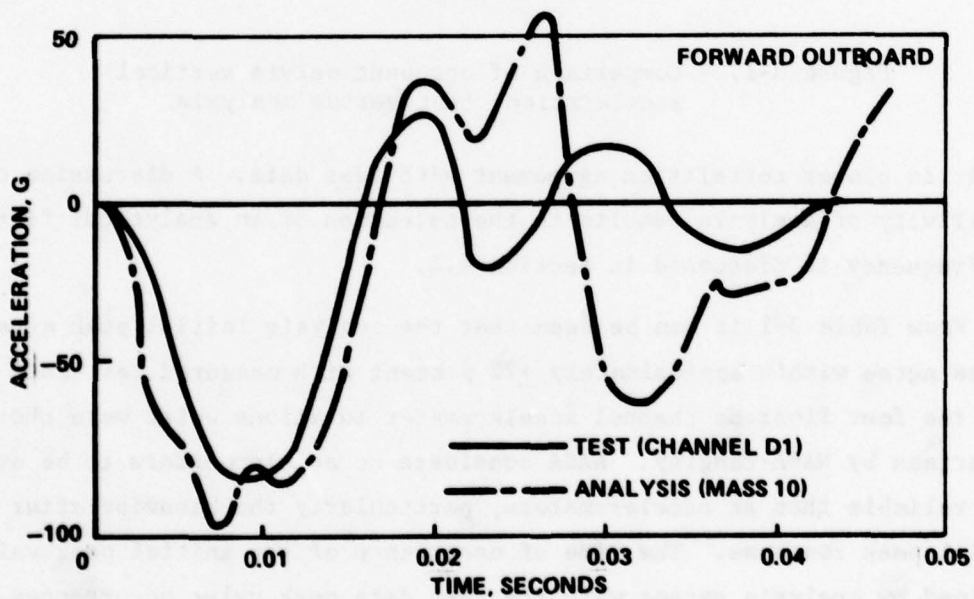
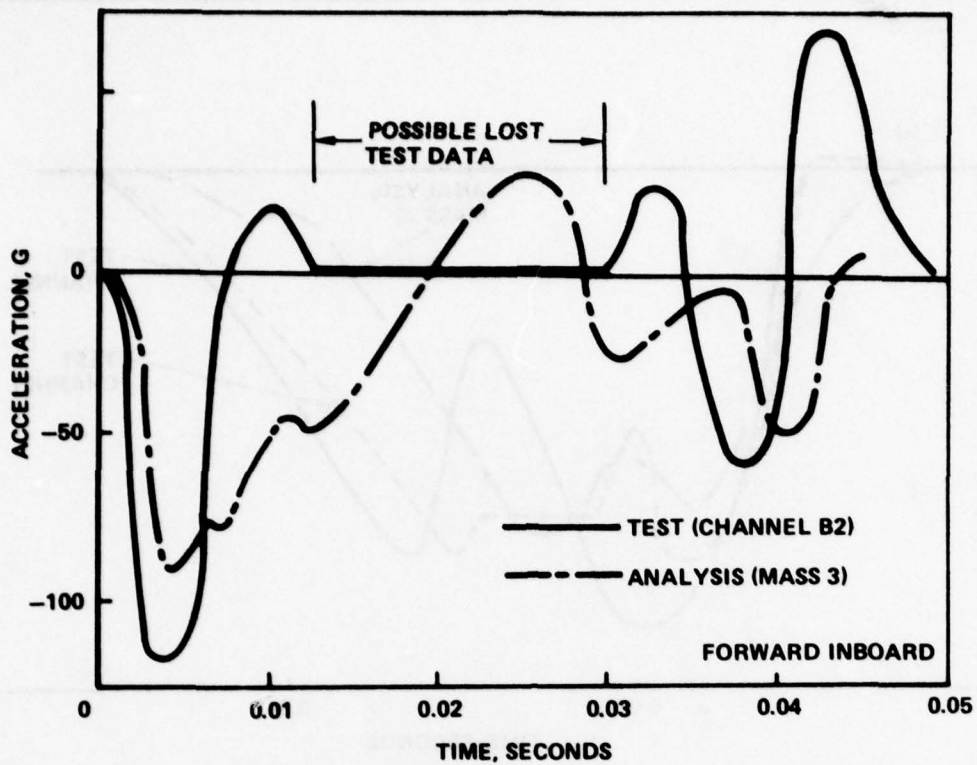


Figure 3-2. - Comparison of fuselage floor vertical acceleration, test versus analysis.

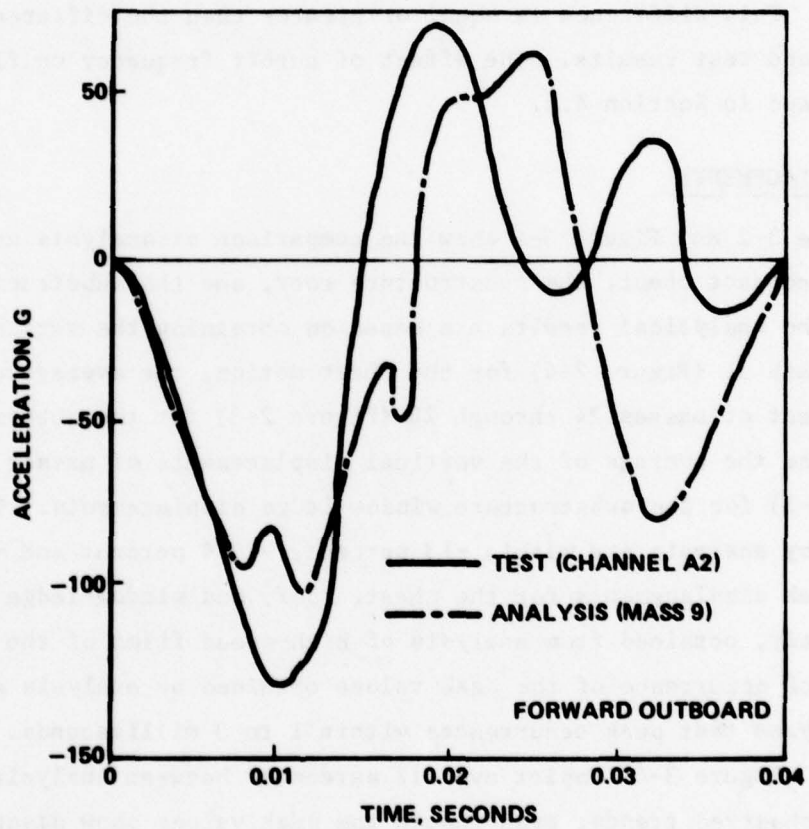
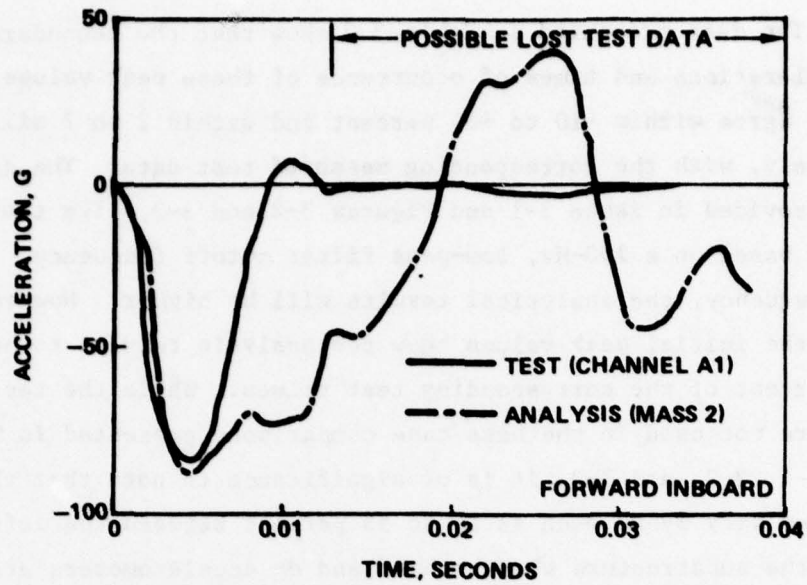


Figure 3-3. - Comparison of fuselage floor vertical acceleration, test versus analysis

regime. The data presented in Table 3-2 show that the secondary (rebound) peak accelerations and times of occurrence of these peak values, obtained by analysis, agree within -10 to +34 percent and within 2 to 7 milliseconds, respectively, with the corresponding measured test data. The analytical floor results provided in Table 3-1 and Figures 3-2 and 3-3, like the occupant pelvis data, are based on a 100-Hz, low-pass filter cutoff frequency. For a 150-Hz cutoff frequency, the analytical results will be higher. However, the comparisons for the initial peak values show the analysis results to be within -11.7 to +34 percent of the corresponding test values. While the test ac accelerometers are not used in the base case comparisons presented in Table 3-1 and Figures 3-1, 3-2, and 3-3, it is of significance to note that the measured test values vary by as much as 16 to 55 percent between the left and right sides of the substructure when both ac and dc accelerometers are included in the data. This difference is equal or greater than the difference between analysis and test results. The effect of cutoff frequency on floor responses is discussed in Section 4.4.

3.2 DISPLACEMENTS

Table 3-2 and Figure 3-4 show the comparison of analysis and test motions for the occupant chest, the substructure roof, and the substructure window-ledge. The analytical results are based on obtaining the vertical displacement of mass 31 (Figure 2-4) for the chest motion, the average of the vertical displacement of masses 24 through 28 (Figure 2-3) for the substructure roof motion, and the average of the vertical displacements of masses 14 through 17 (Figure 2-3) for the substructure window-ledge displacements. The peak values obtained by analysis are within -13 percent, -27.4 percent and +43.3 percent of the peak displacements for the chest, roof, and window-ledge motions, respectively, obtained from analysis of high-speed films of the crash test. The time of occurrence of the peak values obtained by analysis agree with the film-analyzed test peak occurrences within 1 to 3 milliseconds. The motion histories (Figure 3-4) depict overall agreement between analysis determined and test-observed trends, even though the peak values show disagreements of between 13 and 43 percent.

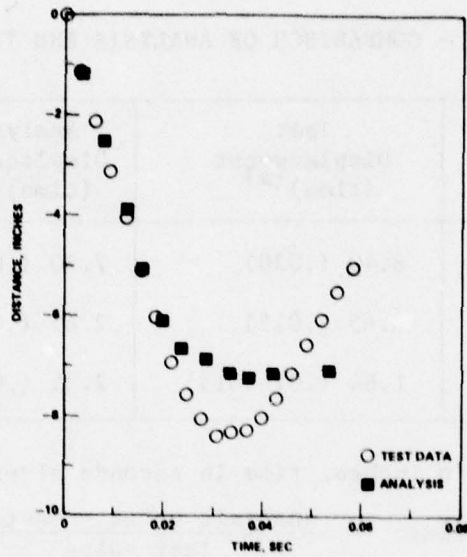
TABLE 3-2. - COMPARISON OF ANALYSIS AND TEST PEAK MOTIONS

	Test Displacement (time) ^(a)	Analysis Displacement (time) ^(a)	Percent Difference (time) ^(b)
Occupant Chest	8.40 (.030)	7.30 (.033)	-13.1 (.003)
Roof	3.65 (.015)	2.65 (.013)	-27.4 (.002)
Window Ledge	1.64 (.01-.015)	2.35 (.012)	43.3 (.002-.003)
<p>(a) Displacement in inches, time in seconds after impact</p> <p>(b) Percent difference = $\frac{\text{analysis value} - \text{test value}}{\text{test value}} \times 100$</p>			

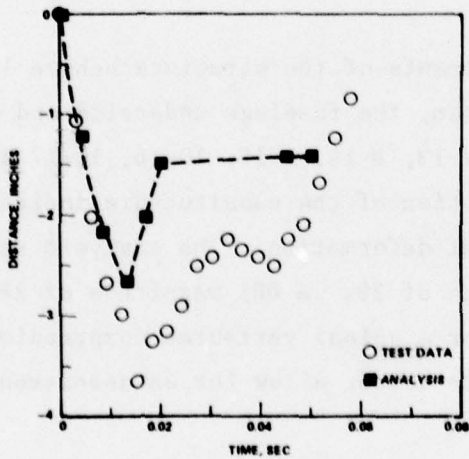
The analytical results indicate that lower fuselage deformation of up to 1.4 inches occurs, which appears to be approximately twice as high as the average deformation observed in the test high-speed film review. A review of the post-crash test condition of the structure indicates that overall deformation of the structure may not have exceeded 0.6 inches based on the average of the front and rear deformation.

The analysis shows that all the elements of the structure behave linearly, except for the seat cushion and pan, the fuselage underside and several elements of the shell structure (beams 7-13, 8-14, 9-15, 10-16, 11-17 and 12-18, Figure 2-3). The postcrash condition of the substructure indicates little in the way of permanent structural deformation. The analysis results show a Dynamic Response Index (DRI) value of 28. A DRI magnitude of 28 indicates a high potential (>50 percent) for a spinal vertebrae compression-type injury to occur. The available test data do not allow for an assessment of this type of injury potential.

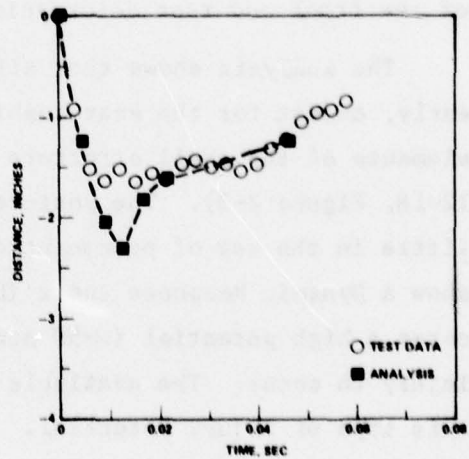
Variation of the analytical filter cutoff frequency has no effect on the motion results since filtering is a post-processing procedure in KRASH and does not alter any of the basic results.



(a) OCCUPANT CHEST



(b) SUBSTRUCTURE ROOF



(c) SUBSTRUCTURE WINDOW-LEDGE

Figure 3-4. - Comparison of analysis and test motions.

3.3 COMPUTER COST AND PERFORMANCES

The KRASH analysis was performed on an IBM 370-3330 digital computer. For the size case and impact condition analyzed (see Section 2.0) the approximate cost per computer run is \$135. The analysis (machine) time, including all printed and plotted data, is 6.9 minutes per run.

SECTION 4

KRASH SENSITIVITY STUDY RESULTS

An analysis using program KRASH is based on the premises that:

- Nonlinear load-deflection behavior can be approximated
- Only a portion of the major structural elements need be modeled nonlinearly for post-failure behavior.

Since the use of KRASH is designed to obtain overall responses, depict significant dynamic phenomenon, and represent response trends using approximate modeling techniques, it is understandable that different users might model aircraft structure or select input data which varies in some respects. To determine the consequence, insofar as dynamic response results are concerned, of establishing a model and an analysis which might vary, a limited sensitivity investigation was performed. The base case results which best represent the estimated properties of the structure and occupant are described in Section 3.0. In this section the results of varying the following parameters are discussed:

- External spring load-deflection representation
- Occupant axial stiffness
- Seat maximum force level
- Analytical filter cutoff frequency selection
- Math model size

There was little in the way of nonlinear behavior, other than in the crushable lower fuselage, occupant seat cushion and pan deflection, and several elements in the airframe shell, noted in the analysis of the substructure for the defined impact condition. Consequently, the above noted parameters are considered representative of areas wherein different users may have differences of opinion with regard to modeling representations.

4.1 EXTERNAL SPRING LOAD-DEFLECTION REPRESENTATION

The representation of the crushable lower fuselage structure within the framework of KRASH's external spring input requirements is perhaps the most sensitive and critical concern for modeling. The data for the base case representation were obtained following the procedures outlined in References 4 and 5. A sample calculation is shown in Appendix A. The most likely area of variation in a user's thinking would be in the representation of the slope of the load-deflection curve in the nonlinear region. The base case assumes a constant load in the nonlinear region until bottoming occurs. This curve (condition A) is shown in Figure 4-1, along with possible user input variations. Condition B provides for a constant 20-percent increase in the assumed maximum forces associated with the crushable structure. Conditions C and D represent sloping 20-percent force changes (increasing and decreasing, respectively) up until bottoming occurs. All the curves are based on a 0.1-inch initial linear region and a 3-inch deflection before bottoming occurs. Both values are determined following the procedure outlined in References 4 and 5. The results would not be altered to any significant degree if the linear deflection value were in the range of 0.01 to as much as 0.3 inch, which leaves significant margin for modeling variation. Since the maximum deflection of the crushable structure in the base analysis does not exceed 1.6 inches the selection of 3 inches for bottoming to occur, is also of little consequence in this analysis. Thus, it is reasonable to assume that the selection of the peak force and the rate at which force varies with deflection will be most influential on the results for this analysis. The results of this parameter sensitivity investigation are shown in Figure 4-2. The 20-percent constant increase in external spring force maximum load results in an approximately 15 to 20-percent increase in peak floor accelerations at the four floor dc channel accelerometer locations. Changing the slope (conditions C and D) has a substantially less effect on the peak responses. The sloping ± 20 percent change results in a variation of the peak floor accelerations of between ± 3 to ± 11 percent. The occupant pelvis responses are not affected by these changes because in this model and under the defined impact conditions the pelvis responses are influenced primarily by the seat and occupant

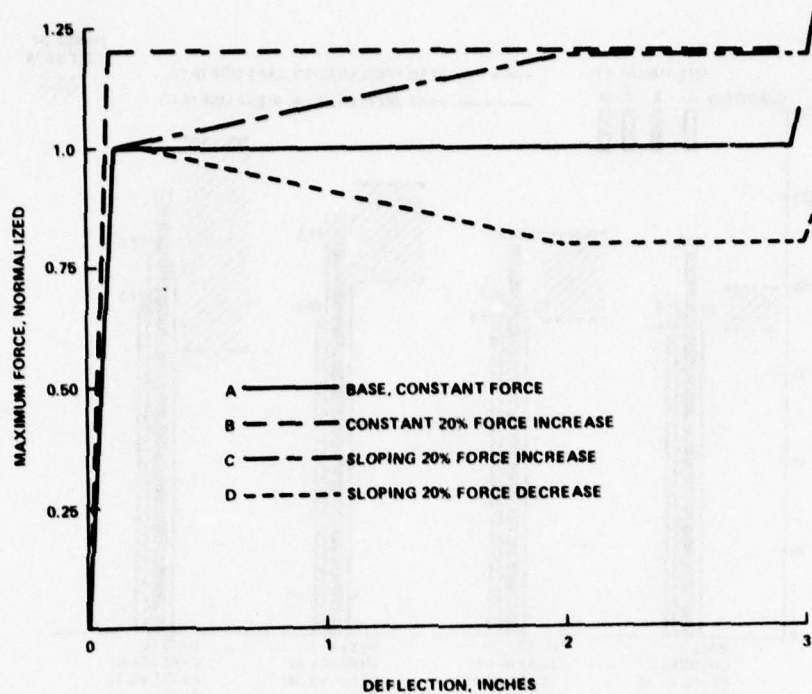


Figure 4-1. - Normalized force versus external spring load-deflection characteristics.

characteristics. As can be anticipated, the maximum deflection of the external spring decreases as the force level increases and vice versa. For the range of external spring characteristics investigated, the average floor deformation ranges from 1 to 1.5 inches. The range of test-measured peak accelerations is also shown in Figure 4-2. The analysis results for the range of load-deflection behavior investigated are within the range of the measured ac and dc accelerometer data. When considering dc accelerometer data alone the analysis peak values are no more than 30 percent different than the test peak values except at the aft outboard floor location where the difference is 50 percent and the ac and dc accelerometers differ by 75 percent (using dc accelerometer values as base values). The results presented in Figure 4-2 indicate that the sensitivity of the analysis results are comparable to the sensitivity of the test measurements. The results further indicate that all four external spring

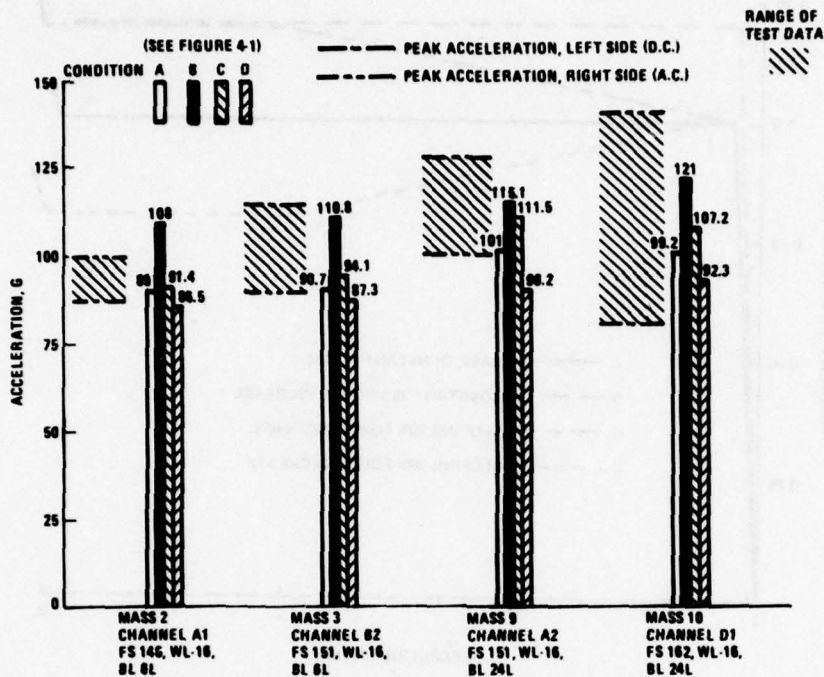


Figure 4-2. - Peak acceleration as a function of external spring load-deflection characteristics.

load-deflection curves, which can be considered to represent four different users, "on the average" represent the dynamic behavior of the structure reasonably well.

4.2 OCCUPANT AXIAL STIFFNESS REPRESENTATION

The representation of the occupant is controlled by the user in program KRASH by the selection of mass, area, and damping properties assigned to the corresponding masses and beam elements. The lower and upper torso masses (30 to 31 in Figure 2-4) are assigned mass weight and inertia properties as described in References 5 and 6 and in Appendix A. The connecting link between masses 31 and 32 represents the properties of the upper spine. The axial stiffness of this element is determined from the area, modulus of elasticity, and length properties assigned to this element. The data in Reference 7 suggest that the human upper torso has specific frequency and damping values.

Translated into KRASH data this requires the axial frequency and the damping of the human spine to be 14 Hz and 41 percent of critical, respectively. Depending on the actual properties of the anthropomorphic dummy used in a particular test it is possible that the frequency and/or the damping can be different than the values suggested for humans. In this particular case the spinal axial stiffness is not defined for the dummies used in the test.

For the human properties defined in Reference 7, KRASH is coded to compute the desired frequency and damping. For all other spinal stiffness, the user can easily determine the proper values to input. Knowing the desired frequency, the input mass values, and the length of the spinal element, combinations of modulus of elasticity and cross section area may be determined for input into KRASH. Damping, as a percent of critical, can be user selected for any individual element.

To evaluate the consequence of different spinal axial properties on the response of the structure and occupant, a variation in upper torso axial frequency from 14 to 61 Hz was examined. The results of this investigation are presented in Figure 4-3. As shown in Figure 4-3, as the axial frequency increases the analytical results tend to reproduce the two peaks (camel hump) effect exhibited in the test data for the occupant lower torso. Using an axial frequency, of 61 Hz., a maximum seat force of 5570 pounds and 0.41 damping the analysis results are 20 to 30 percent lower than the test data. For a higher seat force, the occupant lower torso acceleration values increase. For a lower axial stiffness the occupant lower torso initial peak value increases while the second peak value decreases, until it actually goes negative at 14 Hz. Changing the damping value while holding all other parameters constant tends to affect the second peak value more than the initial peak value. During a separate study using a simplified 5-mass system, changing damping from 0.31 to 0.04 increased the occupant lower torso first peak value by 2.5 percent and the second peak value by 29 percent.

The parameter sensitivity analyses involving the occupant representation illustrates the importance of providing input data representative of the elements being modeled. It may well be that the properties of test dummies

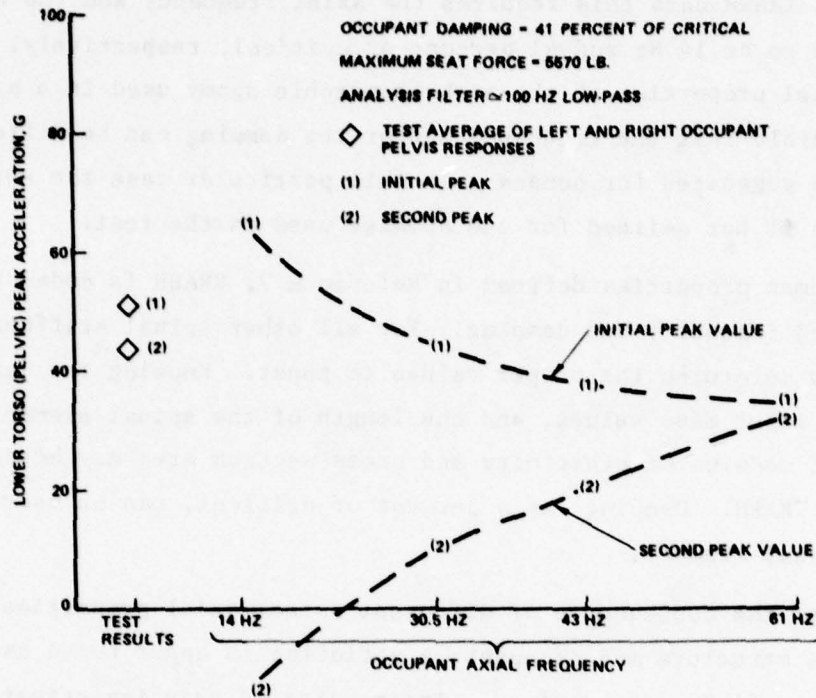


Figure 4-3. - Lower torso (pelvis) response as a function of occupant axial stiffness

differ from the corresponding human properties. It appears from the results of this investigation that the "camel hump" effect noted in the test data means that the dummy spine is stiffer than originally anticipated in setting up a representation based on Reference 7 data. The fact that the occupant upper torso responses follow very closely the occupant lower torso responses in both magnitude and time of occurrence, supports the contention that the spinal connection of the dummies used in the substructure test are relatively stiff.

4.3 SEAT MAXIMUM FORCE

The seat-cushion and pan-stiffness properties used in the analysis are representative of those installed in the particular type of airplane used in the substructure test. Figure 4-4 shows a general force-deflection curve for a light aircraft passenger seat. Since the curve provided in Figure 4-4

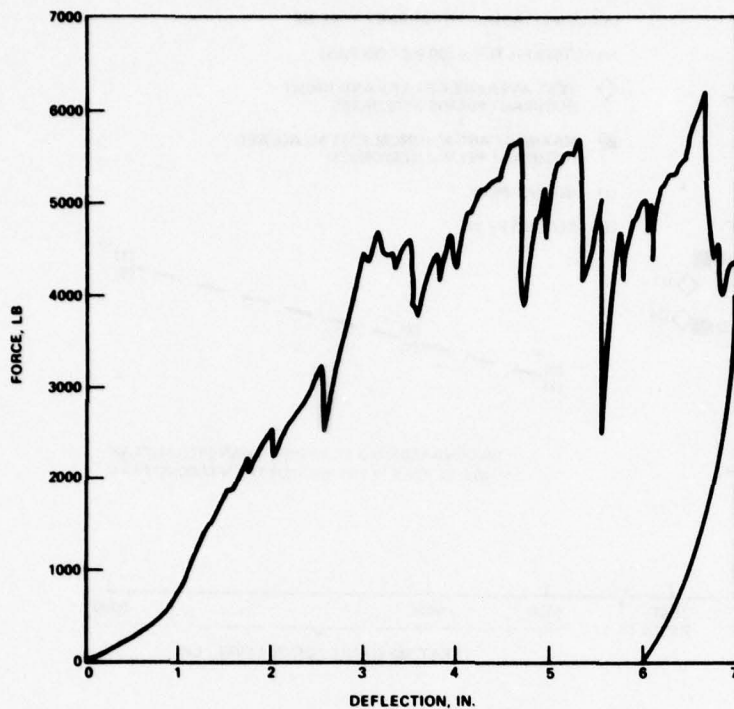


Figure 4-4. - Typical force-deflection curve for a light-aircraft passenger seat.

is not the actual load-deflection for the seat installation in the substructure test, an investigation into the effect of the variation in maximum seat force on occupant response was performed. The change in cushion and pan stiffness effects the occupant response to a lesser extent than the force cutoff value in this particular situation and was not fully explored. Figure 4-5 shows the results of the force cutoff changes. The occupant pelvis responses increase as the maximum force level increases. For a maximum cutoff force of 5570 pounds the analysis results are approximately 30 to 19 percent lower than the average of the measured responses for the two peak accelerations. For the 6455 pounds used in the base analysis the analytical results are approximately 19 and 7 percent lower than the average of the measured responses for the two peak accelerations. If the cutoff force was as high as 9000 pounds, the analytical results would be 8 and 18 percent higher than the average of the

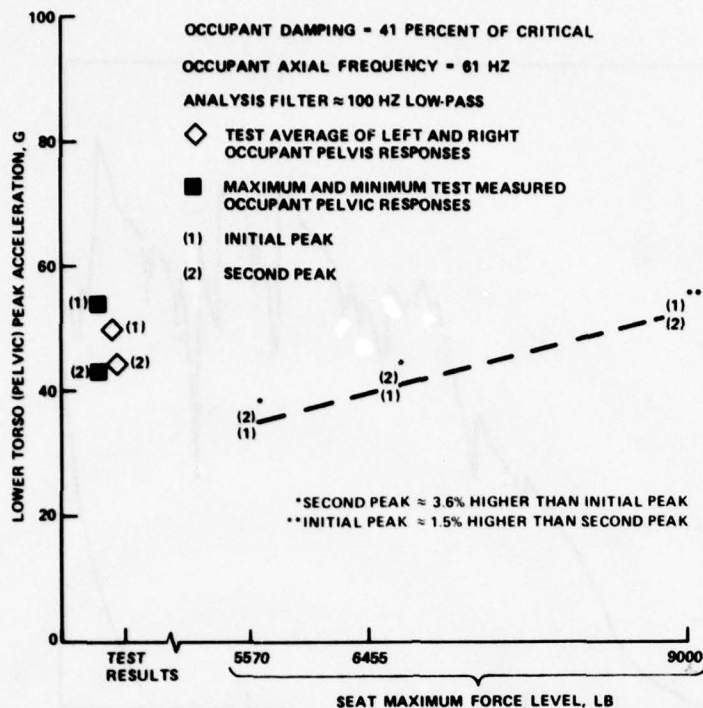


Figure 4-5. - Lower torso (pelvis) response as a function of seat maximum force level.

measured responses. The ranges investigated represent a deviation of approximately -15 to +28 percent from the nominal 6455 pounds used. For the three force levels evaluated (5570, 6455, and 9000 pounds), the initial peak acceleration level obtained by analysis for the occupant upper torso is approximately 6 percent, 17.4 percent, and 58 percent higher, respectively, than the corresponding average of the head and chest measured values. The upper torso response is more akin to the DRI value than the lower torso response. Consequently, the analysis may show a more conservative DRI value than is indicated by test response data. User-selected values of between 5500 and 6500 pounds appear to provide reasonable representations of the seat load-deflection characteristics.

4.4 ANALYTICAL FILTER CUTOFF FREQUENCY

Analysis of the current substructure test data indicated that a 100-Hz, low-pass digital filter is approximately equivalent to the least-square-fit (LSF) filtering performed by NASA-Langley. The LSF data were used for the tabulation of test results. Previous NASA evaluation of equivalent filtering

indicated that 180 Hz, low-pass filtering could be equivalent to the LSF data. Recognizing that equivalent filtering is difficult to define because of the different data reduction processes that are used and the wide range of types of structures or elements being considered, an evaluation was performed to ascertain the effects of the analytical results and subsequent correlation with test results of different analytical filter cutoff frequencies. As noted earlier, KRASH filtering is a post-processing technique and doesn't change any computed values.

Figure 4-6 shows the result of the analysis for a cutoff frequency range from 100 to 150 Hz. For the floor responses the analytically obtained peak values increase by approximately 4 to 18 percent in changing from a 100-Hz to 150-Hz cutoff frequency. However, as can be observed in Figure 4-6, the results are for the most part still within the range of recorded test values at the respective locations. The analytical responses for the occupant lower torso are less sensitive to the cutoff frequency change. The data in Figure 4-6 shows a variation of less than 5 percent for the initial lower torso peak value and less than 2 percent for the second peak value. The occupant responses exhibit lower frequency (broader response) characteristics than the floor responses and consequently are not expected to be as sensitive to the higher cutoff frequencies.

4.5 MODEL SIZE VARIATION

The base 32 mass, 57 member symmetrical math model shown in Figures 2-3 and 2-4 provides an adequate representation of the substructure and impact condition evaluated, as attested to by the close agreement with available test data. The results, analytical and test, indicate that the airframe shell structure, which accounts for approximately 28 percent of the total substructure airframe weight, did not deform appreciably, due in part to the stabilizing effect of the end closures (tension rods), during the 27.5 ft/sec vertical impact. Consequently, the occupant responses may not be altered very much from that which would be expected if the upper shell structure flexibility were ignored and the mass and inertia effects were accounted for. This situation is particularly significant since the 32 mass, 57 member model and test results show that the shell structure motion does not pose any lethal threat to the



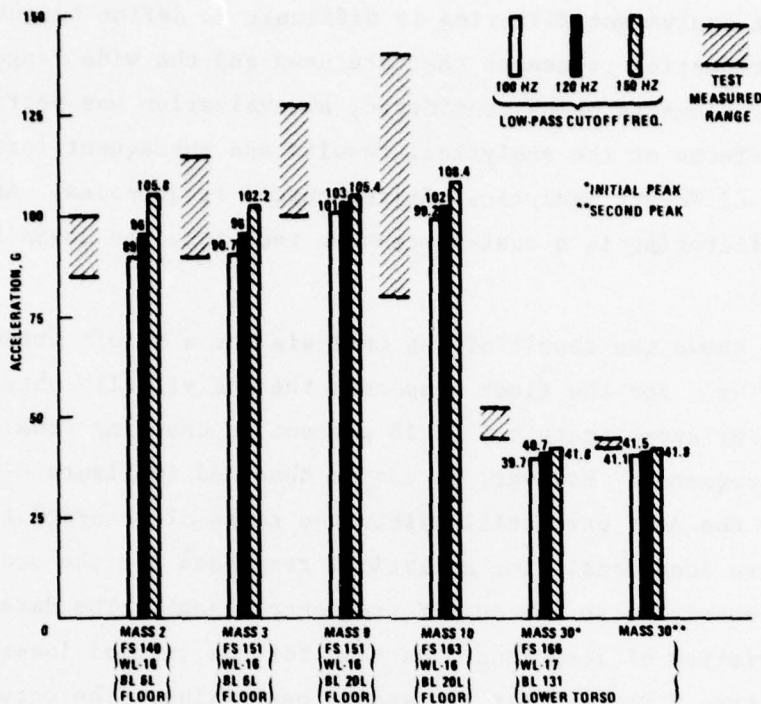


Figure 4-6. Floor and occupant peak responses as a function of analysis filter cutoff frequency.

occupants either through failure or excessive motion. If prior to or during the analysis, the user can establish that the representation of the shell structure is not critical, insofar as the occupant and floor responses are concerned, a smaller more economical math model can be pursued. To assess the tradeoff between accuracy and model analysis cost for the substructure and impact condition described in this report the following KRASH math models were investigated:

- 16 mass, 32 member symmetrical half structure (runmod=1)
- 6 mass, 8 member symmetrical half structure (runmod=1)
- 5 mass, 5 member full structure (runmod=0)

The 16 mass, 32 member model is shown in Figure 4-7. The model is the same as the base 32 mass, 57 member model except that the mass associated with the shell structure is distributed among the floor masses. The 6 mass,

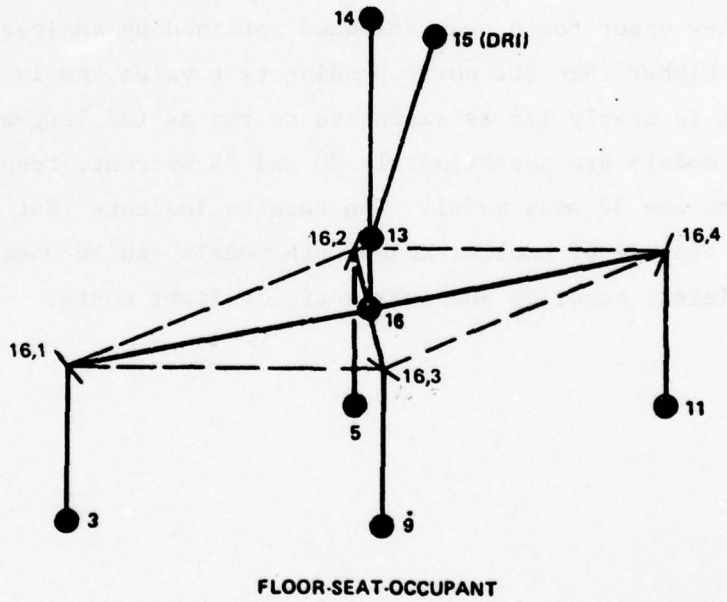
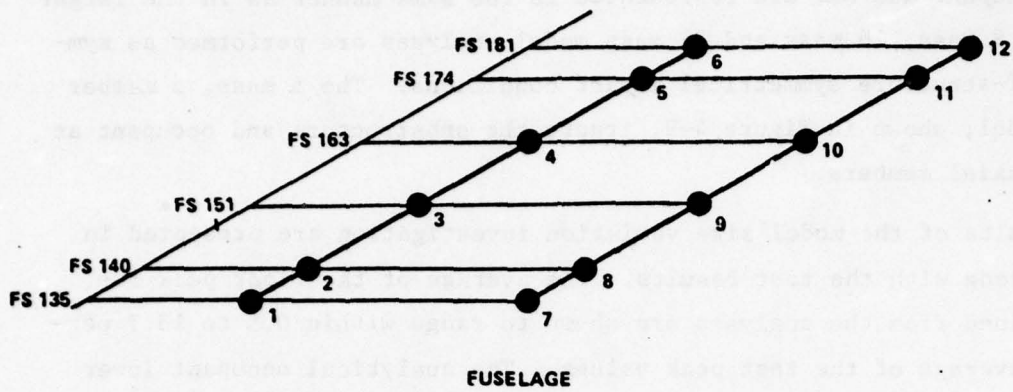


Figure 4-7. 16 mass, 32 member symmetrical math model.



8 member model, shown in Figure 4-8, lumps half the airframe weight at mass locations 1 and 2. The stiffness of the seat is represented by 2 members instead of 4 as in the larger 16 mass and 32 mass models. The seat cushion, seat pan, occupant and DRI are represented in the same manner as in the larger models. The 8 mass, 16 mass and 32 mass model analyses are performed as symmetrical half-structure symmetrical impact conditions. The 5 mass, 5 member full math model, shown in Figure 4-9, treats the substructure and occupant as a series of axial members.

The results of the model size variation investigation are presented in Table 4-1, along with the test results. The average of the floor peak responses obtained from the analyses are shown to range within 0.5 to 13.7 percent of the average of the test peak values. The analytical occupant lower torso responses are within 19 to 22 percent of the test value for the first peak and between 3 and 7 percent of the test values for the second peak. The primary upper torso peak response obtained by analyses are from 15 to 24 percent higher than the corresponding test value. As is anticipated the smallest model is nearly 1/8 as expensive to run as the largest model. The 6 and 16 mass models are approximately 20 and 75 percent, respectively, as expensive to run as the 32 mass model. The results indicate that for this particular situation the use of smaller KRASH math models can be used to assess trends with sufficient accuracy and substantially lower costs.

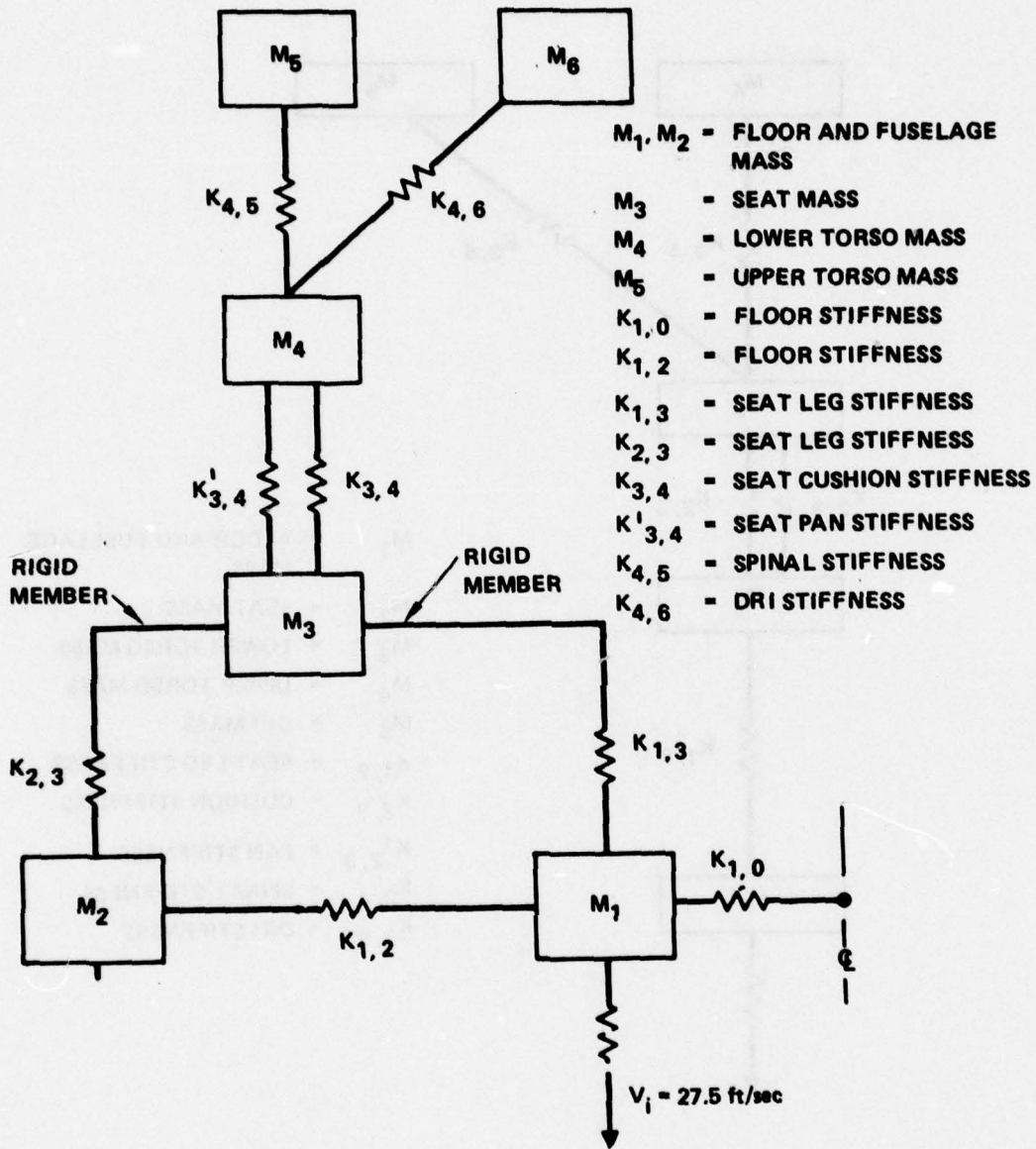


Figure 4-8. 6 mass, 8 member symmetrical math model.

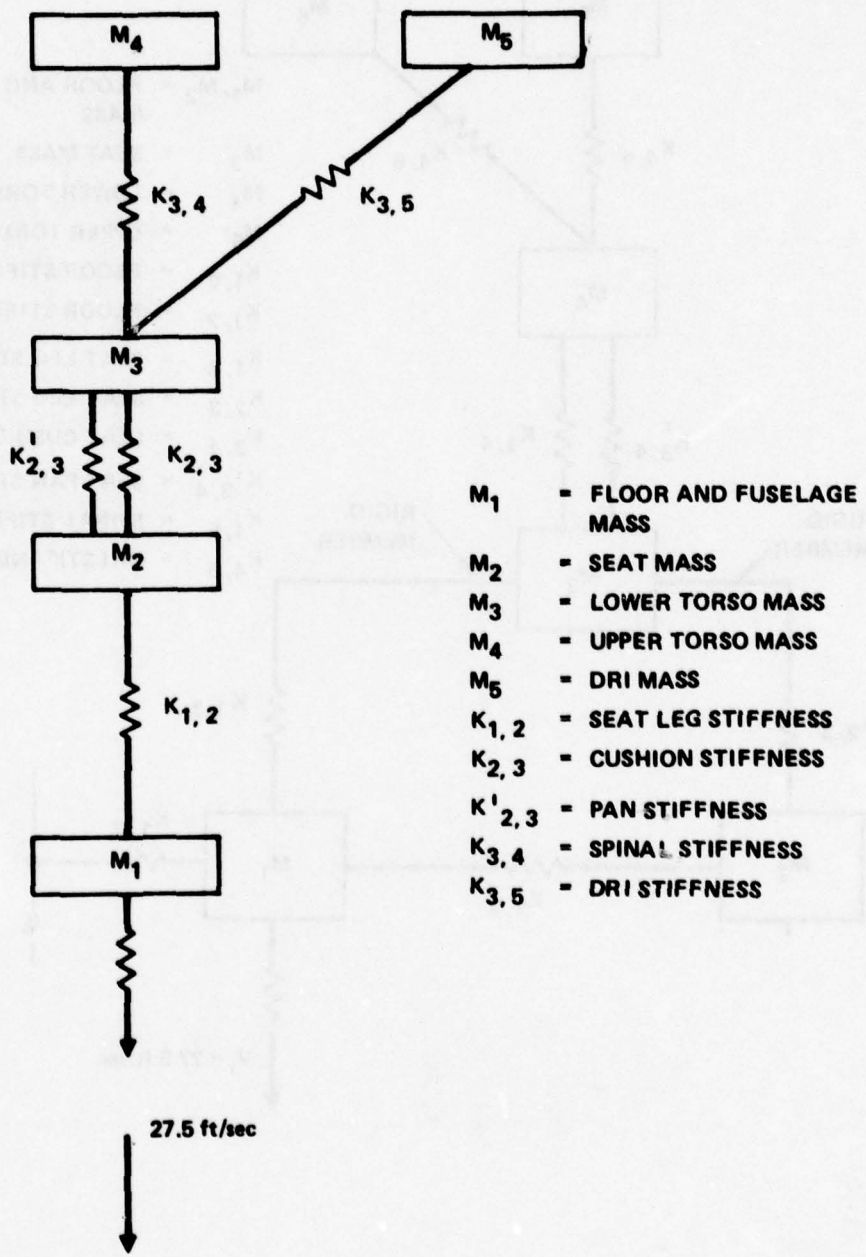


Figure 4-9. 5 mass, 5 member full math model.



TABLE 4-1. COMPARISON OF RESULTS FOR DIFFERENT SIZE MATH MODELS (a)

Location	Analysis Results (Peak Acceleration - g) (b)					Test Results (Peak Acceleration - g) (b)
	Masses Beams	32	16	6	5	
Floor						
		89(.004)	91.2(.005)	99(.005)	88.5(.008)	84.9(.004)
		90.7(.004)	92.6(.007)	105(.008)		128.7(.010)
		101(.011)	94(.011)			115.7(.004)
		99.2(.004)	98.5(.007)			80.8(.008)
Average (Time Range)		95(.004-.011)	94(.005-.011)	102(.005-.008)	88.5(.008)	102.5(.004-.010)
Lower Torso		39.7(.017)	38.4(.018)	39.8(.017)	39.7(.017)	49(.018-.020)
		41.1(.026)	38.4(.027)	42. (.028)	45.4(.030)	44.1(.030-.032)
Upper Torso		50.5(.022)	49.5(.022)	50.8(.022)	53.5(.019)	43(.020) (c)
Analysis Time (Machine Minutes) (d)		6.9	4.75	1.1	.67	---
Approximate Cost (d)		\$135	\$91	\$26	\$17	---

(a) Analysis results are based on 85 Hz low-pass filter, 27.5 ft/sec vertical velocity, 0.131 radian nose-up pitch, \approx 6500 pound seat force cutoff, and integration interval = .00001 seconds

(b) Time of occurrence in seconds after impact is shown in parenthesis

(c) Averaging of head and chest values

(d) Based on IBM 370-3330 digital computer

SECTION 5

CONCLUSIONS

The analysis of a twin-engine, low-wing airplane substructure subjected to a 27.5 ft/sec vertical impact has demonstrated program KRASH's capability to quantitatively represent the significant dynamic response phenomena, namely:

- Primary floor acceleration magnitudes and times of occurrence
- Occupant response magnitudes, time of occurrence and response shape, particularly the "camel-hump" effect
- Occupant and structure motion trends

The results of the sensitivity investigation using program KRASH indicate that for the parameters varied, the structure, and the impact condition evaluated, user-selected data for input into KRASH can vary as much as 20 percent and still provide a reasonable assessment of overall dynamic behavior. Furthermore, the range of dynamic response peak values obtained from variations in KRASH user selected input data is comparable to the spread in the measured test data between the left and right sides.

The results of the test and analysis correlation and sensitivity studies provide valuable information which can be used to enhance future modeling of crash impact conditions.

For some structural configurations and impact conditions simple approximate models are a cost-effective method of representing large structural segments with acceptable accuracy for qualitatively assessing dynamic behavior and response trends.

REFERENCES

1. Wittlin, G., Gamon, M.A. "Experimental Program for the Development of Improved Helicopter Structural Crashworthiness Analytical and Design Techniques," Lockheed-California Company, USAAMRDL-TR-72, U.S. Army Air Mobility Research and Development Laboratory, Ft. Eustis, Va., May 1973.
2. Wittlin, G., Gamon, M.A., LaBarge, W.L., "Full Scale Crash Test Experimental Verification of a Method of Analysis for General Aviation Airplane Structural Crashworthiness," Lockheed-California Company, FAA-RD-77-188, U.S. Dept. of Transportation, Federal Aviation Administration, System Research and Development, Wash., D.C., February 1978.
3. Vaughan, V., Jr., Alfaro, Bou E., "Impact Dynamics Research Facility for Full Scale Aircraft Crash Testing," NASA TN D-8179, April 1976.
4. Wittlin, G., Park, K.C., "Development and Experimental Verification of Procedures to Determine Nonlinear Load-Deflection Characteristics of Helicopter Substructures Subjected to Crash Forces," Lockheed-California Company, USAAMRDL TR 74-12, U.S. Army Air Mobility Research and Development Laboratory, Ft. Eustis, Va., May 1974.
5. Gamon, M.A., Wittlin, G., LaBarge, W.L., "General Aviation Airplane Structural Crashworthiness User's Manual, Input-Output Techniques and Applications," VOLUME II, Lockheed-California Co., FAA-RD-77-189II, Federal Aviation Administration, Wash., D.C., February 1978.
6. Laananen, D.H., "Development of a Scientific Basis for Analysis of Aircraft Seating Systems," FAA-RD-74-130, U.S. Dept. of Transportation, Federal Aviation Administration, Systems Research and Development Services, Wash., D.C., 1975.
7. Turnbow, J.W., et al, "Crash Survival Design Guide," USAAMRDL-TR-71-22 Eustis Directorate, U.S. Army Air Mobility Research and Development Laboratory, Fort Eustis, Va., Oct. 1971.



APPENDIX A KRASH MODEL CALCULATIONS

This appendix provides the sample calculations for determining the structure and occupant mass locations, mass properties, beam properties, and the external spring load-deflection characteristics.

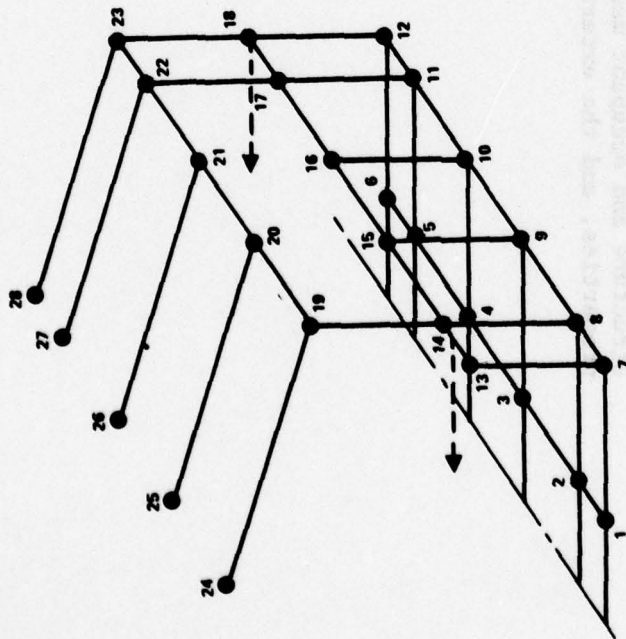


Figure A-1. — Fuselage model.

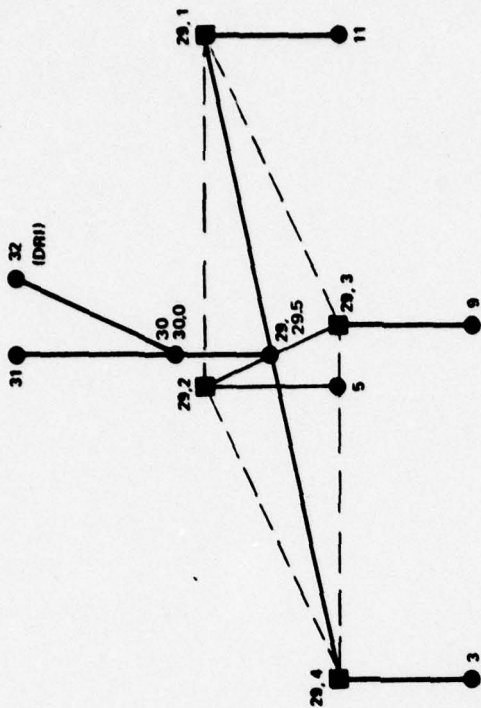


Figure A-2. — Floor seat-occupant model.

SEAT-OCCUPANT-REPRESENTATION

<u>MASS REPRESENTATIONS</u>			<u>MEMBER REPRESENTATIONS</u>	
<u>Mass</u>	<u>Representation</u>	<u>Weight (lb)</u> \overline{X} ^③	<u>ith - jth Masses</u>	<u>Representation</u>
3, 5, 9, 11	Seat leg attachment at floor	①	3 - 29,1	Seat legs
29,1, 29,2, 29,3, 29,4	Seat leg attachment at pan	20.86	5 - 29,2	
30	Lower torso pelvis region	72.86 ^②	9 - 29,3	
			11 - 29,4	
31	Upper torso chest region	72.86 ^②	29 - 30	Seat cushion, compression only member
32	DRI	72.86 ^②	29,5 - 30,1	Seat pan
			30 - 31	Upper torso (spine)
			30 - 32	DRI
			11 - 30	Seat belt, tension only member
			5 - 30	Seat belt, tension only member

Notes

- ① Distributed weight from floor structure +6 percent of occupant weight at each of the forward floor seat leg attachment locations.
- ② 44 percent of occupant weight
- ③ Height in inches above the floor

MASS MOMENT OF INERTIA OF 50-PERCENTILE MAN, 161.5 lb (Reference 6)

Element	Fraction of Total Mass (m/m_T)	Weight (lb)	Mass lb sec ² in.	Mass Moment of Inertia (lb - sec ² - in.)		
				Roll I_x	Pitch I_y	Yaw I_z
Lower Torso	0.2778	44.86	0.1162	4.331	8.703	8.703
Upper Torso	0.2264	36.56	0.09471	2.623	2.623	2.623
Head & Neck	0.0792	12.79	0.03313	0.311	0.311	0.201
Upper Arm	0.0264	4.26 (2)	0.01104	0.164	0.164	0.0241
Forearm & Hand	0.0214	3.46 (2)	0.00896	0.0241	0.218	0.218
Thigh	0.1001	16.17 (2)	0.04189	0.307	1.270	1.270
Leg & Foot	0.0604	9.75 (2)	0.02526	1.192	1.192	0.120
Total		161.5	0.41334			

UPPER TORSO 50-PERCENTILE MAN, 161.5 lb (Reference 6)

$$I_x = 3.357 + 2\{.164 + .01104 [(5.81 - 5.24)^2 + (6.34)^2]\} + 2\{.0241 + .00896 [(11.99 - 5.81)^2 + (6.34)^2]\}$$

$$+ .311 + .03313 [(5.81 + 6.06)^2] = 3.357 + 1.2227 + 1.4529 + 4.9789 = \underline{11.0115}$$

$$I_y = 2.623 + 2\{.164 + .01104 [(5.81 - 5.24)^2]\} + 2\{.218 + .00896 [(11.99 - 5.81)^2 + (8.95)^2]\}$$

$$+ .311 + .03313 [(5.81 + 6.06)^2 + (.75)^2] = 2.623 + .3352 + 2.5559 + 4.9976 = \underline{10.5117}$$

$$I_z = 2.623 + 2\{.0241 + .01104 [(6.34)^2]\} + 2\{.218 + .00896 [(6.34)^2 + (8.95)^2]\} + .201 + .03313 (75)^2$$

$$= 2.623 + .93572 + 2.59174 + .21964 = \underline{6.3701}$$

For 165.6 # MAN

$$I_x = 11.2946$$

$$I_y = 10.7785$$

$$I_z = 6.5318$$

LOWER TORSO 50-PERCENTILE MAN, 161.5 lb

$$I_x = 8.703 + .1162 (5.35)^2 + 2 \{ .307 + .04189 (3.39)^2 \} = 8.703 + 3.3259 + 1.57681 = \underline{13.6057}$$

$$I_y = 4.331 + .1162 (5.35)^2 + 2 \{ 1.270 + .04189 (7.09)^2 \} = 4.331 + 3.3259 + 6.7515 = \underline{14.4084}$$

$$I_z = 8.703 + .1162 (0) + 2 \{ 1.270 + .04189 [(3.39)^2 + (7.09)^2] \} = 8.703 + 0 + 7.71427 = \underline{16.4173}$$

For 165.6 lb Man

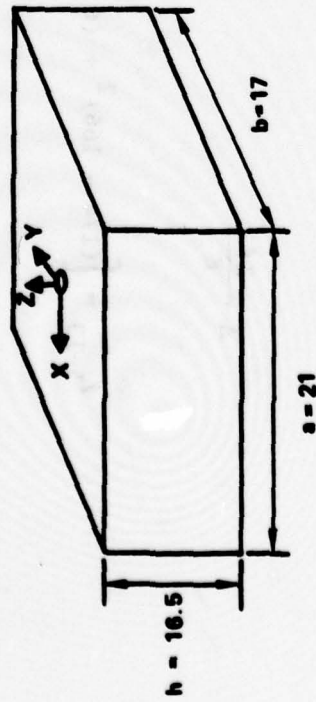
$$I_x = \underline{13.9511}$$

$$I_y = \underline{14.7742}$$

$$I_z = \underline{16.8341}$$

MASS MOMENT OF INERTIA OF SEAT (MASS 29)

Mass = 20/386



$$I'_x = \frac{20}{12(386)} (17^2 + 16.5^2) = 2.4234$$

$$I'_y = \frac{20}{12(386)} (21^2 + 16.5^2) = 3.0797$$

$$I'_z = \frac{20}{12(386)} (21^2 + 17^2) = 3.1520$$

About Top Center

$$I_x = 2.4234 + \frac{20}{386} \left(\frac{16.5}{2} \right)^2 = 5.9500$$

$$I_y = 3.0797 + \frac{20}{386} \left(\frac{16.5}{2} \right)^2 = 6.6062$$

$$I_z = 3.1520$$

SEAT BELT

Seat Belt Attaches from Mass 30 to Mass 11 and from Mass 30 to Mass 5

Estimated stiffness of seat belt = 1000 lb/in.

For the purpose of seat belt calculations assume the seat belt material to be aluminum - material #4

$$E = 10.5 \times 10^6$$

$$K = \frac{AE}{\ell}$$

$$A = \frac{K\ell}{E}$$

$$\ell_{5-13} = \left[(174 - 166)^2 + (6 - 13)^2 + (-16 - 4)^2 \right]^{1/2} = 22.6495$$

$$\ell_{11-13} = \left[(174 - 166)^2 + (20 - 13)^2 + (-16 - 4)^2 \right]^{1/2} = 22.6495$$

$$A = \frac{(1 \times 10^3)(22.6495)}{10.5 \times 10^6} = .0021571$$

SEAT CUSHION

Estimated seat cushion stiffness = 500 lb/in.

For the purpose of seat cushion calculations assume the cushion material to be aluminum - material #4
 $E = 10.5 \times 10^6$.

$$K = \frac{AE}{l}$$

$$A = \frac{Kl}{E}$$

Assume thickness of cushion to be 4"

$$A = \frac{(500)(4)}{(10.5 \times 10^6)} = .00019 \text{ (in}^2\text{)}$$

Estimated seat pan stiffness = 2000 lb/in.

$$A = \frac{Kl}{E} = \frac{(2000)(4)}{(10.5 \times 10^6)} = .0007619 \text{ (in}^2\text{)}$$

EXTERNAL SPRING REPRESENTATION

STIFFENER AREA - MASSES 2 THROUGH 6

$$\text{AREA} = (12)(.032) + (a + b)(.032)$$

$$= (12 + a + b)(.032)$$

$$\Delta = \text{AREA/REF AREA}^*$$

$$\text{REF. AREA} = 3.376 \text{ (in}^2\text{)}$$

BULKHEAD AREA - MASSES 8 THROUGH 12

$$\text{Reference Area} = .956^*$$

$$\text{Area} = (14 - 6)(.032) = .256$$

$$\Delta = .268$$

Peak load = 670 lb at a deflection = .05 inches

F.S.	a	b	A	Δ	Peak Load at Deflection = 0.1 inch
135	0	2.5	0.464	0.137	1644
140	2.5	0.65	0.645	0.191	2292
151.3	5.65	5.65	0.746	0.221	2652
162.6	5.65	5.7	0.747	0.221	2652
174	5.7	3.5	0.678	0.201	2412
184	3.5	0	0.496	0.147	1764

*Reference Area based on USAMRDL TR 74-12 TEST SPECIMEN DATA. See Reference FAA-RD-77-188II, page 4-62.

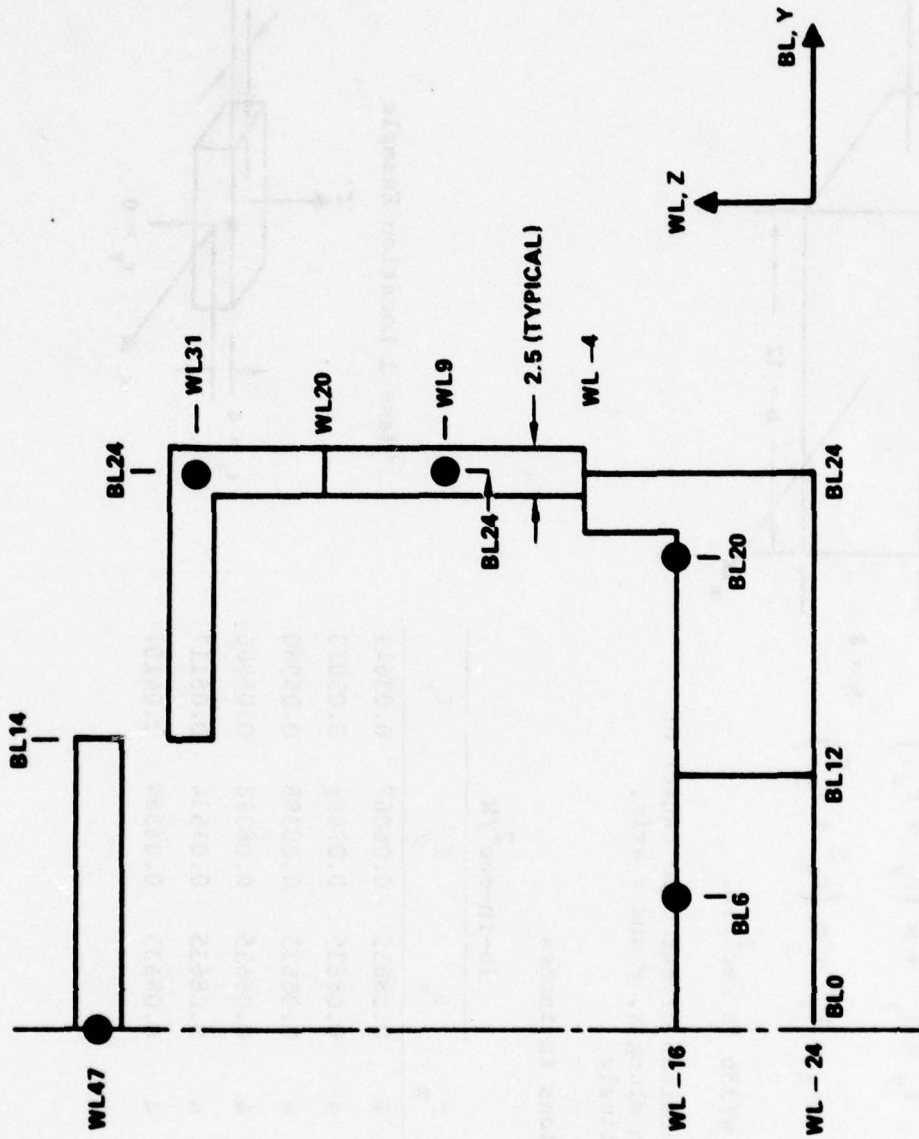


Figure A-3. - Mass moment of inertia schematic.

MASSES 1-6

$$I_x' = \frac{m}{12} (b^2 + h^2)$$

$$I_x = I_x' + m (r_z^2 + r_y^2)$$

$$I_y' = \frac{m}{12} (a^2 + h^2)$$

$$I_y = I_y' + m (r_x^2 + r_z^2)$$

$$I_z' = \frac{m}{12} (b^2 + a^2)$$

$$I_z = I_z' + m (r_x^2 + r_y^2)$$

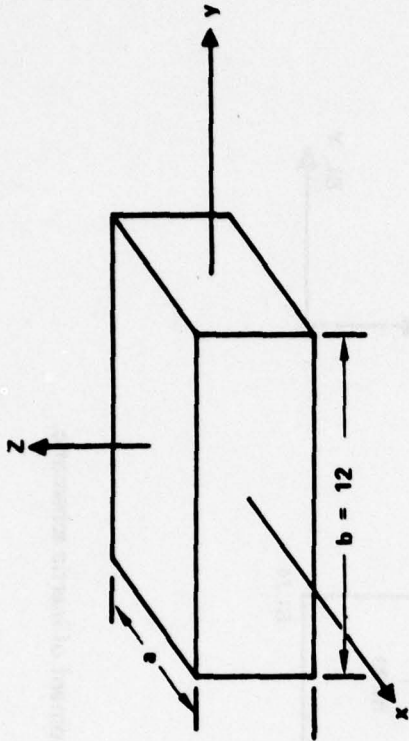
$h = 8$

$$m = \text{mass} = w/386 \text{ lb sec}^2/\text{in.}$$

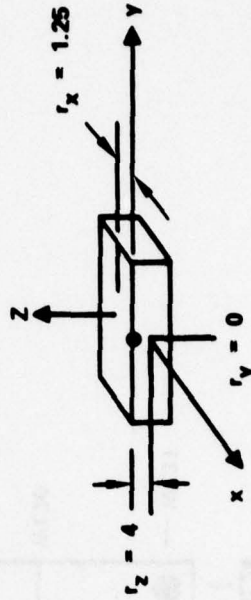
r_x, r_y, r_z = mass location offset from center of section along x, y and z axis, respectively

a, b, h = dimensions in inches

Mass	a	r_x	r_y	r_z	lb-in-sec ² /W		
					I_x	I_y	I_z
*1	2.5	1.25	0	4	0.08635	0.06067	0.03649
2	8.0	1.5	0	4	0.08635	0.07491	0.05073
3	11.5	0.25	0	4	0.08635	0.08398	0.05980
4	11.5	0.25	0	4	0.08635	0.08398	0.05980
5	9	1.	0	4	0.08635	0.07534	0.05117
6	3.5	1.75	0	4	0.08635	0.06584	0.04167



*Mass 1 Location Example



MASSES 7-12

$$I_{1x}' = \frac{m}{12} (b_1^2 + h_1^2) \quad I_{2x}' = \frac{m}{12} (b_2^2 + h_2^2)$$

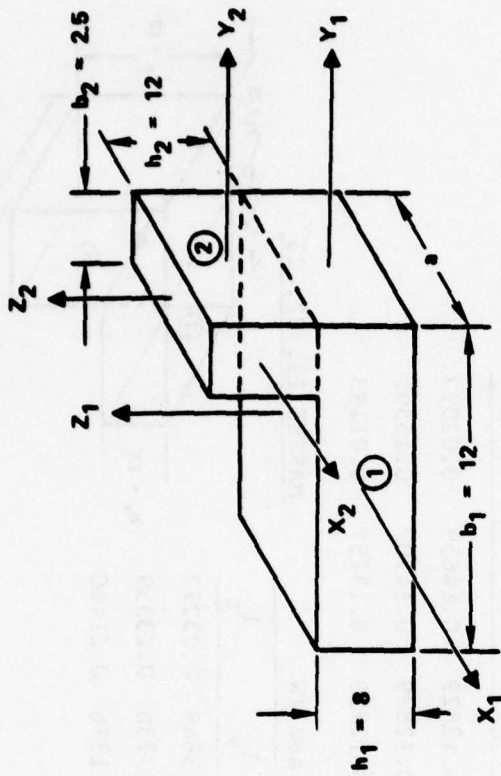
$$I_{1y}' = \frac{m}{12} (a^2 + h_1^2) \quad I_{2y}' = \frac{m}{12} (a^2 + h_2^2)$$

$$I_{1z}' = \frac{m}{12} (a^2 + b_1^2) \quad I_{2z}' = \frac{m}{12} (a^2 + b_2^2)$$

$$I_x = I_{1x}' + m (r_{1z}^2 + r_{1y}^2) + I_{2x}' + m (r_{1z}^2 + r_{1y}^2)$$

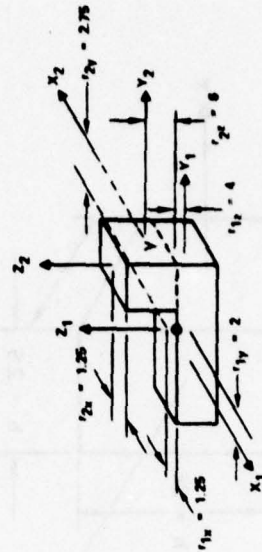
$$I_y = I_{1y}' + m (r_{1x}^2 + r_{1z}^2) + I_{2y}' + m (r_{1x}^2 + r_{1z}^2)$$

$$I_z = I_{1z}' + m (r_{1x}^2 + r_{1y}^2) + I_{2z}' + m (r_{1x}^2 + r_{1y}^2)$$



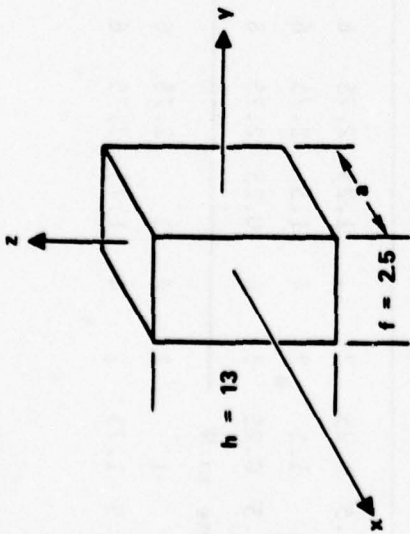
SKETCH B

*Mass 7 Location Example

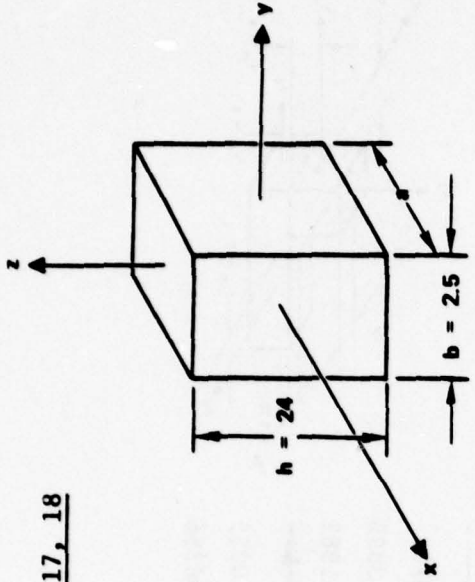


Mass	a	lb-in-sec ² /W								
		r_{1x}	r_{1y}	r_{1z}	r_{2x}	r_{2y}	r_{2z}	I_x	I_y	I_z
* 7	2.5	1.25	2	4	1.25	2.75	6	0.245	0.19042	0.0732
8	8	1.5	2	4	1.5	2.75	6	0.242	0.2189	0.13808
9	11.5	0.25	2	4	0.25	2.75	6	0.242	0.23705	0.11982
10	Same as 9									
11	9	1	2	4	1	2.75	6	0.245	0.21974	0.10255
12	3.5	1.75	2	4	1.75	2.75	6	0.245	0.20077	0.08356

MASSES 13, 15, 16



MASSES 14, 17, 18



SKETCH C

SKETCH D

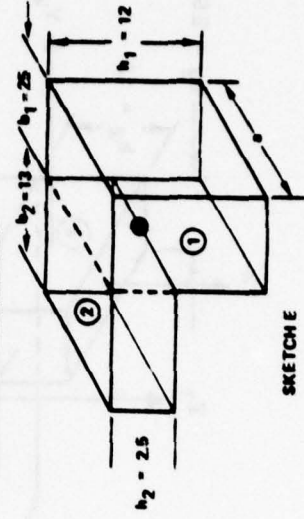
1b-in-sec²/W

Mass	a	r _x	r _y	r _z	I _x	I _y	I _z	
13	2.5	1.25	0	6.5	0.14728	0.15134	0.00675	
15	11.5	0.25	0	6.5	0.14728	0.17465	0.03006	
16	Same as 15							
14	8	1.5	0	1	0.12829	0.14659	0.02099	
17	9	1	0	1	0.12829	0.14702	0.15501	
18	3.5	1.75	0	1	0.12829	0.13752	0.01193	

1b-in-sec²/W

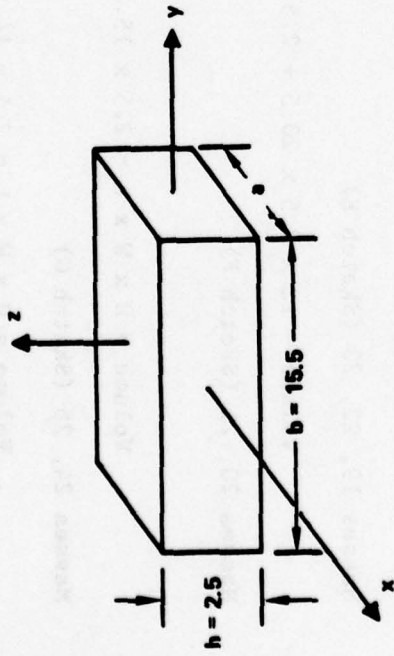
MASS	a	r _{1x}	r _{1y}	r _{1z}	r _{2x}	r _{2y}	r _{2z}	I _x	I _y	I _z
19	8	1.5	0	5	1.5	7.75	0	0.29064	0.13649	0.23272
22	9	1.0	0	5	1	7.75	0	0.29064	0.13736	0.23359
23	3.5	1.75	0	5	1.75	7.75	0	0.29064	0.11836	0.21460

MASSES 19, 22, 23

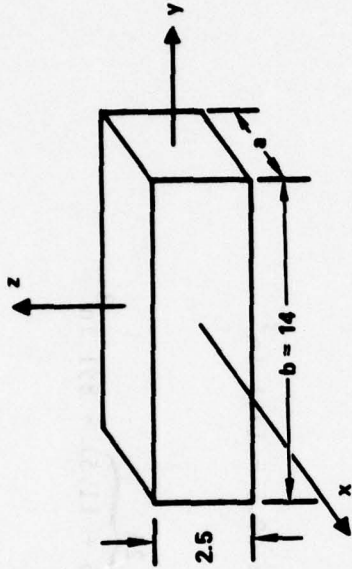


SKETCH E

MASSES 20, 21



MASSES 24-28



SKETCH F

SKETCH G

Mass	a	r_x	r_y	r_z	lb-in sec ² /W		
					I_x	I_y	I_z
20	11.5	0.25	6.5	0	0.16267	0.08058	0.13952
21	Same as 20				→		
24	8	1.5	7	0	0.17061	0.021	0.1889
25	11.5	0.25	7	0	0.17061	0.03006	0.19797
26	Same as 25				→		
27	9	1	7	0	0.17061	0.2143	0.18933
28	3.5	1.75	7	0	0.17061	0.01193	0.17983

MASS DISTRIBUTION BASED ON VOLUME

Masses 1-6 (Sketch A)

$$\text{Volume} = H \times W \times L = 8 \times 12 \times \overbrace{(2.5 + 8 + 11.5 + 11.5 + 9 + 3.5)}^{46} = 4416 \text{ in}^3$$

Masses 7-12 (Sketch B)

$$\text{Volume} = 8 \times 12 \times 46 + 2.5 \times 12 \times 46 = 5796 \text{ in}^3$$

Masses 13, 15, 16 (Sketch C)

$$\text{Volume} = H \times W \times L = 13 \times 2.5 \times \overbrace{(2.5 + 11.5 + 11.5)}^{25.5} = 828.75 \text{ in}^3$$

Masses 14, 17, 18 (Sketch D)

$$\text{Volume} = H \times W \times L = 24 \times 2.5 \times \underbrace{(8 + 9 + 3.5)}_{20.5} = 1230 \text{ in}^3$$

Masses 19, 22, 23 (Sketch E)

$$\text{Volume} = 12 \times 2.5 \times 20.5 + 2.5 \times 13 \times 20.5 = 1281 \text{ in}^3$$

Masses 20, 21 (Sketch F)

$$\text{Volume} = H \times W \times L = 2.5 \times 15.5 \times \overbrace{(11.5 + 11.5)}^{23} = 891 \text{ in}^3$$

Masses 24, 28 (Sketch G)

$$\text{Volume} = H \times W \times L = 2.5 \times 14 \times 46 = 1610 \text{ in}^3$$

$$\text{Total Volume} = 16053.25 \text{ in}^3$$

Density of Aluminum = 0.1 lb/in³

Assume 5% of volume is structure

$$\text{Weight} = 16053.25 \times 0.1 \times 0.05 = 80.265 \text{ lb}$$

Actual Weight = 86.5 lb for half

$$\Delta \text{Weight} = 86.5 - 80.265 = 6.235 \text{ lb}$$

Assume weight on floor is slightly heavier

$$\text{Volume of floor structure masses 1-12} = 0.05 [(8 \times 12 \times 46)2] = 441.6 \text{ in}^3$$

$$\Delta \text{Density} = 6.235/441.6 = 0.014119 \text{ lb/in}^3$$

Weight Calculations

Masses 1-6

$$\text{Weight} = (8)(12)(0.05)(0.1 + 0.04119)a = 0.54768a$$

Masses 7-12

$$\text{Weight} = (8)(12)(0.05)(0.1 + 0.04119)a + 12(2.5)(0.5)(0.1)a = 0.69768a$$

Masses 13, 15, 16

$$\text{Weight} = 13 (0.25)(0.05)(0.1)a = 0.1625a$$

Masses 14, 17, 18

$$\text{Weight} = 2.5 (24)(0.05)(0.1)a = 0.3a$$

Masses 19, 22, 23

$$\text{Weight} = 2.5(12)(0.05) 0.1a + 13 (2.5)(0.05)(0.1)a = 0.3125a$$

Masses 20, 21

$$\text{Weight} = (15.5)(2.5)(0.05)(0.1)a = 0.19375a$$

Masses 24-28

$$\text{Weight} = 14(2.5)(0.05)(0.1)a = 0.175a$$

See Table V-1 for appropriate mass "a" values (lengths) and weights

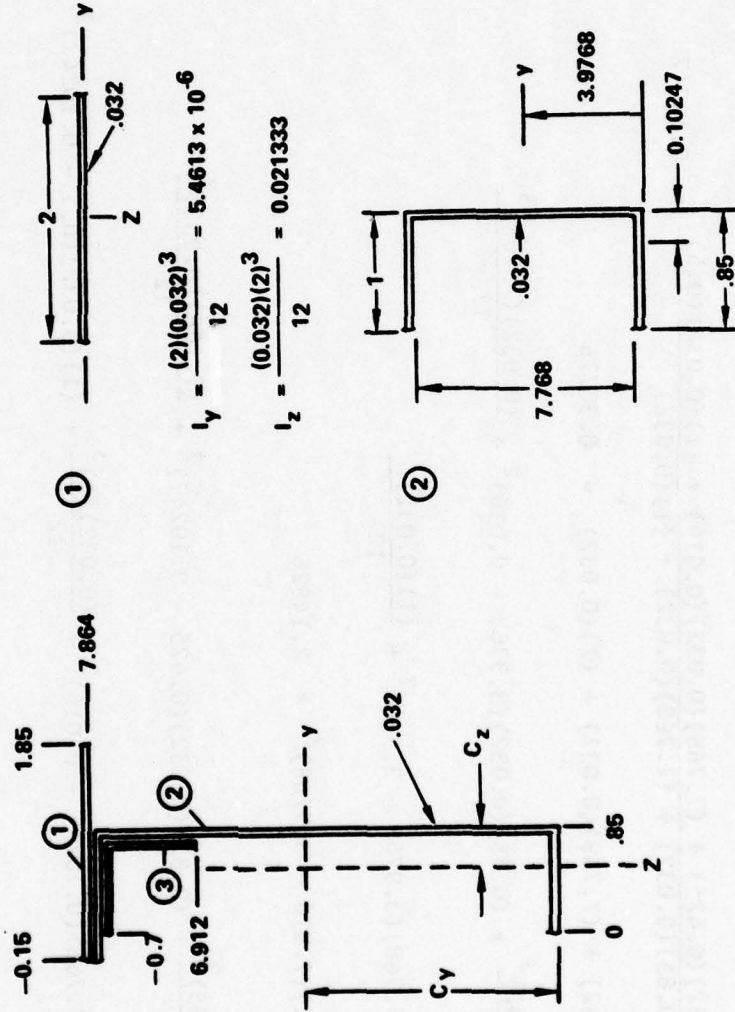
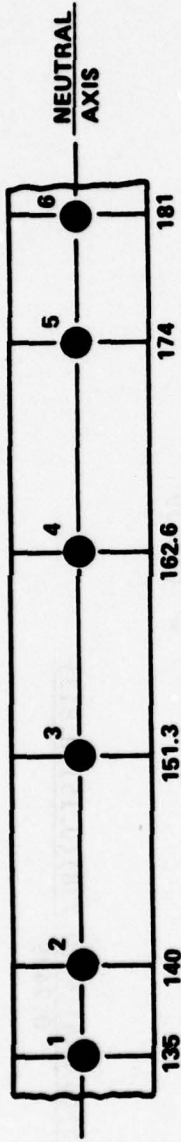
TABLE V-1. - MASS LOCATIONS AND PROPERTIES

Mass No.	a in.	x (in.)	y (in.)	z (in.)	WT l.B.	I _x	I _y (lb-in-sec ²)	I _z
1	2.5	135	6	-16	1.37	0.1183	0.0831	0.05
2	8	140	6	-16	4.38	0.3782	0.328	0.222
3*	11.5	151	6	-16	16.3	4.34	4.4	0.5
4	11.5	163	6	-16	6.3	0.544	0.529	0.377
5	9.	174	6	-16	4.93	0.426	0.371	0.252
6	3.5	181	6	-16	1.91	0.165	0.126	0.0796
7	2.5	135	20	-16	1.75	0.429	0.333	0.128
8	8	140	20	-16	5.58	1.35	1.22	0.771
9*	11.5	151	20	-16	18.03	5.72	5.68	1.09
10	11.5	163	20	-16	8.02	1.94	1.9	0.961
11	9	174	20	-16	6.28	1.54	1.38	0.644
12	3.5	181	20	-16	2.44	0.598	0.49	0.204
13	2.5	135	28	9	0.41	0.06	0.062	0.0028
14	8	140	28	9	2.4	0.308	0.352	0.0504
15	11.5	151	28	9	1.87	0.275	0.326	0.0562
16	11.5	163	28	9	1.87	0.275	0.326	0.0562
17	9	174	28	9	2.7	0.346	0.397	0.4185
18	3.5	181	28	9	1.05	0.134	0.144	0.0125
19	8	140	28	31	2.05	0.595	0.2798	0.477
20	11.5	151	28	31	2.23	0.362	0.1797	0.311
21	11.5	163	28	31	2.23	0.362	0.1797	0.311
22	9	174	28	31	2.81	0.8167	0.386	0.656
23	3.5	181	28	31	1.1	0.319	0.13	0.236
24	8	140	0	47.0	2.8	0.477	0.059	0.529
25	11.5	151	0	47.0	4.02	0.686	0.1206	0.796
26	11.5	163	0	47.0	4.02	0.686	0.1206	0.796
27	9	174	0	47.0	3.15	0.537	0.0675	0.596
28	3.5	181	0	47.0	1.23	0.21	0.0147	0.221
29	-	166	13	-1.7		Seat		
30	-	166	13	5.7		Cushion - Lower Torso		
31	-	166	13	20.89		Upper Torso		
32	-	166	13	20.89		DRI		

*Includes weight and inertia for occupant legs

BEAM PROPERTIES

LONGITUDINAL BEAM ASSEMBLY AREA PROPERTIES - MEMBERS 1-2, 2-3, 3-4, 4-5, 5-6



$$\textcircled{2} \quad C_y = \frac{(0.85)(0.032)(0.016) + (7.768)(0.032)(3.916) + (0.032)(1)(7.816)}{(0.85)(0.032) + (7.768)(0.032) + (1)(0.032)} = 3.9768$$

$$C_z = \frac{(0.85)(0.032)(0.425) + (7.768)(0.032)(0.016) + (1)(0.032)(0.5)}{(0.85)(0.032) + (7.768)(0.032) + (1)(0.032)} = 0.10247$$

$$A = (0.85)(0.032) + (7.768)(0.032) + (1)(0.032) = 0.30776$$

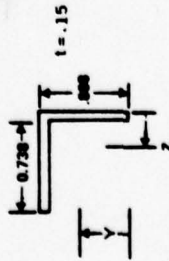
$$I_y = \frac{(0.85)(0.032)^3}{12} + (0.85)(0.032)(3.9768 - 0.016)^2 + \frac{(0.032)(7.768)^3}{12}$$

$$+ (0.032)(7.768)(3.9768 - 3.916)^2 + \frac{(1)(0.032)^3}{12}$$

$$+ (1)(0.032)(7.816 - 3.9768)^2 = 2.14926$$

$$I_z = \frac{(0.032)(0.85)^3}{12} + (0.85)(0.032)(0.425 - 0.10247)^2 + \frac{(7.768)(0.032)^2}{12}$$

$$+ (0.032)(7.768)(0.1024 - 0.016)^2 + \frac{(0.032)(1)^3}{12} + (1)(0.032)(0.5 - 0.10247)^2 = 0.0140706$$



$\textcircled{3}$

$$A = (0.888)(0.15) + (0.738)(0.15) = 0.2439$$

$$C_y = \frac{(0.888)(0.15)(0.444) + (0.738)(0.15)(0.813)}{0.2439}$$

$$C_y = 0.61148$$

$$C_z = 0.27652$$

$$I_y = \frac{(0.15)(0.855)^2}{12} + (0.888)(0.15)(0.61148 - 0.444)^2 + \frac{(0.738)(0.15)^3}{12} + (0.738)(0.15)(0.813 - 0.61148)^2$$

$$= 0.017192$$

$$I_z = \frac{(0.885)(0.15)^3}{12} + (0.888)(0.15)(0.27652 - 0.075)^2 + \frac{(0.15)(0.738)^3}{12} + (0.738)(0.15)(0.519 - 0.27652)^2$$

$$= 0.017192$$

Total

$$A_T = 0.064 + 0.307776 + 0.2439 = 0.615674$$

$$C_y = \frac{(0.064)(7.848) + (0.307776)(3.9768) + (0.2439)(7.52348)}{0.615674} = 5.78425$$

$$C_z = \frac{(0.064)(0) + (0.307776)(0.10247) + (0.2439)(0.30852)}{0.615674} = 0.27740$$

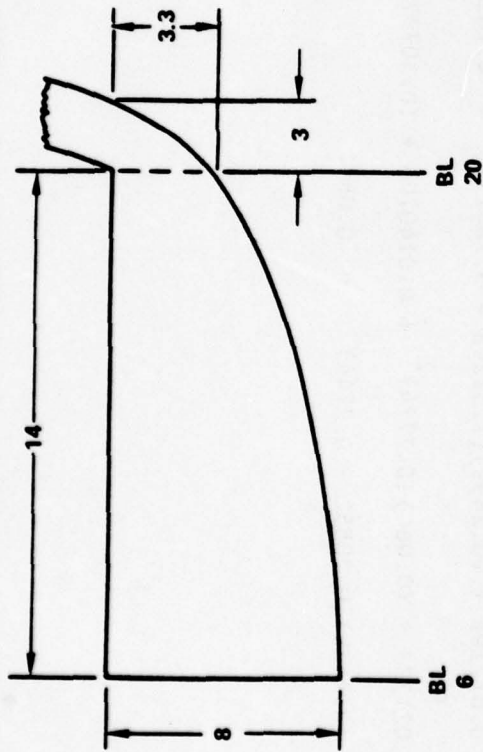
$$I_y = 5.4613 \times 10^{-6} + (0.064)(7.848 - 5.78425)^2 + 2.14926 + (0.307776)(5.78425 - 3.9768)^2$$

$$+ 0.017192 + (0.2439)(7.52348 - 5.78425)^2 = 4.18228$$

$$I_z = 0.021333 + (0.064)(0.2774)^2 + 0.0140706 + (0.307776)(0.2744 - 0.10247)^2 + 0.017192$$

$$+ (0.2439)(0.30852 - 0.2744)^2 = 0.0671$$

FUSELAGE STATION 135 - 181 - MEMBERS 1-7, 2-8, 3-9, 4-10, 5-11, 6-12



$$\text{Average Section Height} = \frac{8 + 3.3}{2} = 5.65$$

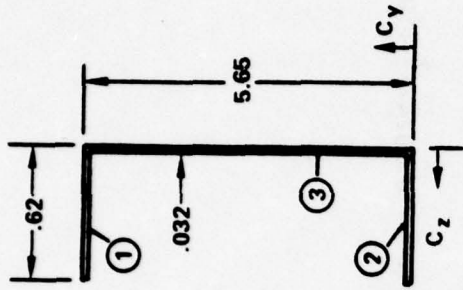
$$\textcircled{1} \text{ and } \textcircled{2} \quad A = 0.01984$$

$$C_y = 0.016$$

$$C_z = 0.31$$

$$I_y = \frac{0.62(0.032)^3}{12} = 1.693 \times 10^{-6}$$

$$I_z = \frac{0.032(0.62)^3}{12} = 6.3554 \times 10^{-4}$$



$$\text{Area} = 2(0.62)(0.032) + (5.686)(0.032) = 0.21843$$

$$\textcircled{1} \quad A = (5.586)(0.032) = 0.17875$$

$$C_y = 2.793$$

$$C_z = 0.016$$

$$I_y = \frac{0.032(5.586)^3}{12} = 0.46481$$

$$I_z = \frac{5.586(0.032)^3}{12} = 1.5254 \times 10^{-5}$$

Total Section

$$A = 0.21843$$

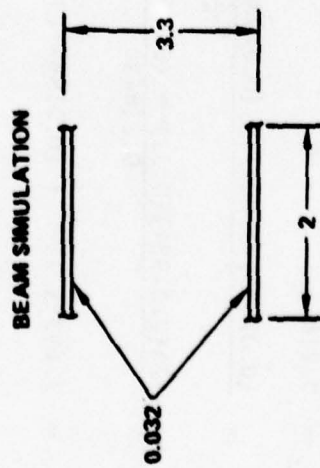
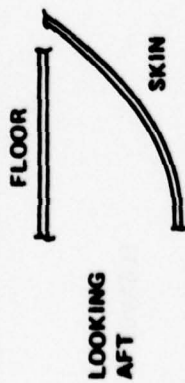
$$C_y = \frac{(0.01984)(5.634) + (0.01984)(0.016) + (0.17875)(2.825)}{0.21843} = 2.825$$

$$C_z = \frac{(2)(0.01984)(0.31) + (0.17875)(0.016)}{0.21843} = 0.06941$$

$$I_y = 1.693 \times 10^{-6} + (0.01984)(5.634 - 2.825)^2 + 0.46481 + (0.17875)(0) + 1.693 \times 10^{-6} \\ + (0.01984)(2.825 - 0.016)^2 = 0.77791$$

$$I_z = (6.3554 \times 10^{-4})(2) + (2)(0.01984)(0.31 - 0.06941)^2 + 1.5254 \times 10^{-5} + (0.17875)(0.06941 - 0.016)^2 \\ = 0.0040931$$

STRUCTURE BETWEEN RINGS - MEMBERS - 7-8, 8-9, 9-10, 10-11, 11-12



$$A = (2)(2)(0.032) = 0.128$$

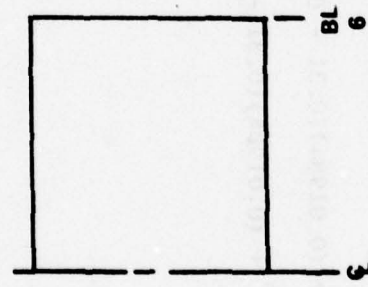
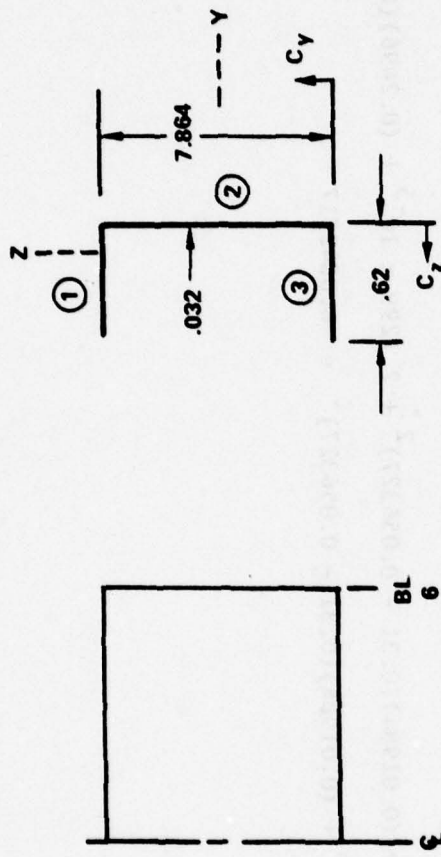
$$C_y = 1.65$$

$$C_z = 1.0$$

$$I_y = 2 \left[\frac{(2)(0.032)^3}{12} + (0.064)(1.634)^2 \right] = 0.34176$$

$$I_z = (2) \frac{(0.032)(2)^3}{12} = 0.042667$$

FUSELAGE STATION 135 - 181 - MEMBERS 1-0, 2-0, 3-0, 4-0, 5-0, 6-0



①, ③ $A = (0.62)(0.032) = 0.01984$

$C_y = 0.016$

$C_z = 0.31$

$I_y = \frac{(0.62)(0.032)^3}{12} = 1.6930 \times 10^{-6}$

$I_z = \frac{(0.032)(0.62)^3}{12} = 6.3554 \times 10^{-4}$

② $A = (7.8)(0.032) = 0.2496$

$C_y = 3.9$

$C_z = 0.016$

$$I_y = \frac{(0.032)(7.8)^3}{12} = 1.2655$$

$$I_z = \frac{(7.8)(0.032)^3}{12} = 2.1299 \times 10^5$$

Total

$$A = 2(0.01984) + 0.2496 = 0.28928$$

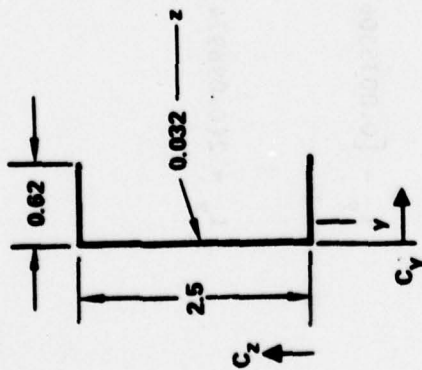
$$C_y = \frac{(0.01984)(0.016) + (0.2456)(3.932) + (0.01984)(7.848)}{0.28928} = 3.932$$

$$C_z = \frac{(2)(0.31)(0.01984) + (0.2496)(0.016)}{0.28928} = 0.056327$$

$$I_y = 1.6930 \times 10^{-6} + (0.01984)(3.932 - 0.016)^2 + 1.2655 + (0.2496)(3.932 - 3.932)^2 \\ + 1.6930 \times 10^{-6} + (0.01984)(7.848 - 3.932)^2 = 1.87400$$

$$I_z = 6.3554 \times 10^{-4} + (0.01984)(0.31 - 0.056327)^2 + 2.1299 \times 10^{-5} + (0.2496)(0.056327 - 0.016)^2 \\ + 6.3554 \times 10^{-4} + (0.01984)(0.31 - 0.056327)^2 = 0.0042517$$

BEAMS 7-13, 8-14, 9-15, 10-16, 12-18, 17-22, 18-23



$$A = 2 (0.62)(0.032) + (2.5 - 0.064)(0.032) = 0.11763$$

$$C_z = 1.25$$

$$C_y = \frac{2(0.62)(0.032)(0.31) + (2.5 - 0.064)(0.032)(0.016)}{0.11763} = 0.11517$$

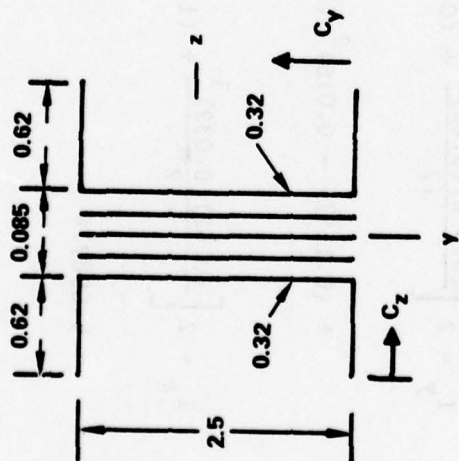
$$I_y = 2 \left[\frac{(0.032)(0.62)^3}{12} + (0.31 - 0.11517)^2 (0.62)(0.032) \right] + \frac{(2.5 - 0.064)(0.032)^3}{12}$$

$$+ (0.11517 - 0.016)^2 (2.5 - 0.064)(0.032) = 0.0035506$$

$$I_z = 2 \left[\frac{(0.62)(0.032)^3}{12} + (1.25 - 0.016)^2 (0.62)(0.032) \right] + \frac{(0.032)(2.5 - 0.064)^3}{12}$$

$$= 0.098974$$

BEAM 11-17



$$A = 4(0.62)(0.032) + 2(2.5 - 0.064)(0.032) + (0.085)(2.5) = 0.44776$$

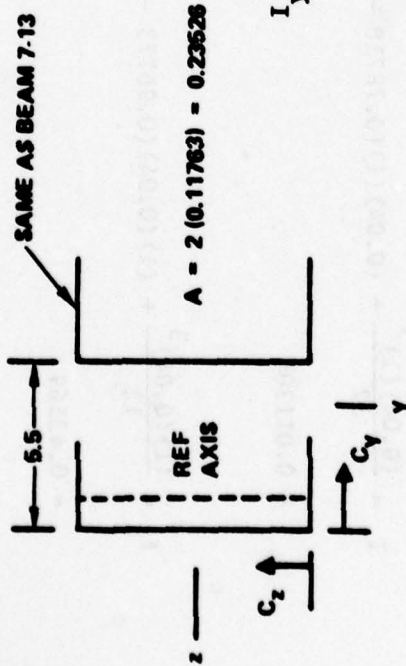
$$C_y = 1.25$$

$$C_z = 0.6625$$

$$I_y = [0.0035506 + (0.11517 + 0.0425)^2 (0.11763)] (2) + \frac{(2.5)(0.085)^3}{12} = 0.013077$$

$$I_z = 2(0.098974) + \frac{(0.085)(2.5)^3}{12} = 0.308625$$

BEAM 14-19



$$C_y = \frac{(0.11763)(0.11517) + (0.11763)(0.11517 + 5.5)}{0.23526}$$

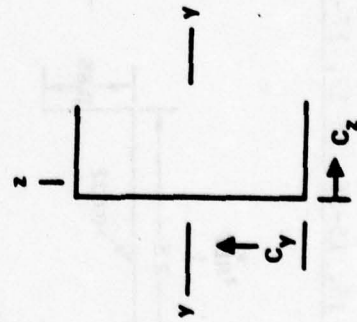
$$= 3.09396$$

$$C_z = 1.25$$

$$I_y(\text{REF AXIS}) = (0.0035506)(2) + (0.11763)(5.5)^2 = 3.56541$$

$$I_z = 2(0.098974) = 0.197948$$

BEAMS 19-24, 20-25, 21-26, 22-27, 23-28 (See Beam 7-13)



$$A = 0.11763$$

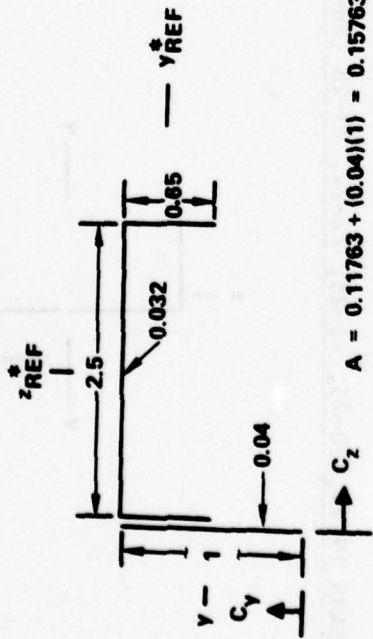
$$C_y = 1.25$$

$$C_z = 0.11517$$

$$I_y = 0.098974$$

$$I_z = 0.0035506$$

BEAMS 13-14, 14-15, 15-16, 16-17, 17-18



$$A = 0.11763 + (0.04)(1) = 0.15763$$

*Z_{REF} = 1.25, Y_{REF} = 0.11517, FROM BEAM 7-13 DATA

$$A = 0.11763 + (0.04)(1) = 0.15763$$

$$C_y = \frac{(1)(0.04)(0.5) + (0.11763)(1 - 0.11517)}{0.11763 + 0.04} = 0.78718$$

$$C_z = \frac{(1)(0.04)(0.02) + (1.25 + 0.04)(0.11763)}{0.15763} = 0.96773$$

$$I_y = \frac{(0.04)(1)^3}{12} + (0.04)(1)(0.78718 - 0.5)^2 + 0.0035506 + (0.11763)(1 - 0.11517 - 0.78718)^2$$

$$= 0.011304$$

$$I_z = \frac{(1)(0.04)^3}{12} + (1)(0.04)(0.96773 - 0.02)^2 + 0.098974 + (0.11763)(2.54 - 0.96773)^2$$

$$= 0.42569$$

APPENDIX B ANALYSIS COMPUTER PRINT

This section contains the KRASH program print showing the math model input data, model parameter data, mass position plots and selected output data. The math input data consists of the following:

- Echo print
- Program size and control data
- Initial conditions
- Mass, mode point, external spring, and beam data

The model parameter data provides the following:

- Vehicle weight, cg, inertia and initial ground impact position
- Beam loads, deflections, uncoupled frequencies, damping terms and Euler angles.

The time-equal-zero data consists of the following:

- Mass accelerations
- Vehicle cg translational velocity
- Energy distribution
- Mass energy deviation

The mass position plots at time = 0.0 are presented for the following:

- xz plane (aft-up)
- yz plane (side-up)

The selected output data consists of the following:

- Rupture/yield summary
- Energy summary
- Position plots at time = 0.054
- History plots of:
 - A mass filtered and unfiltered acceleration
 - A beam force and deflection
 - An external spring
 - The DRI element
 - The vehicle cg translational velocity

ECHO OF THE INPUT DATA IN CARD IMAGE FORMAT

CARD NO.	1	2	3	4	5	6	7	8
51	1	30	166.	13.	5.6			00000510
52	2	3	6.0	0.0	50000.0			00000520
53	3	3	6.0	0.0	50000.0			00000530
54	4	3	6.0	0.0	50000.0			00000540
55	5	3	6.0	0.0	50000.0			00000550
56	6	3	6.0	0.0	50000.0			00000560
57	8	3	3.3	0.0	20000.0			00000570
58	9	3	3.3	0.0	20000.0			00000580
59	10	3	3.3	0.0	20000.0			00000590
60	11	3	3.3	0.0	20000.0			00000600
61	12	3	3.3	0.0	20000.0			00000610
62	0.100	0.700	1.000	2.5	2290.0	2290.0		00000620
63	0.100	0.700	1.000	2.5	2650.0	2650.0		00000630
64	0.100	0.700	1.000	2.5	2650.0	2650.0		00000640
65	0.100	0.700	1.000	2.5	2410.0	2410.0		00000650
66	0.100	0.700	1.000	2.5	1760.0	1760.0		00000660
67	0.045	0.055	0.15	1.1	1380.	1380.		00000670
68	0.045	0.055	0.15	1.1	1380.	1380.		00000680
69	0.045	0.055	0.15	1.1	1380.	1380.		00000690
70	0.045	0.055	0.15	1.1	1380.	1380.		00000700
71	0.045	0.055	0.15	1.1	1380.	1380.		00000710
72	1	2	0.615674	4.18228	0.060521			5.78 .667 400000720
73	2	3	0.615674	4.18228	0.060521			5.78 .667 400000730
74	3	4	0.615674	4.18228	0.060521			5.78 .667 400000740
75	4	5	0.615674	4.18228	0.060521			5.78 .667 400000750
76	5	6	0.615674	4.18228	0.060521			5.78 .667 400000760
77	7	8	0.128	0.34176	0.042667			1.65 1.0 400000770
78	8	9	0.128	0.34176	0.042667			1.65 1.0 400000780
79	9	10	0.128	0.34176	0.042667			1.65 1.0 400000790
80	10	11	0.128	0.34176	0.042667			1.65 1.0 400000800
81	11	12	0.128	0.34176	0.042667			1.65 1.0 400000810
82	1	0	0.28928	1.874	0.0042517			3.93 .564 400000820
83	2	0	0.28928	1.874	0.0042517			3.93 .564 400000830
84	3	0	0.28928	1.874	0.0042517			3.93 .564 400000840
85	4	0	0.28928	1.874	0.0042517			3.93 .564 400000850
86	5	0	0.28928	1.874	0.0042517			3.93 .564 400000860
87	6	0	0.28928	1.874	0.0042517			3.93 .564 400000870
88	1	7	0.21843	0.77791	0.0040931			2.82 .550 400000880
89	2	8	0.21843	0.77791	0.0040931			2.82 .550 400000890
90	3	9	0.21843	0.77791	0.0040931			2.82 .550 400000900
91	4	10	0.21843	0.77791	0.0040931			2.82 .550 400000910
92	5	11	0.21843	0.77791	0.0040931			2.82 .550 400000920
93	6	12	0.21843	0.77791	0.0040931			2.82 .550 400000930
94	7	13	0.11763	0.003551	0.098974			.115 1.25 400000940
95	8	14	0.11763	0.003551	0.098974			.115 1.25 400000950
96	9	15	0.11763	0.003551	0.098974			.115 1.25 400000960
97	10	16	0.11763	0.003551	0.098974			.115 1.25 400000970
98	11	17	0.44776	0.013077	0.308625			.663 1.25 400000980
99	12	18	0.11763	0.003551	0.098974			.115 1.25 400000990
100	17	22	0.11763	0.003551	0.098974			.115 1.25 400001000
101	18	23	0.11763	0.003551	0.098974			.115 1.25 400001010

ECHO OF THE INPUT DATA IN CARD IMAGE FORMAT

CARD NO.	1	2	3	4	5	6	7	8
102	14	19	J.23526	3.565610	0.197948	3.09	1.25	400001020
103	19	24	1.11763	0.098974	0.003551	1.25	.115	400001030
104	20	25	0.11763	0.098974	0.003551	1.25	.115	400001040
105	21	26	0.11763	0.098974	0.003551	1.25	.115	400001050
106	22	27	0.11763	0.098974	0.003551	1.25	.115	400001060
107	23	28	0.11763	0.098974	0.003551	1.25	.115	400001070
108	13	14	0.15763	0.011304	0.425691	.787	.968	400001080
109	14	15	0.15763	0.011304	0.425691	.787	.968	400001090
110	15	16	0.15763	0.011304	0.425691	.787	.968	400001100
111	16	17	0.15763	0.011304	0.425691	.787	.968	400001110
112	17	18	0.15763	0.011304	0.425691	.787	.968	400001120
113	19	25	0.33012	3.798130	17.74063	.787	.968	400001130
114	20	21	0.33012	3.798130	17.74063			400001140
115	21	22	0.33012	3.798130	17.74063			400001150
116	22	23	0.33012	3.798130	17.74063			400001160
117	3	1	0.188	0.18000	0.54000	0.06	0.06	600001170
118	5	2	0.188	0.18000	0.54000	0.06	0.06	600001180
119	9	3	0.188	0.18000	0.54000	0.06	0.06	600001190
120	11	4	0.188	0.18000	0.54000	0.06	0.06	600001200
121	30	3	0.02000	0.0075	0.0075			400001210
122	30	32	0.009504	0.0048	0.0048			1000001220
123	5	30	0.0021571					400001230
124	11	30	0.0021571					400001240
125	29	30	0.000381					400001250
126	5	29	1	30	0.001170			400001260
127	14	0	0.11045					100001270
128	18	0	0.11045					100001280
129	5	30	1					00001290
130	11	30	1					00001300
131	29	30	-1					00001310
132	5	29	1	30	-1	0.00		00001320
133	14	0	1					00001330
134	18	0	1					00001340
135	0.04							00001350
136	30	31	.41					00001360
137	29	30	1					00001370
138	5	29	1	30	1	0.75		00001380
139	14	19	1	5	.082			00001390
140	14	19	2	5	.48			00001391
141	14	19	3	5	.194			00001400
142	17	22	1	5	.054			00001410
143	17	22	2	5	.48			00001411
144	17	22	3	5	5.2			00001420
145	18	23	1	5	.054			00001430
146	18	23	2	5	.48			00001431
147	18	23	3	5	5.2			00001440
148	19	24	1	5	.037			00001450
149	19	24	2	5	1.03			00001451
150	19	24	3	5	1.03			00001460
151	20	25	1	5	.037			00001470
152	20	25	2	5	1.03			00001471

ECHO OF THE INPUT DATA IN CARD IMAGE FORMAT

CARD NO.	1	2	3	4	5	6	7	8	
153	20	25	3	5	1.03			00001480	
154	21	26	1	5	.037			00001490	
155	21	26	2	5	1.03			00001491	
156	21	26	3	5	1.030			00001500	
157	22	27	1	5	.037			00001510	
158	22	27	2	5	1.03			00001511	
159	22	27	3	5	1.03			00001520	
160	23	28	1	5	.037			00001530	
161	23	28	2	5	1.03			00001531	
162	23	28	3	5	1.03			00001540	
163	7	13	1	5	.045			00001550	
164	7	13	2	5	.682			00001551	
165	7	13	3	5	1.287			00001560	
166	8	14	1	5	.045			00001570	
167	8	14	2	5	.682			00001571	
168	8	14	3	5	1.287			00001580	
169	9	15	1	5	.045			00001590	
170	9	15	2	5	.682			00001591	
171	9	15	3	5	1.287			00001600	
172	10	16	1	5	.045			00001610	
173	10	16	2	5	.682			00001611	
174	10	16	3	5	1.287			00001620	
175	11	17	1	5	.045			00001630	
176	11	17	2	5	.682			00001631	
177	11	17	3	5	1.287			00001640	
178	12	18	1	5	.045			00001650	
179	12	18	2	5	.682			00001651	
180	12	18	3	5	1.287			00001660	
181	0.	.75	.003					00001661	
182	.75	.003						00001662	
183	.751	1.						00001663	
184	3.5	1.						00001664	
185	3.51	3.						00001665	
186	4.	3.						00001666	
187	5.	3.						00001667	
188	6.	0.						00001668	
189	7.	3.						00001669	
190	20.	3.						00001670	
191	30	32						00001675	
192	2	6	3		5.0	10.0		00001680	
193	2	6	6	24	25	26		00001690	
194	2	6	3		5.0	5.0		00001700	
195	8	10	12	14	16	18		00001710	
196	3	5	3		5.	10.		00001720	
197	4	10	16	21	26			00001730	
198	2	5	3		5.0	10.0		00001740	
199	3	5	29	30	31			00001750	
200	2	3	3		5.0	10.0		00001760	
201	9	11	29	30	31			00001770	
202	2	3	0	0	0	0	1	1	0
203	3	3	0	0	0	0	1	1	0

ECHO OF THE INPUT DATA IN CARD IMAGE FORMAT

CARD NO.	1	2	3	4	5	6	7	8
204	5	0	0	0	0	1	1	0
205	9	0	0	0	0	1	1	0
206	10	0	0	0	0	1	1	0
207	11	0	0	0	0	1	1	0
208	14	1	0	0	0	1	1	0
209	19	1	0	0	0	1	1	0
210	21	1	0	0	0	1	1	0
211	15	1	0	0	0	1	1	0
212	20	1	0	0	0	1	1	0
213	25	1	0	0	0	1	1	0
214	17	1	0	0	0	1	1	0
215	22	1	0	0	0	1	1	0
216	27	1	0	0	0	1	1	0
217	29	1	0	0	0	1	1	0
218	30	1	0	0	0	1	1	0
219	31	1	0	0	0	1	1	0
220	32	1	0	0	0	1	1	0
221	46	1	1	1	1	1	1	0
222	49	1	1	1	1	1	1	0
223	50	1	1	1	1	1	1	0
224	54	1	1	1	1	1	1	0
225	55	1	1	1	1	1	1	0
226	56	1	1	1	1	1	1	0
227	57	1	1	1	1	1	1	0
228	46	1	1	1	1	1	1	0
229	49	1	1	1	1	1	1	0
230	50	1	1	1	1	1	1	0
231	54	1	1	1	1	1	1	0
232	55	1	1	1	1	1	1	0
233	56	1	1	1	1	1	1	0
234	57	1	1	1	1	1	1	0
235	23	1	1	1	1	1	1	0
236	24	1	1	1	1	1	1	0
237	25	1	1	1	1	1	1	0
238	26	1	1	1	1	1	1	0
239	27	1	1	1	1	1	1	0
240	28	1	1	1	1	1	1	0
241	29	1	1	1	1	1	1	0
242	30	1	1	1	1	1	1	0
243	31	1	1	1	1	1	1	0
244	32	1	1	1	1	1	1	0
245	33	1	1	1	1	1	1	0
246	34	1	1	1	1	1	1	0
247	35	1	1	1	1	1	1	0
248	36	1	1	1	1	1	1	0
249	2	0	1	1	1	1	1	0
250	3	0	1	1	1	1	1	0
251	4	0	1	1	1	1	1	0
252	5	0	1	1	1	1	1	0
253	6	0	1	1	1	1	1	0
254	32	0	1	1	1	1	1	0

PROGRAM SIZE DATA

NUMBER OF:

MASSES	SPRINGS	BEAMS	TABLES	KP HE OR IXY	NON- ZERO	MASS PENETR.	VOLUME CHANGE	DRI ELEMENTS	MTL TYPES	ACCEL. TABLES	NON- STANDARD MAX. FORCE	NON- ZERO PHI..	NON- STANDARD STIFFNESS MODE	NO. PTS.		
NI	NSP	NS	MLB	NHI	NVCH	MVP	NVCH	NORI	NMTL	NACC	NVBM	NFBM	NPH	ND	NKM	NMP
32	10	57	44	0	0	0	0	1	0	0	0	0	0	1	0	6

NSC= 0 NIC= 1 ITOLL= 10% NTOL2= 50% NTOL3= 100%

PROGRAM DATA MANAGEMENT CONTROL DATA

RESTART: TITLE -
 CASE -
 TIME - 0

SAVE: TITLE -
 CASE -
 TIMES - 0 0 0 0 0

VARIABLE INTEGRATION CONTROL DATA

VAR. INT. FLAG = 0 EL = 0.0 EU = 0.0 LOMER RATIO = 0.0 UPPER RATIO = 0.0

PROGRAM CONTROL DATA

PRINT INTERVAL/ INTEGRATION INTERVAL	INTEGRATION INTERVAL	MAX. TIME	PLOW FORCE STARTING TIME	FILTER CUTOFF FREQUENCY	CASE TYPE INDICATOR
DP/DT 100	DT 0.000010	THAX 0.054000	PLOWT 0.0	FCUT 85.000	RUNPOO 1.000

TIME HISTORY PRINT CONTROL CARDS

STRAIN	TOTAL BEAM	EXT. SPRING	ENERGY	STRESS	ACCEL
FORCES	DEFLECTIONS	DATA	DATA	DATA	DATA
0	0	0	0	0	0

NO. OF MASS POSITION PLOTS EACH TIME= 5 PLOT PRINT FACTOR = 18

PLANE I.D. NO. OF POINTS

2	6
2	6
3	5
2	5
2	5

VEHICLE INITIAL CONDITIONS

VEHICLE TRANSLATIONAL VELOCITIES IN GROUND AXES (IN/SEC)
 VEHICLE ROTATIONAL VELOCITIES IN VEHICLE AXES (RAD/SEC)
 EULER ANGLES OF VEHICLE RELATIVE TO GROUND (RADIAN)

XROOT YROOT ZROOT
 P' Q' R'
 PHI' THETA' PSI'
 0.0 0.0 3.340000 02
 0.0 0.0 0.0
 0.0 1.310000-02 0.0

GENERALIZED SURFACE DATA

BETA = 0.0 DEGREES
 XGIM = 0.0
 JGIN = 0.0

MASS DATA

WEIGHTS MASS COORDINATES F.S., B.L., M.L.

I	M	X''	Y''	Z''
1	1.370000 00	1.350000 02	6.000000 00	-1.600000 01
2	4.380000 00	1.400000 02	6.000000 00	-1.600000 01
3	1.630000 01	1.510000 02	6.000000 00	-1.600000 01
4	6.300000 00	1.630000 02	6.000000 00	-1.600000 01
5	4.930000 00	1.740000 02	6.000000 00	-1.600000 01
6	1.910000 00	1.810000 02	6.000000 00	-1.600000 01
7	1.750000 00	1.350000 02	2.000000 01	-1.600000 01
8	5.580000 00	1.400000 02	2.000000 01	-1.600000 01
9	1.802000 01	1.510000 02	2.000000 01	-1.600000 01
10	8.020000 00	1.630000 02	2.000000 01	-1.600000 01
11	6.280000 00	1.740000 02	2.000000 01	-1.600000 01
12	2.440000 00	1.810000 02	2.000000 01	-1.600000 01
13	4.100000-01	1.350000 02	2.800000 01	9.000000 00
14	2.406000 00	1.400000 02	2.800000 01	9.000000 00
15	1.870000 00	1.510000 02	2.800000 01	9.000000 00
16	1.870000 00	1.630000 02	2.800000 01	9.000000 00
17	2.700000 00	1.740000 02	2.800000 01	9.000000 00
18	1.050000 00	1.810000 02	2.800000 01	9.000000 00
19	2.050000 00	1.400000 02	2.800000 01	3.100000 01
20	2.230000 00	1.510000 02	2.800000 01	3.100000 01
21	2.230000 00	1.630000 02	2.800000 01	3.100000 01
22	2.810000 00	1.740000 02	2.800000 01	3.100000 01
23	1.100000 00	1.810000 02	2.800000 01	3.100000 01
24	2.800000 00	1.400000 02	0.0	4.700000 01
25	4.020000 00	1.510000 02	0.0	4.700000 01
26	4.020000 00	1.630000 02	0.0	4.700000 01
27	3.150000 00	1.740000 02	0.0	4.700000 01
28	1.230000 00	1.810000 02	0.0	4.700000 01
29	2.050000 01	1.660000 02	1.300000 01	-1.700000 00
30	7.296000 01	1.660000 J2	1.300000 01	5.800000 00
31	7.286000 01	1.660000 02	1.300000 01	2.089000 01
32	7.286000 01	1.660000 02	1.300000 01	2.089000 01

MASS MOMENTS OF INERTIA (LB-IN-SEC**2)

I	IX	IY	IZ
1	1.183000-01	8.312000-02	4.999000-02
2	3.782200-01	3.281100-01	2.222000-01
3	4.344000 00	4.400000 00	5.000000-01
4	5.440100-01	5.291000-01	3.767400-01
5	4.257100-01	3.714300-01	2.522700-01
6	1.654000-01	1.261000-01	8.000000-02
7	4.275000-01	3.323000-01	1.277200-01
8	1.350400 00	1.221500 00	7.705000-01
9	5.720000 00	5.680000 00	1.091000 00
10	1.942100 00	1.902330 00	9.616100-01
11	1.540000 00	1.300000 00	6.440300-01
12	5.970000-01	4.899000-01	2.038500-01
13	5.960000-02	6.130000-02	2.730000-03
14	3.079000-01	3.518000-01	5.038000-02
15	2.754200-01	3.266000-01	5.620000-02
16	2.754200-01	3.266000-01	5.620000-02
17	3.463900-01	3.969600-01	4.185300-01
18	1.347100-01	1.444000-01	1.253000-02
19	5.956000-01	2.792000-01	4.770000-01
20	3.627600-01	1.797000-01	3.111300-01
21	3.627600-01	1.797000-01	3.111300-01
22	8.167000-01	3.860000-01	6.564000-01
23	3.185000-01	1.296000-01	2.350000-01
24	4.780000-01	5.880000-02	5.289200-01
25	6.858500-01	1.208400-01	7.958400-01
26	6.858500-01	1.208400-01	7.958400-01
27	5.374200-01	6.704000-02	5.963900-01
28	2.098500-01	1.467000-02	2.211900-01
29	5.950000 00	6.606200 00	3.152000 00
30	1.395110 01	1.477420 01	1.683410 01
31	1.131160 01	1.079890 01	6.531800 00
32	1.131160 01	1.079890 01	6.531800 00

MODE POINT DATA

MASS N.P. MODE POINT COORDINATES F.S.B.L.M.L.

I	M	X	Y	Z
29	1	1.510000 02	6.000000 00	-1.700000 00
29	2	1.740000 02	6.000000 00	-1.700000 00
29	3	1.510000 02	2.000000 01	-1.700000 00
29	4	1.740000 02	2.000000 01	-1.700000 00
29	5	1.660000 02	1.300000 01	-1.700000 00
30	1	1.660000 02	1.300000 01	5.800000 00

EXTERNAL SPRING DATA

SPRING	I	K	M	FR.E LENTH	FRICION COEFFICIENT	BOTTOMING SPRINGS	PLOWING FORCE	GROUND FLEXIBILITY
	I	K	M	LBAR(IKHM)	MU(IKHM)	KE(IKHM)	FORCE(IKHM)	GFLEX(IKHM)
2	3	0	0	8.000000 00	0.0	5.000000 04	0.0	0.0
3	3	0	0	8.000000 00	0.0	5.000000 04	0.0	0.0
4	3	0	0	8.000000 00	0.0	5.000000 04	0.0	0.0
5	3	0	0	8.000000 00	0.0	5.000000 04	0.0	0.0
6	3	0	0	8.000000 00	0.0	5.000000 04	0.0	0.0
8	3	0	0	3.300000 00	0.0	2.000000 04	0.0	0.0
9	3	0	0	3.300000 00	0.0	2.000000 04	0.0	0.0
10	3	0	0	3.300000 00	0.0	2.000000 04	0.0	0.0
11	3	0	0	3.300000 00	0.0	2.000000 04	0.0	0.0
12	3	0	0	3.300000 00	0.0	2.000000 04	0.0	0.0

DEFLECTION COORDINATES

SPRING	I	K	M	SA(IKHM)	SB(IKHM)	SF(IKHM)	FSPDI(IKHM)	FSPDF(IKHM)
2	3	0	0	1.000000-01	1.000000 00	2.500000 00	2.290000 03	2.290000 03
3	3	0	0	1.000000-01	1.000000 00	2.500000 00	2.650000 03	2.650000 03
4	3	0	0	1.000000-01	1.000000 00	2.500000 00	2.650000 03	2.650000 03
5	3	0	0	1.000000-01	1.000000 00	2.500000 00	2.410000 03	2.410000 03
6	3	0	0	1.000000-01	1.000000 00	2.500000 00	1.760000 03	1.760000 03
8	3	0	0	4.500000-02	1.500000-01	1.100000 00	1.380000 03	1.380000 03
9	3	0	0	4.500000-02	1.500000-01	1.100000 00	1.380000 03	1.380000 03
10	3	0	0	4.500000-02	1.500000-01	1.100000 00	1.380000 03	1.380000 03
11	3	0	0	4.500000-02	1.500000-01	1.100000 00	1.380000 03	1.380000 03
12	3	0	0	4.500000-02	1.500000-01	1.100000 00	1.380000 03	1.380000 03

MATERIAL PROPERTIES

MATERIAL NO.	MODULUS OF ELASTICITY	MODULUS OF RIGIDITY	TENSION STRESS	COMPRESS. STRESS	SHEAR STRESS
1	3.00000 07	1.10000 07	75000.	75000.	37500.
2	3.00000 07	1.10000 07	205000.	205000.	80000.
3	2.80000 07	1.25000 07	70000.	46000.	36000.
4	1.05000 07	4.00000 06	47000.	39000.	22000.
5	1.00000 07	3.80000 06	35000.	34000.	17000.
6	1.00000 07	3.80000 06	16000.	16000.	17000.
7	1.00000 06	3.00000 05	16000.	16000.	17000.
8	1.00000 06	0.0	16000.	16000.	17000.
9	1.00000 06	3.00000 05	16000.	16000.	17000.

10 1.00000 06 3.00000 05 16000. 16000. 17000.

INTERNAL BEAM DATA

BEAM	AREA			MOMENTS OF INERTIA			DISTANCES FROM NEUTRAL AXIS TO EXTREME FIBRES			TORSION			DAMPING RATIO	L	P-CODES			BEAM												
	I	J	M	A	Y	Z	Z1	Z2	Z3	XIQ	Y	Z			Y	Z	Y		Z	I	J	M								
1	1	2	0	0	6.1570	-01	4.1820	00	6.0520	-02	4.2430	00	5.7800	00	6.6700	-01	0.0	5.0000	00	4.0000	-02	4	0	0	0	1	2	0	0	0
2	1	2	0	0	6.1570	-01	4.1820	00	6.0520	-02	4.2430	00	5.7800	00	6.6700	-01	0.0	1.1000	01	4.0000	-02	4	0	0	0	2	2	3	0	0
3	3	4	0	0	6.1570	-01	4.1820	00	6.0520	-02	4.2430	00	5.7800	00	6.6700	-01	0.0	1.2000	01	4.0000	-02	4	0	0	0	3	3	4	0	0
4	4	5	0	0	6.1570	-01	4.1820	00	6.0520	-02	4.2430	00	5.7800	00	6.6700	-01	0.0	1.1000	01	4.0000	-02	4	0	0	0	4	4	5	0	0
5	5	6	0	0	6.1570	-01	4.1820	00	6.0520	-02	4.2430	00	5.7800	00	6.6700	-01	0.0	7.0000	00	4.0000	-02	4	0	0	0	5	5	6	0	0
6	7	6	0	0	1.2800	-01	3.4180	-01	4.2670	-02	3.8440	-01	1.6500	00	1.0000	00	0.0	5.0000	00	4.0000	-02	4	0	0	0	6	7	6	0	0
7	6	9	0	0	1.2800	-01	3.4180	-01	4.2670	-02	3.8440	-01	1.6500	00	1.0000	00	0.0	1.1000	01	4.0000	-02	4	0	0	0	7	6	9	0	0
8	9	10	0	0	1.2800	-01	3.4180	-01	4.2670	-02	3.8440	-01	1.6500	00	1.0000	00	0.0	1.2000	01	4.0000	-02	4	0	0	0	8	9	10	0	0
9	10	11	0	0	1.2800	-01	3.4180	-01	4.2670	-02	3.8440	-01	1.6500	00	1.0000	00	0.0	7.0000	00	4.0000	-02	4	0	0	0	10	11	12	0	0
10	11	12	0	0	1.2800	-01	3.4180	-01	4.2670	-02	3.8440	-01	1.6500	00	1.0000	00	0.0	1.2000	01	4.0000	-02	4	0	0	0	11	1	0	0	0
11	1	0	0	0	2.8930	-01	1.8740	00	4.2520	-03	1.6780	00	3.9300	00	5.6400	-01	0.0	1.2000	01	4.0000	-02	4	0	0	0	12	2	0	0	0
12	2	0	0	0	2.8930	-01	1.8740	00	4.2520	-03	1.6780	00	3.9300	00	5.6400	-01	0.0	1.2000	01	4.0000	-02	4	0	0	0	13	3	0	0	0
13	3	0	0	0	2.8930	-01	1.8740	00	4.2520	-03	1.6780	00	3.9300	00	5.6400	-01	0.0	1.2000	01	4.0000	-02	4	0	0	0	14	4	0	0	0
14	4	0	0	0	2.8930	-01	1.8740	00	4.2520	-03	1.6780	00	3.9300	00	5.6400	-01	0.0	1.2000	01	4.0000	-02	4	0	0	0	15	5	0	0	0
15	5	0	0	0	2.8930	-01	1.8740	00	4.2520	-03	1.6780	00	3.9300	00	5.6400	-01	0.0	1.2000	01	4.0000	-02	4	0	0	0	16	6	0	0	0
16	6	0	0	0	2.8930	-01	1.8740	00	4.2520	-03	1.6780	00	3.9300	00	5.6400	-01	0.0	1.4000	01	4.0000	-02	4	0	0	0	17	1	7	0	0
17	1	7	0	0	2.1840	-01	7.7790	-01	4.0930	-03	7.8200	-01	2.8200	00	5.5000	-01	0.0	1.4000	01	4.0000	-02	4	0	0	0	18	2	8	0	0
18	2	8	0	0	2.1840	-01	7.7790	-01	4.0930	-03	7.8200	-01	2.8200	00	5.5000	-01	0.0	1.4000	01	4.0000	-02	4	0	0	0	19	3	9	0	0
19	3	9	0	0	2.1840	-01	7.7790	-01	4.0930	-03	7.8200	-01	2.8200	00	5.5000	-01	0.0	1.4000	01	4.0000	-02	4	0	0	0	20	4	10	0	0
20	4	10	0	0	2.1840	-01	7.7790	-01	4.0930	-03	7.8200	-01	2.8200	00	5.5000	-01	0.0	1.4000	01	4.0000	-02	4	0	0	0	21	5	11	0	0
21	5	11	0	0	2.1840	-01	7.7790	-01	4.0930	-03	7.8200	-01	2.8200	00	5.5000	-01	0.0	1.4000	01	4.0000	-02	4	0	0	0	22	6	12	0	0
22	6	12	0	0	1.1760	-01	3.5510	-03	9.8970	-02	1.0250	-01	1.1500	-01	1.2500	00	0.0	2.6250	01	4.0000	-02	4	0	0	0	23	7	13	0	0
23	7	13	0	0	1.1760	-01	3.5510	-03	9.8970	-02	1.0250	-01	1.1500	-01	1.2500	00	0.0	2.6250	01	4.0000	-02	4	0	0	0	24	8	14	0	0
24	8	14	0	0	1.1760	-01	3.5510	-03	9.8970	-02	1.0250	-01	1.1500	-01	1.2500	00	0.0	2.6250	01	4.0000	-02	4	0	0	0	25	9	15	0	0
25	9	15	0	0	1.1760	-01	3.5510	-03	9.8970	-02	1.0250	-01	1.1500	-01	1.2500	00	0.0	2.6250	01	4.0000	-02	4	0	0	0	26	10	16	0	0
26	10	16	0	0	1.1760	-01	3.5510	-03	9.8970	-02	1.0250	-01	1.1500	-01	1.2500	00	0.0	2.6250	01	4.0000	-02	4	0	0	0	27	11	17	0	0
27	11	17	0	0	4.4780	-01	1.3080	-02	3.0680	-01	3.2170	-01	6.3000	-01	1.2500	00	0.0	2.6250	01	4.0000	-02	4	0	0	0	28	12	18	0	0
28	12	18	0	0	1.1760	-01	3.5510	-03	9.8970	-02	1.0250	-01	1.1500	-01	1.2500	00	0.0	2.2000	01	4.0000	-02	4	0	0	0	29	17	22	0	0
29	17	22	0	0	1.1760	-01	3.5510	-03	9.8970	-02	1.0250	-01	1.1500	-01	1.2500	00	0.0	2.2000	01	4.0000	-02	4	0	0	0	30	18	23	0	0
30	18	23	0	0	1.1760	-01	3.5510	-03	9.8970	-02	1.0250	-01	1.1500	-01	1.2500	00	0.0	3.2250	01	4.0000	-02	4	0	0	0	31	14	19	0	0
31	14	19	0	0	2.4530	-01	3.5650	00	1.9790	-01	3.7630	00	3.0900	00	1.2500	00	0.0	3.2250	01	4.0000	-02	4	0	0	0	32	19	24	0	0
32	19	24	0	0	1.1760	-01	3.5510	-03	9.8970	-02	1.0250	-01	1.1500	-01	1.2500	00	0.0	3.2250	01	4.0000	-02	4	0	0	0	33	20	25	0	0
33	20	25	0	0	1.1760	-01	3.5510	-03	9.8970	-02	1.0250	-01	1.1500	-01	1.2500	00	0.0	3.2250	01	4.0000	-02	4	0	0	0	34	21	26	0	0
34	21	26	0	0	1.1760	-01	3.5510	-03	9.8970	-02	1.0250	-01	1.1500	-01	1.2500	00	0.0	3.2250	01	4.0000	-02	4	0	0	0	35	22	27	0	0
35	22	27	0	0	1.1760	-01	3.5510	-03	9.8970	-02	1.0250	-01	1.1500	-01	1.2500	00	0.0	3.2250	01	4.0000	-02	4	0	0	0	36	23	28	0	0
36	23	28	0	0	1.1760	-01	3.5510	-03	9.8970	-02	1.0250	-01	1.1500	-01	1.2500	00	0.0	3.2250	01	4.0000	-02	4	0	0	0	37	13	14	0	0
37	13	14	0	0	1.1760	-01	3.5510	-03	9.8970	-02	1.0250	-01	1.1500	-01	1.2500	00	0.0	5.0000	00	4.0000	-02	4	0	0	0	38	14	15	0	0
38	14	15	0	0	1.1760	-01	3.5510	-03	9.8970	-02	1.0250	-01	1.1500	-01	1.2500	00	0.0	5.0000	00	4.0000	-02	4	0	0	0	39	15	16	0	0
39	15	16	0	0	1.1760	-01	3.5510	-03	9.8970	-02	1.0250	-01	1.1500	-01	1.2500	00	0.0	1.2000	01	4.0000	-02	4	0	0	0	40	16	17	0	0
40	16	17	0	0	1.1760	-01	3.5510	-03	9.8970	-02	1.0250	-01	1.1500	-01	1.2500	00	0.0	1.1000	01	4.0000	-02	4	0	0	0	41	17	18	0	0
41	17	18	0	0	1.1760	-01	3.5510	-03	9.8970	-02	1.0250	-01	1.1500	-01	1.2500	00	0.0	7.0000	00	4.0000	-02	4	0	0	0	42	17	18	0	0
42	17	18	0	0	3.3010	-01	3.7980	00	1.7740	01	2.1540	01	0.0	0.0	0.0	0.0	0.0	1.1000	01	4.0000	-02	4	0	0	0	43	20	21	0	0
43	20	21	0	0	3.3010	-01	3.7980	00	1.7740	01	2.1540	01	0.0	0.0	0.0	0.0	0.0	1.1000	01	4.0000	-02	4	0	0	0	44	21	22	0	0
44	21	22	0	0	3.3010	-01	3.7980	00	1.7740	01	2.1540	01	0.0	0.0	0.0	0.0	0.0	1.1000	01	4.0000	-02	4	0	0	0	45	22	23	0	0
45	22	23	0	0	3.3010	-01	3.7980	00	1.7740	01	2.1540	01	0.0	0.0	0.0	0.0	0.0	7.0000	00	4.0000	-02	4	0	0	0	46	3	29	0	1
46	3	29	0	1	1.8800	-01	1.8000	-01	5.4000	-01	7.2000	-01	6.0000	-02	6.0000	-02	0.0	1.4300	01	4.0000	-02	4	0	0	0	47	5	29	0	2
47	5	29	0	2	1.8800	-01	1.8000	-01	5.4000	-01	7.2000	-01	6.0000	-02	6.0000	-02	0.0	1.4300	01	4.0000	-02	4	0	0	0	48	9	29	0	3
48	9	29	0	3	1.8800	-01	1.8000	-01	5.4000	-01	7.2000	-01	6.0000	-02	6.0000	-02	0.0	1.4300	01	4.0000	-02	4	0	0	0	49	11	29	0	4
49	11	29	0	4	1.8800	-01	1.8000	-01	5.4000	-01	7.2000	-01	6.0000	-02	6.0000	-02	0.0	1.4300	01	4.0000	-02	4	0	0	0					

1.5090 01 4.1000-01 4 0 0 0 0 50 30 31 0 0
 1.5090 01 3.111D-0110 0 0 0 0 0 51 30 32 0 0
 2.425D 01 4.0000-02 4 0 0 0 0 52 5 30 0 0
 2.425D 01 4.0000-02 4 0 0 0 0 53 11 30 0 0
 7.500D 00 4.0000-02 4 0 0 0 0 54 29 30 0 0
 7.500D 00 4.0000-02 4 0 0 0 0 55 29 30 5 1
 5.600D 01 4.0000-02 1 0 0 0 0 56 14 0 0 0
 5.600D 01 4.0000-02 1 0 0 0 0 57 18 0 0 0

0.0
 0.0
 0.0
 0.0
 0.0
 0.0
 0.0

0.0
 0.0
 0.0
 0.0
 0.0
 0.0
 0.0

0.0
 0.0
 0.0
 0.0
 0.0
 0.0
 0.0

0.0
 0.0
 0.0
 0.0
 0.0
 0.0
 0.0

UNSYMMETRICAL BEAM DATA

BEAM	TENSION-COMPRESSION FLAG	DEADBAND
IJ I J M N	IJUB	DB
52 5 30 0 0	1	0.0
53 11 30 0 0	1	0.0
54 29 30 0 0	-1	0.0
55 29 30 5 1	-1	0.0
56 14 0 0 0	1	0.0
57 18 0 0 0	1	0.0

NONLINEAR BEAM DATA

BEAM	DIRECTION	STANDARD TABLE NO.	LINEAR DEFLECTION	BOTTOMING DEFLECTION
IJ I J M N	L	NP	LDP	LDP1
54 29 30 0 0	1	8	7.5000E-01	0.0
55 29 30 5 1	1	10	0.0	0.0
31 14 19 0 0	1	5	8.2000E-02	0.0
31 14 19 0 0	2	5	4.8000E-01	0.0
31 14 19 0 0	3	5	1.9400E-01	0.0
29 17 22 0 0	1	5	5.4000E-02	0.0
29 17 22 0 0	2	5	4.8000E-01	0.0
29 17 22 0 0	3	5	5.2000E 00	0.0
30 18 23 0 0	1	5	5.4000E-02	0.0
30 18 23 0 0	2	5	4.8000E-01	0.0
30 18 23 0 0	3	5	5.2000E 00	0.0
32 19 24 0 0	1	5	3.7000E-02	0.0
32 19 24 0 0	2	5	1.0300E 00	0.0
32 19 24 0 0	3	5	1.0300E 00	0.0
33 20 25 0 0	1	5	3.7000E-02	0.0
33 20 25 0 0	2	5	1.0300E 00	0.0
33 20 25 0 0	3	5	1.0300E 00	0.0
34 21 26 0 0	1	5	3.7000E-02	0.0
34 21 26 0 0	2	5	1.0300E 00	0.0
34 21 26 0 0	3	5	1.0300E 00	0.0
35 22 27 0 0	1	5	3.7000E-02	0.0
35 22 27 0 0	2	5	1.0300E 00	0.0
35 22 27 0 0	3	5	1.0300E 00	0.0
36 23 28 0 0	1	5	3.7000E-02	0.0
36 23 28 0 0	2	5	1.0300E 00	0.0
36 23 28 0 0	3	5	1.0300E 00	0.0
23 7 13 0 0	1	5	4.5000E-02	0.0

23	7	13	0	0	2	5	6.82000E-01	0.0
23	7	13	0	0	3	5	1.28700E 00	0.0
24	8	14	0	0	1	5	4.50000E-02	0.0
24	8	14	0	0	2	5	6.82000E-01	0.0
24	8	14	0	0	3	5	1.28700E 00	0.0
25	9	15	0	0	1	5	4.50000E-02	0.0
25	9	15	0	0	2	5	6.82000E-01	0.0
25	9	15	0	0	3	5	1.28700E 00	0.0
26	10	16	0	0	1	5	4.50000E-02	0.0
26	10	16	0	0	2	5	6.82000E-01	0.0
26	10	16	0	0	3	5	1.28700E 00	0.0
27	11	17	0	0	1	5	4.50000E-02	0.0
27	11	17	0	0	2	5	6.82000E-01	0.0
27	11	17	0	0	3	5	1.28700E 00	0.0
28	12	18	0	0	1	5	4.50000E-02	0.0
28	12	18	0	0	2	5	6.82000E-01	0.0
28	12	18	0	0	3	5	1.28700E 00	0.0

KR TABLE FOR I,J,M,N,L = 29 30 0 0 1

1	0.0	1.00000E 00
2	7.50000E-01	1.00000E 00
3	7.50750E-01	-1.00000E 00
4	1.50000E 00	-1.00000E 00
5	1.50075E 00	0.0
6	7.50000E 00	0.0
7	1.12500E 01	0.0
8	1.50000E 01	0.0

KR TABLE FOR I,J,M,N,L = 29 30 5 1 1

1	0.0	3.00000E-03
2	7.50000E-01	3.00000E-03
3	7.51000E-01	1.00000E 00
4	3.50000E 00	1.00000E 00
5	3.51000E 00	0.0
6	4.00000E 00	0.0
7	5.00000E 00	0.0
8	6.00000E 00	0.0
9	7.00000E 00	0.0
10	2.00000E 01	0.0

KR TABLE FOR I,J,M,N,L = 14 19 0 0 1

1	0.0	1.00000E 00
2	8.20000E-02	1.00000E 00
3	8.20819E-02	0.0
4	8.20000E-01	0.0
5	1.64000E 00	0.0

KR TABLE FOR I,J,M,N,L = 14 19 0 0 2

1	0.0	1.00000E 00
2	4.80000E-01	1.00000E 00
3	4.80430E-01	0.0
4	4.80000E 00	0.0
5	9.60000E 00	0.0

KR TABLE FOR I,J,M,N,L = 14 19 0 0 3

1	0.0	1.00000E 00
2	1.94000E-01	1.00000E 00
3	1.94194E-01	0.0
4	1.94000E 00	0.0
5	3.88000E 00	0.0

KR TABLE FOR I,J,M,N,L = 17 22 0 0 1

1	0.0	1.00000E 00
2	5.40000E-02	1.00000E 00
3	5.40540E-02	0.0
4	5.40000E-01	0.0
5	1.08000E 00	0.0

KR TABLE FOR I,J,M,N,L = 17 22 0 0 2

1	0.0	1.00000E 00
2	4.80000E-01	1.00000E 00
3	4.80480E-01	0.0
4	4.80000E 00	0.0
5	9.60000E 00	0.0

KR TABLE FOR I,J,M,N,L = 17 22 0 0 3

1	0.0	1.00000E 00
2	5.20000E 00	1.00000E 00
3	5.20520E 00	0.0
4	5.20000E 01	0.0
5	1.04000E 02	0.0

KR TABLE FOR I,J,M,N,L = 18 23 0 0 1

1	0.0	1.00000E 00
2	5.40000E-02	1.00000E 00
3	5.40540E-02	0.0
4	5.40000E-01	0.0
5	1.08000E 00	0.0

KR TABLE FOR I,J,M,N,L = 18 23 0 0 2

1	0.0	1.00000E 00
2	4.80000E-01	1.00000E 00
3	4.80480E-01	0.0
4	4.80000E 00	0.0
5	9.60000E 00	0.0

KR TABLE FOR I,J,M,N,L = 18 23 0 0 3

1	0.0	1.00000E 00
2	5.20000E 00	1.00000E 00
3	5.20520E 00	0.0
4	5.20000E 01	0.0
5	1.04000E 02	0.0

KR TABLE FOR I,J,M,N,L = 19 24 0 0 1

1	0.0	1.00000E 00
2	3.70000E-02	1.00000E 00
3	3.70370E-02	0.0
4	3.70000E-01	0.0
5	7.40000E-01	0.0

KR TABLE FOR I,J,M,N,L = 19 24 0 0 2

1	0.0	1.00000E 00
2	1.03000E 00	1.00000E 00
3	1.03103E 00	0.0
4	1.03000E 01	0.0
5	2.06000E 01	0.0

KR TABLE FOR I,J,M,N,L = 19 24 0 0 3

1	0.0	1.00000E 00
2	1.03000E 00	1.00000E 00
3	1.03103E 00	0.0

4 1.03000E 01 0.0
5 2.06000E 01 0.0

KR TABLE FOR I,J,M,N,L = 20 25 0 0 1

1 0.0 1.00000E 00
2 3.70000E-02 1.00000E 00
3 3.70370E-02 0.0
4 3.70000E-01 0.0
5 7.40000E-01 0.0

KR TABLE FOR I,J,M,N,L = 20 25 0 0 2

1 0.0 1.00000E 00
2 1.03000E 00 1.00000E 00
3 1.03103E 00 0.0
4 1.03000E 01 0.0
5 2.06000E 01 0.0

KR TABLE FOR I,J,M,N,L = 20 25 0 0 3

1 0.0 1.00000E 00
2 1.03000E 00 1.00000E 00
3 1.03103E 00 0.0
4 1.03000E 01 0.0
5 2.06000E 01 0.0

KR TABLE FOR I,J,M,N,L = 21 26 0 0 1

1 0.0 1.00000E 00
2 3.70000E-02 1.00000E 00
3 3.70370E-02 0.0
4 3.70000E-01 0.0
5 7.40000E-01 0.0

KR TABLE FOR I,J,M,N,L = 21 26 0 0 2

1 0.0 1.00000E 00
2 1.03000E 00 1.00000E 00
3 1.03103E 00 0.0
4 1.03000E 01 0.0
5 2.06000E 01 0.0

KR TABLE FOR I,J,M,N,L = 21 26 0 0 3

1 0.0 1.00000E 00
2 1.03000E 00 1.00000E 00
3 1.03103E 00 0.0
4 1.03000E 01 0.0
5 2.06000E 01 0.0

KR TABLE FOR I,J,M,N,L = 22 27 0 0 1

1 0.0 1.00000E 00
2 3.70000E-02 1.00000E 00
3 3.70370E-02 0.0
4 3.70000E-01 0.0
5 7.40000E-01 0.0

KR TABLE FOR I,J,M,N,L = 22 27 0 0 2

1 0.0 1.00000E 00
2 1.03000E 00 1.00000E 00
3 1.03103E 00 0.0
4 1.03000E 01 0.0
5 2.06000E 01 0.0

KR TABLE FOR I,J,M,N,L = 22 27 0 0 3

1 0.0 1.00000E 00
2 1.03000E 00 1.00000E 00
3 1.03103E 00 0.0
4 1.03000E 01 0.0
5 2.06000E 01 0.0

1 0.0 1.00000E 00
 2 1.03000E 00 1.00000E 00
 3 1.03103E 00 0.0
 4 1.03000E 01 0.0
 5 2.06000E 01 0.0

KR TABLE FOR I,J,M,N,L = 23 28 0 0 1
 1 0.0 1.00000E 00
 2 3.70000E-02 1.00000E 00
 3 3.70370E-02 0.0
 4 3.70000E-01 0.0
 5 7.40000E-01 0.0

KR TABLE FOR I,J,M,N,L = 23 28 0 0 2
 1 0.0 1.00000E 00
 2 1.03000E 00 1.00000E 00
 3 1.03103E 00 0.0
 4 1.03000E 01 0.0
 5 2.06000E 01 0.0

KR TABLE FOR I,J,M,N,L = 23 28 0 0 3
 1 0.0 1.00000E 00
 2 1.03000E 00 1.00000E 00
 3 1.03103E 00 0.0
 4 1.03000E 01 0.0
 5 2.06000E 01 0.0

KR TABLE FOR I,J,M,N,L = 7 13 0 0 1
 1 0.0 1.00000E 00
 2 4.00000E-02 1.00000E 00
 3 4.0450E-02 0.0
 4 4.00000E-01 0.0
 5 9.00000E-01 0.0

KR TABLE FOR I,J,M,N,L = 7 13 0 0 2
 1 0.0 1.00000E 00
 2 6.82000E-01 1.00000E 00
 3 6.82682E-01 0.0
 4 6.82000E 00 0.0
 5 1.36400E 01 0.0

KR TABLE FOR I,J,M,N,L = 7 13 0 0 3
 1 0.0 1.00000E 00
 2 1.26700E 00 1.00000E 00
 3 1.26829E 00 0.0
 4 1.26700E 01 0.0
 5 2.57400E 01 0.0

KR TABLE FOR I,J,M,N,L = 8 14 0 0 1
 1 0.0 1.00000E 00
 2 4.50000E-02 1.00000E 00
 3 4.50450E-02 0.0
 4 4.50000E-01 0.0
 5 9.00000E-01 0.0

KR TABLE FOR I,J,M,N,L = 8 14 0 0 2
 1 0.0 1.00000E 00
 2 6.82000E-01 1.00000E 00
 3 6.82682E-01 0.0
 4 1.36400E 01 0.0

5 1.36400E 01 0.0
 KR TABLE FOR I,J,M,N,L = 8 14 0 0 3

1 0.0 1.00000E 00
 2 1.26700E 00 1.00000E 00
 3 1.26829E 00 0.0
 4 1.26700E 01 0.0
 5 2.57400E 01 0.0

KR TABLE FOR I,J,M,N,L = 9 15 0 0 1

1 0.0 1.00000E 00
 2 4.50000E-02 1.00000E 00
 3 4.50450E-02 0.0
 4 4.50000E-01 0.0
 5 9.00000E-01 0.0

KR TABLE FOR I,J,M,N,L = 9 15 0 0 2

1 0.0 1.00000E 00
 2 6.82000E-01 1.00000E 00
 3 6.82682E-01 0.0
 4 6.82000E 00 0.0
 5 1.36400E 01 0.0

KR TABLE FOR I,J,M,N,L = 9 15 0 0 3

1 0.0 1.00000E 00
 2 1.26700E 00 1.00000E 00
 3 1.26829E 00 0.0
 4 1.26700E 01 0.0
 5 2.57400E 01 0.0

KR TABLE FOR I,J,M,N,L = 10 16 0 0 1

1 0.0 1.00000E 00
 2 4.50000E-02 1.00000E 00
 3 4.50450E-02 0.0
 4 4.50000E-01 0.0
 5 9.00000E-01 0.0

KR TABLE FOR I,J,M,N,L = 10 16 0 0 2

1 0.0 1.00000E 00
 2 6.82000E-01 1.00000E 00
 3 6.82682E-01 0.0
 4 6.82000E 00 0.0
 5 1.36400E 01 0.0

KR TABLE FOR I,J,M,N,L = 10 16 0 0 3

1 0.0 1.00000E 00
 2 1.26700E 00 1.00000E 00
 3 1.26829E 00 0.0
 4 1.26700E 01 0.0
 5 2.57400E 01 0.0

KR TABLE FOR I,J,M,N,L = 11 17 0 0 1

1 0.0 1.00000E 00
 2 4.50000E-02 1.00000E 00
 3 4.50450E-02 0.0
 4 4.50000E-01 0.0
 5 9.00000E-01 0.0

KR TABLE FOR I,J,M,N,L = 11 17 0 0 2

1 0.0 1.00000E 00

0.0	3.049500 05	0.0	1.414270 06	0.0	1.829750 06	0.0	0.0
0.0	0.0	0.0	0.0	0.0	0.0	0.0	0.0
0.0	1.829750 06	0.0	0.0	0.0	1.463000 07	0.0	2.118240 05
0.0	-2.647790 04	0.0	0.0	0.0	0.0	0.0	0.0
4 5 0 0							
5.876890 05	0.0	0.0	0.0	0.0	0.0	0.0	0.0
0.0	5.729260 03	0.0	0.0	0.0	0.0	0.0	-3.151090 04
0.0	0.0	0.0	0.0	0.0	0.0	0.0	0.0
0.0	3.959180 05	0.0	1.542840 06	0.0	2.177550 06	0.0	0.0
0.0	0.0	0.0	0.0	0.0	0.0	0.0	0.0
0.0	2.177550 06	0.0	0.0	0.0	1.596870 07	0.0	0.0
0.0	0.0	0.0	0.0	0.0	0.0	0.0	2.310800 05
5 6 0 0							
9.235110 05	0.0	0.0	0.0	0.0	0.0	0.0	0.0
0.0	2.223220 04	0.0	0.0	0.0	0.0	0.0	-7.781270 04
0.0	0.0	0.0	0.0	0.0	5.377220 06	0.0	0.0
0.0	0.0	0.0	2.424460 06	0.0	0.0	0.0	0.0
0.0	5.377220 06	0.0	0.0	0.0	2.509370 07	0.0	0.0
0.0	0.0	0.0	0.0	0.0	0.0	0.0	3.631260 05
7 8 0 0							
2.688000 05	0.0	0.0	0.0	0.0	0.0	0.0	0.0
0.0	4.300630 04	0.0	0.0	0.0	0.0	0.0	-1.075210 05
0.0	0.0	0.0	0.0	0.0	8.612350 05	0.0	0.0
0.0	0.0	0.0	3.075420 05	0.0	0.0	0.0	0.0
0.0	0.0	0.0	0.0	0.0	2.870780 06	0.0	0.0
0.0	0.0	0.0	0.0	0.0	0.0	0.0	3.584030 05
0.0	-1.075210 05	0.0	0.0	0.0	0.0	0.0	0.0
6 9 0 0							
1.221820 05	0.0	0.0	0.0	0.0	0.0	0.0	0.0
0.0	4.039100 03	0.0	0.0	0.0	0.0	0.0	-2.221500 04
0.0	0.0	0.0	0.0	0.0	1.779410 05	0.0	0.0
0.0	0.0	0.0	1.397920 05	0.0	0.0	0.0	0.0
0.0	0.0	0.0	0.0	0.0	1.304900 06	0.0	0.0
0.0	-2.221500 04	0.0	0.0	0.0	0.0	0.0	1.629100 05
9 10 0 0							
1.120000 05	0.0	0.0	0.0	0.0	0.0	0.0	0.0
0.0	3.111140 03	0.0	0.0	0.0	0.0	0.0	-1.866680 04
0.0	0.0	0.0	0.0	0.0	1.495200 05	0.0	0.0
0.0	0.0	0.0	1.281420 05	0.0	0.0	0.0	0.0
0.0	0.0	0.0	0.0	0.0	1.196160 06	0.0	0.0
0.0	-1.866680 04	0.0	0.0	0.0	0.0	0.0	1.493350 05
10 11 0 0							
1.221820 05	0.0	0.0	0.0	0.0	0.0	0.0	0.0
0.0	4.039100 03	0.0	0.0	0.0	0.0	0.0	-2.221500 04
0.0	0.0	0.0	0.0	0.0	1.779410 05	0.0	0.0
0.0	0.0	0.0	1.397920 05	0.0	0.0	0.0	0.0
0.0	0.0	0.0	0.0	0.0	1.304900 06	0.0	0.0
0.0	-2.221500 04	0.0	0.0	0.0	0.0	0.0	1.629100 05
11 12 0 0							
1.920000 05	0.0	0.0	0.0	0.0	0.0	0.0	0.0
0.0	1.567360 04	0.0	0.0	0.0	0.0	0.0	-5.485760 04
0.0	0.0	0.0	0.0	0.0	4.394060 05	0.0	0.0
0.0	0.0	0.0	2.196730 05	0.0	0.0	0.0	0.0
0.0	0.0	0.0	0.0	0.0	2.050560 06	0.0	0.0
0.0	-5.485760 04	0.0	0.0	0.0	0.0	0.0	2.560020 05
1 0 0 0							
2.531200 05	0.0	0.0	0.0	0.0	0.0	0.0	0.0
0.0	3.100200 02	0.0	0.0	0.0	0.0	0.0	-1.860120 03
0.0	0.0	0.0	0.0	0.0	8.198750 05	0.0	0.0
0.0	0.0	0.0	6.260840 05	0.0	0.0	0.0	0.0
0.0	0.0	0.0	0.0	0.0	6.559000 06	0.0	0.0
0.0	0.0	0.0	0.0	0.0	0.0	0.0	1.488100 04
0.0	-1.860120 03	0.0	0.0	0.0	0.0	0.0	0.0

AD-A069 171

LOCKHEED-CALIFORNIA CO BURBANK

F/G 1/3

SUMMARY OF RESULTS FOR A TWIN-ENGINE, LOW-WING AIRPLANE SUBSTRU--ETC(U)

JAN 79 G WITTLIN

DOT-FA75WA-3707

UNCLASSIFIED

LR-28869

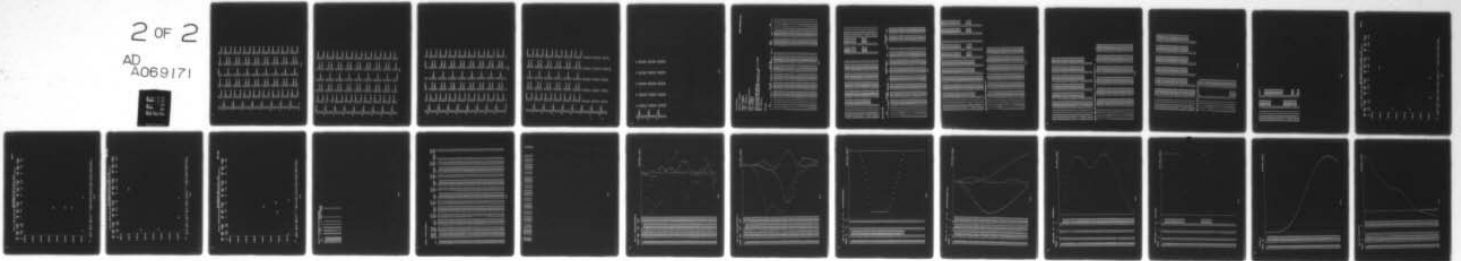
FAA-RD-79-13

NL

2 OF 2

AD
A069171

7E
1/79



END

DATE
FILMED

7-79

DDC

0.0	0.0	0.0	2.234290 05	0.0	0.0	0.0	0.0	0.0	0.0
0.0	0.0	2.500430 05	0.0	2.333730 06	0.0	0.0	0.0	0.0	0.0
5 11 0 0	-1.315640 03	0.0	0.0	0.0	0.0	0.0	0.0	1.227930 04	0.0
1.638230 05	0.0	0.0	0.0	0.0	0.0	0.0	0.0	0.0	0.0
0.0	1.879480 02	0.0	0.0	0.0	0.0	0.0	0.0	-1.315640 03	0.0
0.0	0.0	3.572040 04	0.0	2.500430 05	0.0	0.0	0.0	0.0	0.0
0.0	0.0	0.0	2.234290 05	0.0	0.0	0.0	0.0	0.0	0.0
0.0	0.0	2.500430 05	0.0	2.333730 06	0.0	0.0	0.0	0.0	0.0
0.0	-1.315640 03	0.0	0.0	0.0	0.0	0.0	0.0	1.227930 04	0.0
6 12 0 0	0.0	0.0	0.0	0.0	0.0	0.0	0.0	0.0	0.0
1.638230 05	0.0	0.0	0.0	0.0	0.0	0.0	0.0	0.0	0.0
0.0	1.879480 02	0.0	0.0	0.0	0.0	0.0	0.0	-1.315640 03	0.0
0.0	0.0	3.572040 04	0.0	2.500430 05	0.0	0.0	0.0	0.0	0.0
0.0	0.0	0.0	2.234290 05	0.0	0.0	0.0	0.0	0.0	0.0
0.0	0.0	2.500430 05	0.0	2.333730 06	0.0	0.0	0.0	0.0	0.0
0.0	-1.315640 03	0.0	0.0	0.0	0.0	0.0	0.0	1.227930 04	0.0
7 13 0 0	0.0	0.0	0.0	0.0	0.0	0.0	0.0	0.0	0.0
4.705410 04	0.0	0.0	0.0	0.0	0.0	0.0	0.0	0.0	0.0
0.0	6.895450 02	0.0	0.0	0.0	0.0	0.0	0.0	-9.049870 03	0.0
0.0	0.0	2.473960 01	0.0	3.246920 02	0.0	0.0	0.0	0.0	0.0
0.0	0.0	0.0	1.562360 04	0.0	0.0	0.0	0.0	0.0	0.0
0.0	0.0	3.246920 02	0.0	5.681860 03	0.0	0.0	0.0	0.0	0.0
0.0	-9.049870 03	0.0	0.0	0.0	0.0	0.0	0.0	1.583660 05	0.0
8 14 0 0	0.0	0.0	0.0	0.0	0.0	0.0	0.0	0.0	0.0
4.705410 04	0.0	0.0	0.0	0.0	0.0	0.0	0.0	0.0	0.0
0.0	6.895450 02	0.0	0.0	0.0	0.0	0.0	0.0	-9.049870 03	0.0
0.0	0.0	2.473960 01	0.0	3.246920 02	0.0	0.0	0.0	0.0	0.0
0.0	0.0	0.0	1.562360 04	0.0	0.0	0.0	0.0	0.0	0.0
0.0	0.0	3.246920 02	0.0	5.681860 03	0.0	0.0	0.0	0.0	0.0
0.0	-9.049870 03	0.0	0.0	0.0	0.0	0.0	0.0	1.583660 05	0.0
9 15 0 0	0.0	0.0	0.0	0.0	0.0	0.0	0.0	0.0	0.0
4.705410 04	0.0	0.0	0.0	0.0	0.0	0.0	0.0	0.0	0.0
0.0	6.895450 02	0.0	0.0	0.0	0.0	0.0	0.0	-9.049870 03	0.0
0.0	0.0	2.473960 01	0.0	3.246920 02	0.0	0.0	0.0	0.0	0.0
0.0	0.0	0.0	1.562360 04	0.0	0.0	0.0	0.0	0.0	0.0
0.0	0.0	3.246920 02	0.0	5.681860 03	0.0	0.0	0.0	0.0	0.0
0.0	-9.049870 03	0.0	0.0	0.0	0.0	0.0	0.0	1.583660 05	0.0
10 16 0 0	0.0	0.0	0.0	0.0	0.0	0.0	0.0	0.0	0.0
4.705410 04	0.0	0.0	0.0	0.0	0.0	0.0	0.0	0.0	0.0
0.0	6.895450 02	0.0	0.0	0.0	0.0	0.0	0.0	-9.049870 03	0.0
0.0	0.0	2.473960 01	0.0	3.246920 02	0.0	0.0	0.0	0.0	0.0
0.0	0.0	0.0	1.562360 04	0.0	0.0	0.0	0.0	0.0	0.0
0.0	0.0	3.246920 02	0.0	5.681860 03	0.0	0.0	0.0	0.0	0.0
0.0	-9.049870 03	0.0	0.0	0.0	0.0	0.0	0.0	1.583660 05	0.0
11 17 0 0	0.0	0.0	0.0	0.0	0.0	0.0	0.0	0.0	0.0
1.791120 05	0.0	0.0	0.0	0.0	0.0	0.0	0.0	0.0	0.0
0.0	2.150170 03	0.0	0.0	0.0	0.0	0.0	0.0	-2.821970 04	0.0
0.0	0.0	9.110660 01	0.0	1.195720 03	0.0	0.0	0.0	0.0	0.0
0.0	0.0	0.0	4.902350 04	0.0	0.0	0.0	0.0	0.0	0.0
0.0	0.0	1.195720 03	0.0	2.092410 04	0.0	0.0	0.0	0.0	0.0
0.0	-2.821970 04	0.0	0.0	0.0	0.0	0.0	0.0	4.938220 05	0.0
12 18 0 0	0.0	0.0	0.0	0.0	0.0	0.0	0.0	0.0	0.0
4.705410 04	0.0	0.0	0.0	0.0	0.0	0.0	0.0	0.0	0.0
0.0	6.895450 02	0.0	0.0	0.0	0.0	0.0	0.0	-9.049870 03	0.0
0.0	0.0	2.473960 01	0.0	3.246920 02	0.0	0.0	0.0	0.0	0.0
0.0	0.0	0.0	1.562360 04	0.0	0.0	0.0	0.0	0.0	0.0
0.0	0.0	3.246920 02	0.0	5.681860 03	0.0	0.0	0.0	0.0	0.0
0.0	-9.049870 03	0.0	0.0	0.0	0.0	0.0	0.0	1.583660 05	0.0
17 22 0 0	0.0	0.0	0.0	0.0	0.0	0.0	0.0	0.0	0.0

0.0	0.0	2.04061D 04	0.0	9.49536D 04	0.0
0.0	-1.07274D 06	0.0	0.0	0.0	3.57500D 06
14 15 0 0					
1.50465D 05	0.0	0.0	0.0	0.0	0.0
0.0	4.02903D 04	0.0	0.0	0.0	-2.21641D 05
0.0	0.0	1.07010D 03	0.0	5.68555D 03	0.0
0.0	0.0	0.0	1.50907D 05	0.0	0.0
0.0	0.0	5.68555D 03	0.0	4.31607D 04	0.0
0.0	-2.21641D 05	0.0	0.0	0.0	1.62537D 06
15 16 0 0					
1.37926D 05	0.0	0.0	0.0	0.0	0.0
0.0	3.10400D 04	0.0	0.0	0.0	-1.66240D 05
0.0	0.0	8.24250D 02	0.0	4.94550D 03	0.0
0.0	0.0	0.0	1.45665D 05	0.0	0.0
0.0	0.0	4.94550D 03	0.0	3.95640D 04	0.0
0.0	-1.66240D 05	0.0	0.0	0.0	1.48992D 06
16 17 0 0					
1.50465D 05	0.0	0.0	0.0	0.0	0.0
0.0	4.02903D 04	0.0	0.0	0.0	-2.21641D 05
0.0	0.0	1.07010D 03	0.0	5.68555D 03	0.0
0.0	0.0	0.0	1.50907D 05	0.0	0.0
0.0	0.0	5.68555D 03	0.0	4.31607D 04	0.0
0.0	-2.21641D 05	0.0	0.0	0.0	1.62537D 06
17 18 0 0					
2.36445D 05	0.0	0.0	0.0	0.0	0.0
0.0	1.56376D 05	0.0	0.0	0.0	-5.47317D 05
0.0	0.0	4.15249D 03	0.0	1.45337D 04	0.0
0.0	0.0	0.0	2.49711D 05	0.0	0.0
0.0	0.0	1.45337D 04	0.0	6.78240D 04	0.0
0.0	-5.47317D 05	0.0	0.0	0.0	2.55415D 06
19 20 0 0					
3.15115D 05	0.0	0.0	0.0	0.0	0.0
0.0	1.67943D 06	0.0	0.0	0.0	-9.23666D 05
0.0	0.0	3.59553D 05	0.0	1.97754D 06	0.0
0.0	0.0	0.0	7.83228D 06	0.0	0.0
0.0	0.0	1.97754D 06	0.0	1.45020D 07	0.0
0.0	-9.23666D 06	0.0	0.0	0.0	6.77370D 07
20 21 0 0					
2.6855D 05	0.0	0.0	0.0	0.0	0.0
0.0	1.29359D 06	0.0	0.0	0.0	-7.76153D 06
0.0	0.0	2.76947D 05	0.0	1.66168D 06	0.0
0.0	0.0	0.0	7.17959D 06	0.0	0.0
0.0	0.0	1.66168D 06	0.0	1.32935D 07	0.0
0.0	-7.76153D 06	0.0	0.0	0.0	6.20922D 07
21 22 0 0					
3.15115D 05	0.0	0.0	0.0	0.0	0.0
0.0	1.67943D 06	0.0	0.0	0.0	-9.23666D 06
0.0	0.0	3.59553D 05	0.0	1.97754D 06	0.0
0.0	0.0	0.0	7.83228D 06	0.0	0.0
0.0	0.0	1.97754D 06	0.0	1.45020D 07	0.0
0.0	-9.23666D 06	0.0	0.0	0.0	6.77370D 07
22 23 0 0					
4.95180D 05	0.0	0.0	0.0	0.0	0.0
0.0	6.51697D 06	0.0	0.0	0.0	-2.28094D 07
0.0	0.0	1.39523D 06	0.0	4.88331D 06	0.0
0.0	0.0	0.0	1.23079D 07	0.0	0.0
0.0	0.0	4.88331D 06	0.0	2.27888D 07	0.0
0.0	-2.28094D 07	0.0	0.0	0.0	1.06444D 08
3 29 0 1					
1.31779D 05	0.0	0.0	0.0	0.0	0.0

MODEL PARAMETERS

VEHICLE MT = 5.4366000 02

VEHICLE CG POSITION

X (FS) = 1.625600 02

Y (BL) = 0.0

Z (ML) = 5.322050 00

VEHICLE INERTIAS (IN-LB-SEC**2)

I(XX) = 0.150260 02

I(YZ) = 6.063550 02

I(ZZ) = 5.139550 02

VEHICLE CG INITIAL GROUND COORDINATES

XCG IS THE DISTANCE FROM SLOPE/GROUND INTERSECTION TO VEHICLE CG, +FORWARD

ZCG IS THE DISTANCE FROM GROUND PLANE TO VEHICLE CG, +DOWN

XCG = 0.0

ZCG = -2.956210 01

BEAM LOADS

BEAM		M		N		BUCKLING		AXIAL LOAD		COMPRESSION		SHEAR FORCE		ROLL(X)		MOMENT		YAM(Z)		BEAM			
I	J	I	J	I	J	I	J	TENSION	LATERAL(Y)	VERTICAL(Z)	COMPRESSION	LATERAL(Y)	VERTICAL(Z)	ROLL(X)	PITCH(Y)	I	J	I	J	I	J	M	M
1	1	2	0	0	0	1	00350 06	2.89370 04	2.40110 04	9.07500 03	2.40110 04	9.07500 03	9.07500 03	0.0	2.82200 04	3.53870 03	1	1	2	0	0	0	
2	2	3	0	0	0	2	07330 05	2.89370 04	2.40110 04	9.07500 03	2.40110 04	9.07500 03	9.07500 03	0.0	2.82200 04	3.53870 03	2	2	3	0	0	0	
3	3	4	0	0	0	1	74220 05	2.89370 04	2.40110 04	9.07500 03	2.40110 04	9.07500 03	9.07500 03	0.0	2.82200 04	3.53870 03	3	3	4	0	0	0	
4	4	5	0	0	0	2	07330 05	2.89370 04	2.40110 04	9.07500 03	2.40110 04	9.07500 03	9.07500 03	0.0	2.82200 04	3.53870 03	4	4	5	0	0	0	
5	5	6	0	0	0	5	11990 05	2.89370 04	2.40110 04	9.07500 03	2.40110 04	9.07500 03	9.07500 03	0.0	2.82200 04	3.53870 03	5	5	6	0	0	0	
6	7	6	0	0	0	7	07460 05	6.01600 03	4.99200 03	1.88670 03	4.99200 03	1.88670 03	1.88670 03	0.0	8.07800 03	1.66400 03	6	7	6	0	0	0	
7	8	9	0	0	0	1	46170 05	6.01600 03	4.99200 03	1.88670 03	4.99200 03	1.88670 03	1.88670 03	0.0	8.07800 03	1.66400 03	7	8	9	0	0	0	
8	9	10	0	0	0	1	22820 05	6.01600 03	4.99200 03	1.88670 03	4.99200 03	1.88670 03	1.88670 03	0.0	8.07800 03	1.66400 03	8	9	10	0	0	0	
9	10	11	0	0	0	1	46170 05	6.01600 03	4.99200 03	1.88670 03	4.99200 03	1.88670 03	1.88670 03	0.0	8.07800 03	1.66400 03	9	10	11	0	0	0	
10	11	12	0	0	0	3	60950 05	6.01600 03	4.99200 03	1.88670 03	4.99200 03	1.88670 03	1.88670 03	0.0	8.07800 03	1.66400 03	10	11	12	0	0	0	
11	1	0	0	0	0	1	22390 04	1.35960 04	1.12820 04	4.26400 03	1.12820 04	4.26400 03	4.26400 03	0.0	1.85970 04	2.94000 02	11	1	0	0	0	0	
12	2	0	0	0	0	1	22390 04	1.35960 04	1.12820 04	4.26400 03	1.12820 04	4.26400 03	4.26400 03	0.0	1.85970 04	2.94000 02	12	2	0	0	0	0	
13	3	0	0	0	0	1	22390 04	1.35960 04	1.12820 04	4.26400 03	1.12820 04	4.26400 03	4.26400 03	0.0	1.85970 04	2.94000 02	13	3	0	0	0	0	
14	4	0	0	0	0	1	22390 04	1.35960 04	1.12820 04	4.26400 03	1.12820 04	4.26400 03	4.26400 03	0.0	1.85970 04	2.94000 02	14	4	0	0	0	0	
15	5	0	0	0	0	1	22390 04	1.35960 04	1.12820 04	4.26400 03	1.12820 04	4.26400 03	4.26400 03	0.0	1.85970 04	2.94000 02	15	5	0	0	0	0	
16	6	0	0	0	0	1	22390 04	1.35960 04	1.12820 04	4.26400 03	1.12820 04	4.26400 03	4.26400 03	0.0	1.85970 04	2.94000 02	16	6	0	0	0	0	
17	1	7	0	0	0	8	65660 03	1.02660 04	8.51880 03	3.21970 03	8.51880 03	3.21970 03	3.21970 03	0.0	1.07580 04	2.90240 02	17	1	7	0	0	0	
18	2	8	0	0	0	8	65660 03	1.02660 04	8.51880 03	3.21970 03	8.51880 03	3.21970 03	3.21970 03	0.0	1.07580 04	2.90240 02	18	2	8	0	0	0	
19	3	9	0	0	0	8	65660 03	1.02660 04	8.51880 03	3.21970 03	8.51880 03	3.21970 03	3.21970 03	0.0	1.07580 04	2.90240 02	19	3	9	0	0	0	
20	4	10	0	0	0	8	65660 03	1.02660 04	8.51880 03	3.21970 03	8.51880 03	3.21970 03	3.21970 03	0.0	1.07580 04	2.90240 02	20	4	10	0	0	0	
21	5	11	0	0	0	8	65660 03	1.02660 04	8.51880 03	3.21970 03	8.51880 03	3.21970 03	3.21970 03	0.0	1.07580 04	2.90240 02	21	5	11	0	0	0	
22	6	12	0	0	0	8	65660 03	1.02660 04	8.51880 03	3.21970 03	8.51880 03	3.21970 03	3.21970 03	0.0	1.07580 04	2.90240 02	22	6	12	0	0	0	
23	7	13	0	0	0	2	13640 03	5.52860 03	4.58760 03	1.73390 03	4.58760 03	1.73390 03	1.73390 03	0.0	1.20430 03	3.08800 03	23	7	13	0	0	0	
24	8	14	0	0	0	2	13640 03	5.52860 03	4.58760 03	1.73390 03	4.58760 03	1.73390 03	1.73390 03	0.0	1.20430 03	3.08800 03	24	8	14	0	0	0	
25	9	15	0	0	0	2	13640 03	5.52860 03	4.58760 03	1.73390 03	4.58760 03	1.73390 03	1.73390 03	0.0	1.20430 03	3.08800 03	25	9	15	0	0	0	
26	10	16	0	0	0	2	13640 03	5.52860 03	4.58760 03	1.73390 03	4.58760 03	1.73390 03	1.73390 03	0.0	1.20430 03	3.08800 03	26	10	16	0	0	0	
27	11	17	0	0	0	7	86750 03	2.10450 04	1.74630 04	6.60000 03	1.74630 04	6.60000 03	6.60000 03	0.0	7.69240 02	9.62910 03	27	11	17	0	0	0	
28	12	18	0	0	0	2	13640 03	5.52860 03	4.58760 03	1.73390 03	4.58760 03	1.73390 03	1.73390 03	0.0	1.20430 03	3.08800 03	28	12	18	0	0	0	
29	17	22	0	0	0	3	04130 03	5.52860 03	4.58760 03	1.73390 03	4.58760 03	1.73390 03	1.73390 03	0.0	1.20430 03	3.08800 03	29	17	22	0	0	0	
30	18	23	0	0	0	3	04130 03	5.52860 03	4.58760 03	1.73390 03	4.58760 03	1.73390 03	1.73390 03	0.0	1.20430 03	3.08800 03	30	18	23	0	0	0	
31	14	19	0	0	0	1	69530 05	1.10570 04	9.17510 03	3.46770 03	1.10570 04	3.46770 03	3.46770 03	0.0	4.50000 04	6.17600 03	31	14	19	0	0	0	
32	19	26	0	0	0	1	41540 03	5.52860 03	4.58760 03	1.73390 03	4.58760 03	1.73390 03	1.73390 03	0.0	3.08800 03	1.20430 03	32	19	26	0	0	0	

BEAM	DEFLECTION	TENSION	COMPRESSION	F(Y)	F(Z)	BM(Z)	BM(Y)	X-AXIS	Y-AXIS	Z-AXIS															
33	20	25	0	1.41540	03	5.52060	03	4.50760	03	1.73390	03	0.0	1.73390	03	0.0	3.00000	03	1.20430	03	33	20	25	0	0	
34	21	26	0	1.41540	03	5.52060	03	4.50760	03	1.73390	03	0.0	1.73390	03	0.0	3.00000	03	1.20430	03	34	21	26	0	0	
35	22	27	0	1.41540	03	5.52060	03	4.50760	03	1.73390	03	0.0	1.73390	03	0.0	3.00000	03	1.20430	03	35	22	27	0	0	
36	23	28	0	1.41540	03	5.52060	03	4.50760	03	1.73390	03	0.0	1.73390	03	0.0	3.00000	03	1.20430	03	36	23	28	0	0	
37	13	14	0	1.07430	05	7.40060	03	6.14760	03	2.32350	03	0.0	2.32350	03	0.0	5.60170	02	1.71510	04	37	13	14	0	0	
38	14	15	0	3.07250	04	7.40060	03	6.14760	03	2.32350	03	0.0	2.32350	03	0.0	5.60170	02	1.71510	04	38	14	15	0	0	
39	15	16	0	3.25400	04	7.40060	03	6.14760	03	2.32350	03	0.0	2.32350	03	0.0	5.60170	02	1.71510	04	39	15	16	0	0	
40	16	17	0	3.07250	04	7.40060	03	6.14760	03	2.32350	03	0.0	2.32350	03	0.0	5.60170	02	1.71510	04	40	16	17	0	0	
41	17	18	0	9.56280	04	7.40060	03	6.14760	03	2.32350	03	0.0	2.32350	03	0.0	0.0	0.0	4.21920	04	41	17	18	0	0	
42	19	20	0	1.30120	07	1.55160	04	1.20750	04	4.06600	03	0.0	4.06600	03	0.0	0.0	0.0	4.32021	00	0.0	43	20	21	0	0
43	20	21	0	1.09330	07	1.55160	04	1.20750	04	4.06600	03	0.0	4.06600	03	0.0	0.0	0.0	4.42122	00	0.0	44	21	22	0	0
44	21	22	0	1.30120	07	1.55160	04	1.20750	04	4.06600	03	0.0	4.06600	03	0.0	0.0	0.0	4.52223	00	0.0	45	22	23	0	0
45	22	23	0	3.21310	07	1.55160	04	1.20750	04	4.06600	03	0.0	4.06600	03	0.0	0.0	0.0	4.62324	00	0.0	46	23	24	0	1
46	3	29	0	3.47500	05	3.00000	03	3.00000	03	2.14130	03	0.0	2.14130	03	0.0	4.00000	04	1.44000	05	46	3	29	0	1	
47	5	29	0	3.47500	05	3.00000	03	3.00000	03	2.14130	03	0.0	2.14130	03	0.0	4.00000	04	1.44000	05	47	5	29	0	2	
48	9	29	0	3.47500	05	3.00000	03	3.00000	03	2.14130	03	0.0	2.14130	03	0.0	4.00000	04	1.44000	05	48	9	29	0	3	
49	11	29	0	3.47500	05	3.00000	03	3.00000	03	2.14130	03	0.0	2.14130	03	0.0	4.00000	04	1.44000	05	49	11	29	0	4	
50	30	31	0	1.36530	04	9.40000	02	7.00000	02	2.94000	02	0.0	2.94000	02	0.0	0.0	0.0	5.03031	00	0.0	50	30	31	0	0
51	30	32	0	0.32190	02	1.15150	02	1.15150	02	0.19690	01	0.0	0.19690	01	0.0	0.0	0.0	5.13032	00	0.0	51	30	32	0	0
52	5	30	0	0.0	0.0	1.01300	02	0.41270	01	3.17960	01	0.0	3.17960	01	0.0	0.0	0.0	5.23033	00	0.0	52	5	30	0	0
53	11	30	0	0.0	0.0	1.01300	02	0.41270	01	3.17960	01	0.0	3.17960	01	0.0	0.0	0.0	5.33034	00	0.0	53	11	30	0	0
54	29	30	0	0.0	0.0	1.79070	01	1.40590	01	5.61590	00	0.0	5.61590	00	0.0	0.0	0.0	5.43035	00	0.0	54	29	30	0	0
55	29	30	5	1	0.0	5.49900	01	4.56300	01	1.72460	01	0.0	1.72460	01	0.0	0.0	0.0	5.53036	00	0.0	55	29	30	5	1
56	14	0	0	0.0	0.0	0.20370	03	0.20370	03	2.77510	03	0.0	2.77510	03	0.0	0.0	0.0	5.63037	00	0.0	56	14	0	0	0
57	16	0	0	0.0	0.0	0.20370	03	0.20370	03	2.77510	03	0.0	2.77510	03	0.0	0.0	0.0	5.73038	00	0.0	57	16	0	0	0

BEAM DEFLECTIONS

BEAM	DEFLECTION	TENSION	COMPRESSION	F(Y)	F(Z)	BM(Z)	BM(Y)	X-AXIS	Y-AXIS	Z-AXIS													
1	1	2	0	7.7610	-01	7.2380	-02	1.0570	-02	1.4080	-01	2.1530	-03	4.6410	-02	5.3550	-03	0.0	3.2130	-03	2.7040	-02	0
2	2	3	0	3.5200	-01	4.9240	-02	4.0860	-02	1.5040	00	2.2920	-02	2.2460	-01	2.5920	-02	0.0	7.0690	-03	6.1260	-02	0
3	3	4	0	3.2340	-01	5.3710	-02	4.4570	-02	2.0560	00	2.9760	-02	2.6730	-01	3.0850	-02	0.0	7.7110	-03	6.6820	-02	0
4	4	5	0	3.5200	-01	4.9240	-02	4.0860	-02	1.5040	00	2.2920	-02	2.2460	-01	2.5920	-02	0.0	7.0690	-03	6.1260	-02	0
5	5	6	0	5.5440	-01	3.1330	-02	2.6000	-02	4.0820	-01	5.9070	-03	9.0950	-02	1.0500	-02	0.0	4.4980	-03	3.0980	-02	0
6	7	8	0	2.6320	00	2.380	-02	1.0570	-02	4.3070	-02	5.4770	-03	3.0950	-02	1.0760	-02	0.0	1.1260	-02	1.0570	-02	0
7	8	9	0	1.1960	00	4.9240	-02	4.0860	-02	4.6710	-01	5.0320	-02	1.4980	-01	1.4980	-01	0.0	2.4760	-02	4.0860	-02	0
8	9	10	0	1.0970	00	5.3710	-02	4.4570	-02	6.0440	-01	7.5710	-02	1.7030	-01	1.0810	-01	0.0	2.7010	-02	4.4570	-02	0
9	10	11	0	1.0900	00	3.1330	-02	2.6000	-02	1.2040	-01	1.5030	-02	6.0670	-02	3.6770	-02	0.0	2.4760	-02	4.0860	-02	0
10	11	12	0	0.8350	-02	5.3710	-02	4.4570	-02	1.3750	01	3.1200	-02	3.1610	-01	4.5370	-02	0.0	1.5760	-02	2.6000	-02	0
11	1	0	0	4.8350	-02	5.3710	-02	4.4570	-02	1.3750	01	3.1200	-02	3.1610	-01	4.5370	-02	0.0	1.1340	-02	7.9030	-02	0
12	2	0	0	4.8350	-02	5.3710	-02	4.4570	-02	1.3750	01	3.1200	-02	3.1610	-01	4.5370	-02	0.0	1.1340	-02	7.9030	-02	0
13	3	0	0	4.8350	-02	5.3710	-02	4.4570	-02	1.3750	01	3.1200	-02	3.1610	-01	4.5370	-02	0.0	1.1340	-02	7.9030	-02	0
14	4	0	0	4.8350	-02	5.3710	-02	4.4570	-02	1.3750	01	3.1200	-02	3.1610	-01	4.5370	-02	0.0	1.1340	-02	7.9030	-02	0
15	5	0	0	4.8350	-02	5.3710	-02	4.4570	-02	1.3750	01	3.1200	-02	3.1610	-01	4.5370	-02	0.0	1.1340	-02	7.9030	-02	0
16	6	0	0	4.8350	-02	5.3710	-02	4.4570	-02	1.3750	01	3.1200	-02	3.1610	-01	4.5370	-02	0.0	1.1340	-02	7.9030	-02	0
17	1	7	0	5.2040	-02	6.2670	-02	5.2000	-02	1.7130	01	9.0140	-02	4.4120	-01	8.6050	-02	0.0	1.8440	-02	9.4550	-02	0
18	2	8	0	5.2040	-02	6.2670	-02	5.2000	-02	1.7130	01	9.0140	-02	4.4120	-01	8.6050	-02	0.0	1.8440	-02	9.4550	-02	0
19	3	9	0	5.2040	-02	6.2670	-02	5.2000	-02	1.7130	01	9.0140	-02	4.4120	-01	8.6050	-02	0.0	1.8440	-02	9.4550	-02	0
20	4	10	0	5.2040	-02	6.2670	-02	5.2000	-02	1.7130	01	9.0140	-02	4.4120	-01	8.6050	-02	0.0	1.8440	-02	9.4550	-02	0
21	5	11	0	5.2040	-02	6.2670	-02	5.2000	-02	1.7130	01	9.0140	-02	4.4120	-01	8.6050	-02	0.0	1.8440	-02	9.4550	-02	0
22	6	12	0	5.2040	-02	6.2670	-02	5.2000	-02	1.7130	01	9.0140	-02	4.4120	-01	8.6050	-02	0.0	1.8440	-02	9.4550	-02	0
23	7	13	0	4.5400	-02	1.1750	-01	9.7500	-02	2.5150	00	7.0080	01	6.8240	-01	7.4180	00	0.0	1.8440	-02	9.4550	-02	0
24	8	14	0	4.5400	-02	1.1750	-01	9.7500	-02	2.5150	00	7.0080	01	6.8240	-01	7.4180	00	0.0	1.8440	-02	9.4550	-02	0
25	9	15	0	4.5400	-02	1.1750	-01	9.7500	-02	2.5150	00	7.0080	01	6.8240	-01	7.4180	00	0.0	1.8440	-02	9.4550	-02	0
26	10	16	0	4.5400	-02	1.1750	-01	9.7500	-02	2.5150	00	7.0080	01	6.8240	-01	7.4180	00	0.0	1.8440	-02	9.4550	-02	0
27	11	17	0	4.3930	-02	1.1750	-01	9.7500	-02	3.0700	00	7.2440	01	6.8240	-01	1.2070	00	0.0	1.4710	-01	7.8000	-02	0

28	12	18	0	0	7.91650	02	9.58340	01	1.61420	01	1.33000	02	3.61670	01	1.97520	02
29	17	22	0	0	6.31390	02	9.11940	01	1.72400	01	4.29830	01	2.96220	01	1.40260	02
30	18	23	0	0	1.01060	03	4.46000	02	2.76550	01	1.99230	02	5.01420	01	2.24850	02
31	14	19	0	0	9.96480	02	4.43930	02	6.10630	02	6.16740	02	1.05240	03	2.17170	02
32	19	24	0	0	5.62500	02	4.04980	01	5.54240	01	5.31800	01	1.10960	02	2.36010	01
33	20	25	0	0	5.10960	02	9.53620	00	5.03450	01	5.13950	01	1.17310	02	2.46220	01
34	21	26	0	0	5.10960	02	9.53720	00	5.03450	01	5.13950	01	1.17310	02	2.46220	01
35	22	27	0	0	5.02140	02	9.37160	00	4.94770	01	4.64150	01	1.00370	02	2.12120	01
36	23	28	0	0	8.03040	02	1.49870	01	7.91250	01	8.35960	01	1.60660	02	3.53270	01
37	13	14	0	0	3.04020	03	3.46140	03	5.64050	02	4.21120	02	2.14650	02	5.91400	03
38	14	15	0	0	1.18310	03	6.12270	02	9.97730	01	1.66400	02	8.03460	01	1.24490	03
39	15	16	0	0	1.20100	03	6.69730	02	9.28400	01	1.63690	02	7.83390	01	1.15890	03
40	16	17	0	0	1.15390	03	5.97190	02	9.73150	01	1.61970	02	7.81120	01	9.11560	02
41	17	18	0	0	1.74870	03	1.42100	03	2.31740	02	2.55370	02	1.27380	02	2.30610	03
42	19	20	0	0	1.69840	03	3.92090	03	1.61420	03	9.36090	02	1.63300	03	3.01640	03
43	20	21	0	0	1.59150	03	3.36800	03	1.55840	03	1.00130	03	1.93590	03	3.17970	03
44	21	22	0	0	1.57420	03	3.63420	03	1.68150	03	8.68720	02	1.73080	03	2.85110	03
45	22	23	0	0	2.47480	03	8.97790	03	4.15410	03	1.16640	03	2.43920	03	3.94730	03
46	329	0	1	3.74250	02	1.54470	02	8.91850	01	1.05970	02	6.94920	01	1.23440	02	
47	529	0	2	5.63720	02	2.33470	02	1.34810	02	1.44040	02	1.90440	02	3.10330	02	
48	929	0	3	3.61100	02	1.50310	02	8.67810	01	7.73290	01	6.46220	01	1.14540	02	
49	1129	0	4	5.17100	02	2.12300	02	1.22570	02	9.51980	01	1.05700	02	1.76850	02	
50	3031	0	6	6.11150	01	8.59140	00	8.59140	00	4.62630	00	9.20620	00	9.20040	00	
51	3032	0	0	1.13140	01	2.12110	00	2.12110	00	1.01360	00	2.27290	00	2.27140	00	
52	530	0	0	4.44680	01	0.0	0.0	0.0	0.0	0.0	0.0	0.0	0.0	0.0	0.0	
53	1130	0	0	3.97400	01	0.0	0.0	0.0	0.0	0.0	0.0	0.0	0.0	0.0	0.0	
54	2930	0	1	1.80550	01	0.0	0.0	0.0	0.0	0.0	0.0	0.0	0.0	0.0	0.0	
55	2930	5	1	3.16400	01	0.0	0.0	0.0	0.0	0.0	0.0	0.0	0.0	0.0	0.0	
56	14	0	0	6.94340	02	0.0	0.0	0.0	0.0	0.0	0.0	0.0	0.0	0.0	0.0	
57	18	0	0	1.04970	03	0.0	0.0	0.0	0.0	0.0	0.0	0.0	0.0	0.0	0.0	

DAMPING TERMS (LB/IN-SEC, TRANSLATIONS (1)-(3) AND LB-IN-SEC, ROTATIONS (4)-(6))

I	J	I	J	M	N	(1)	(2)	(3)	(4)	(5)	(6)
1	1	2	0	0	0	3.658260-06	1.684130-05	2.025920-06	1.303510-05	3.475870-06	2.266600-05
2	2	3	0	0	9.869120-06	9.995460-05	1.202400-05	3.799040-05	1.106240-05	6.527350-05	6.057000-05
3	3	4	0	0	1.182570-05	1.306590-04	1.571760-05	4.677420-05	1.437010-05	9.352190-06	6.468950-05
4	4	5	0	0	8.833370-06	8.946450-05	1.076210-05	3.147510-05	4.899980-06	3.271850-05	4.423120-05
5	5	6	0	0	4.971500-06	3.204180-05	3.654460-06	1.773260-05	2.613260-05	1.331930-04	1.480020-04
6	6	7	0	0	9.064960-06	2.266230-05	8.007350-06	8.220220-05	7.021830-05	1.230960-04	1.036810-04
7	7	8	0	0	2.404540-05	1.322490-04	4.672810-05	2.236440-04	6.731950-05	1.230960-04	1.480020-04
8	8	9	0	0	2.866360-05	1.719810-04	6.076680-05	2.690940-04	7.021830-05	1.230960-04	1.480020-04
9	9	10	0	0	2.186210-05	1.202410-04	4.248530-05	1.983010-04	6.263140-05	1.036810-04	1.480020-04
10	10	11	0	0	1.231860-05	4.311500-05	1.523400-05	1.119560-04	3.359220-05	6.221710-05	6.221710-05
11	11	12	0	0	6.698510-06	1.914020-04	9.116820-06	2.061160-05	7.597110-06	1.036810-04	1.480020-04
12	12	0	0	0	1.197720-05	3.422340-04	1.630120-05	4.095140-05	1.358400-05	2.185910-04	2.185910-04
13	13	0	0	0	2.310530-05	6.602070-04	3.144480-05	1.499630-04	4.603640-05	3.279020-04	3.279020-04
14	14	0	0	0	1.436440-05	4.104470-04	1.955030-05	5.200290-05	1.629140-05	2.846300-04	2.846300-04
15	15	0	0	0	1.270700-05	3.630850-04	1.729440-05	4.357100-05	1.441160-05	2.329120-04	2.329120-04
16	16	0	0	0	7.909240-06	2.259970-04	1.076460-05	9.155910-05	8.983050-06	1.311610-04	1.311610-04
17	17	1	7	0	8.818840-06	2.603630-04	1.888600-05	4.364090-05	1.594070-05	1.368420-04	1.368420-04
18	2	8	0	0	1.575920-05	4.652660-04	3.374920-05	8.607260-05	2.846550-05	2.998140-04	2.998140-04
19	3	9	0	0	2.943110-05	8.683090-04	6.302840-05	2.664960-04	8.228530-05	4.227320-04	4.227320-04
20	4	10	0	0	1.889710-05	5.579080-04	4.046920-05	1.088930-04	3.133840-05	3.756110-04	3.756110-04
21	5	11	0	0	1.671900-05	4.936030-04	3.580460-05	9.155910-05	3.024280-05	3.073710-04	3.073710-04
22	6	12	0	0	1.041300-05	3.074280-04	2.230000-05	5.359700-05	1.684640-05	1.730450-04	1.730450-04
23	7	13	0	0	1.081890-05	8.937150-05	4.718290-04	5.630620-05	2.427320-04	4.377050-05	4.377050-05
24	8	14	0	0	2.431750-05	2.008900-04	1.060530-03	1.711190-04	5.314340-04	1.013280-04	1.013280-04
25	9	15	0	0	2.443310-05	2.018350-04	1.065570-03	1.778890-04	5.440400-04	1.073430-04	1.073430-04
26	10	16	0	0	2.311570-05	1.909520-04	1.008110-03	1.758240-04	5.212480-04	1.022170-04	1.022170-04
27	11	17	0	0	1.322080-05	1.206660-04	5.861990-04	1.852410-04	2.940990-04	6.296570-05	6.296570-05

26	12	16	0	0	1.606330-05	1.320590-04	7.014100-04	9.573350-05	3.510540-04	6.444230-05
29	17	22	0	0	2.016570-05	1.396190-04	7.371040-04	2.962200-04	4.298320-04	9.076600-05
30	18	23	0	0	1.259500-05	0.720000-05	6.694070-04	6.390750-05	2.539290-04	5.662670-05
31	14	19	0	0	1.277740-05	0.646510-05	2.094460-05	2.064480-05	1.209000-05	5.862990-05
32	19	24	0	0	2.263530-05	1.212800-03	2.297260-04	2.394210-04	1.147450-04	5.394830-04
33	20	25	0	0	2.491000-05	1.335170-03	2.529010-04	2.477370-04	1.085380-04	5.171130-04
34	21	26	0	0	2.491000-05	1.335170-03	2.529010-04	2.477370-04	1.085380-04	5.171130-04
35	22	27	0	0	2.535630-05	1.356610-03	2.573420-04	2.629830-04	1.268590-04	6.002500-04
36	23	28	0	0	1.505520-05	0.495360-04	1.609150-04	1.523090-04	7.925220-05	3.604140-04
37	13	14	0	0	4.180050-06	3.678440-06	2.257330-05	3.023470-05	5.931780-05	2.152910-06
38	14	15	0	0	1.076200-05	2.079530-05	1.276130-04	7.651060-05	1.504740-04	1.022760-05
39	15	16	0	0	1.060180-05	2.234810-05	1.371430-04	7.770490-05	1.625300-04	1.090660-05
40	16	17	0	0	1.103380-05	2.132050-05	1.308360-04	1.308010-04	1.630010-04	1.396760-05
41	17	18	0	0	7.201020-06	0.953070-06	5.494180-05	4.905810-05	9.995680-05	5.521250-06
42	19	20	0	0	7.496690-06	3.247300-06	7.018150-06	1.357280-05	6.946240-06	4.218020-06
43	20	21	0	0	0.000070-06	3.780380-06	0.170250-06	1.271550-05	6.577030-06	4.004310-06
44	21	22	0	0	0.008810-06	3.503530-06	7.571910-06	1.432670-05	7.356160-06	4.465810-06
45	22	23	0	0	5.144890-06	1.418190-06	3.045030-06	1.091560-05	5.219980-06	3.225410-06
46	3	29	0	1	3.384010-05	0.242510-05	1.427650-04	1.201470-04	1.832210-04	1.031440-04
47	5	29	0	2	2.238790-05	5.453060-05	9.444970-05	0.839220-05	6.685780-05	4.102820-05
48	9	29	0	3	3.47740-05	0.470790-05	1.447180-04	1.644530-04	1.970300-04	1.111610-04
49	11	29	0	4	2.462280-05	5.997420-05	1.038780-04	1.337460-04	1.204580-04	7.199410-05
50	30	31	0	0	2.135430-03	1.519030-02	1.519030-02	2.821000-02	1.417600-02	1.418500-02
51	30	32	0	0	0.753550-03	4.669020-02	4.669020-02	9.770930-02	4.357240-02	4.360010-02
52	5	30	0	0	2.863260-04	0.0	0.0	0.0	0.0	0.0
53	11	30	0	0	3.203920-04	0.0	0.0	0.0	0.0	0.0
54	29	30	0	0	7.051980-04	0.0	0.0	0.0	0.0	0.0
55	29	30	5	1	4.024210-04	0.0	0.0	0.0	0.0	0.0
56	14	0	0	0	1.833740-05	0.0	0.0	0.0	0.0	0.0
57	18	0	0	0	1.212900-05	0.0	0.0	0.0	0.0	0.0

EULER ANGLES, BEAR IJ TO AIRPLANE (RADIANS)

IJ	I	J	M	N	THEIJ(I,J)	PSIIJ(I,J)
1	1	2	0	0	0.0	3.141590 00
2	2	3	0	0	0.0	3.141590 00
3	3	4	0	0	0.0	3.141590 00
4	4	5	0	0	0.0	3.141590 00
5	5	6	0	0	0.0	3.141590 00
6	7	8	0	0	0.0	3.141590 00
7	8	9	0	0	0.0	3.141590 00
8	9	10	0	0	0.0	3.141590 00
9	10	11	0	0	0.0	3.141590 00
10	11	12	0	0	0.0	3.141590 00
11	1	0	0	0	0.0	1.570800 00
12	2	0	0	0	0.0	1.570800 00
13	3	0	0	0	0.0	1.570800 00
14	4	0	0	0	0.0	1.570800 00
15	5	0	0	0	0.0	1.570800 00
16	6	0	0	0	0.0	1.570800 00
17	1	7	0	0	0.0	-1.570800 00
18	2	8	0	0	0.0	-1.570800 00
19	3	9	0	0	0.0	-1.570800 00
20	4	10	0	0	0.0	-1.570800 00
21	5	11	0	0	0.0	-1.570800 00
22	6	12	0	0	0.0	-1.570800 00
23	7	13	0	0	1.261090 00	-1.570800 00
24	8	14	0	0	1.261090 00	-1.570800 00
25	9	15	0	0	1.261090 00	-1.570800 00
26	10	16	0	0	1.261090 00	-1.570800 00
27	11	17	0	0	1.261090 00	-1.570800 00

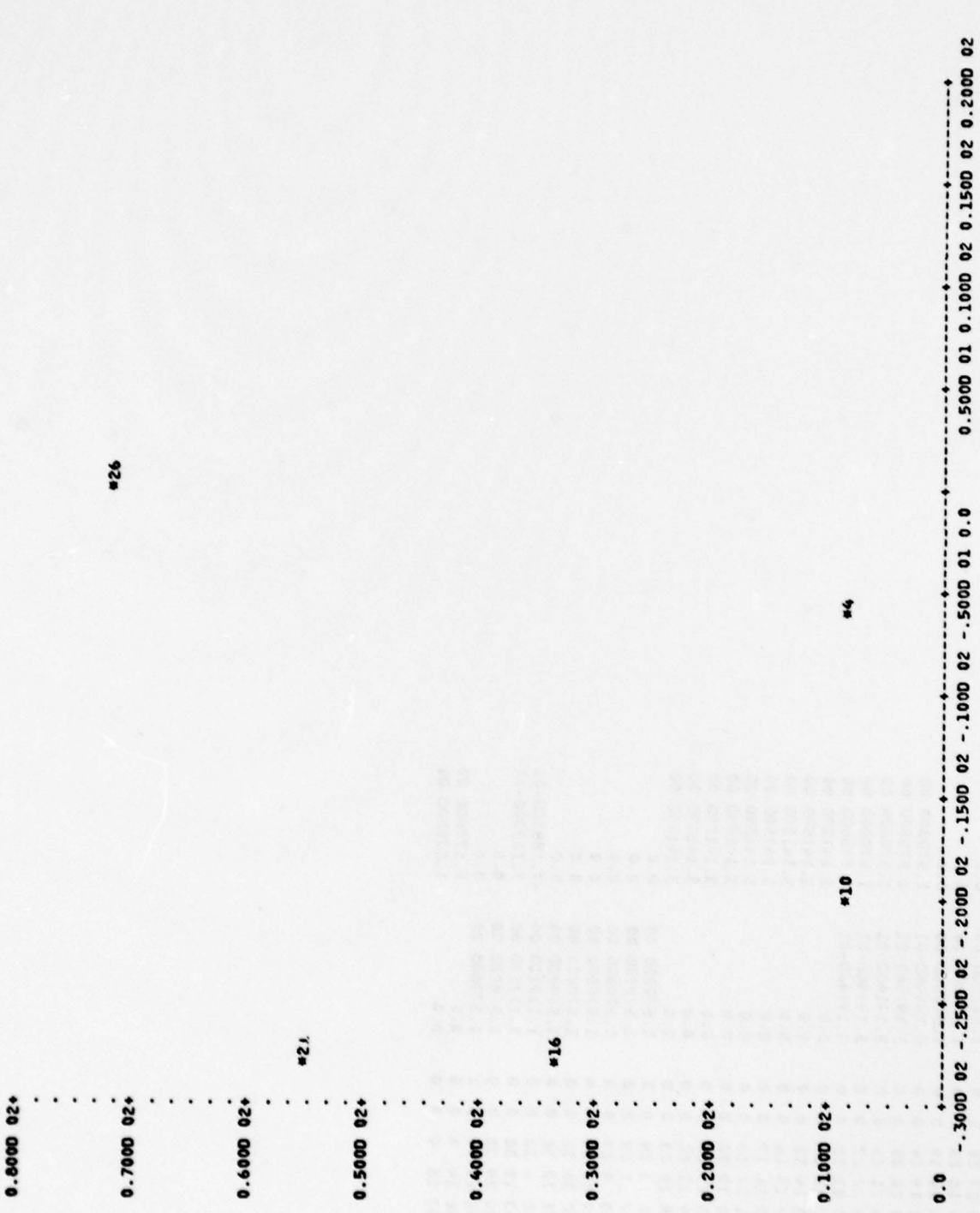
28	12	18	0	0	1.261890	00	-1.570800	00
29	17	22	0	0	1.570800	00	0.0	
30	18	23	0	0	1.570800	00	0.0	
31	14	19	0	0	1.570800	00	0.0	
32	19	24	0	0	5.191460	-01	1.570800	00
33	20	25	0	0	5.191460	-01	1.570800	00
34	21	26	0	0	5.191460	-01	1.570800	00
35	22	27	0	0	5.191460	-01	1.570800	00
36	23	28	0	0	5.191460	-01	1.570800	00
37	13	14	0	0	0.0		3.141590	00
38	14	15	0	0	0.0		3.141590	00
39	15	16	0	0	0.0		3.141590	00
40	16	17	0	0	0.0		3.141590	00
41	17	18	0	0	0.0		3.141590	00
42	19	20	0	0	0.0		3.141590	00
43	20	21	0	0	0.0		3.141590	00
44	21	22	0	0	0.0		3.141590	00
45	22	23	0	0	0.0		3.141590	00
46	3	29	0	1	1.570800	00	0.0	
47	5	29	0	2	1.570800	00	0.0	
48	9	29	0	3	1.570800	00	0.0	
49	11	29	0	4	1.570800	00	0.0	
50	30	31	0	0	1.570800	00	0.0	
51	30	32	0	0	1.570800	00	0.0	
52	5	30	0	0	1.117100	00	-7.188300	-01
53	11	30	0	0	1.117100	00	7.188300	-01
54	29	30	0	0	1.570800	00	0.0	
55	29	30	5	1	1.570800	00	0.0	
56	14	0	0	0	0.0		1.570800	00
57	18	0	0	0	0.0		1.570800	00

TIME = 0

NOTE *** A MODIFIED RIGHT HAND GROUND COORDINATE SYSTEM HAS BEEN USED FOR THIS PLOT ***

MASS POSITION PLOT PLANE ** Y(+RIGHT) - Z(+UP)

MASS NO	HORIZ AXIS	VERTICAL AXIS	MASS NO	HORIZ AXIS	VERTICAL AXIS	MASS NO	HORIZ AXIS	VERTICAL AXIS	MASS NO	HORIZ AXIS	VERTICAL AXIS
4	-6.00	0.2	10	-20.00	0.24	16	-20.00	33.23	21	-20.00	55.23
26	0.0	71.23									



TIME = 0

NOTE *** A MODIFIED RIGHT HAND GROUND COORDINATE SYSTEM HAS BEEN USED FOR THIS PLOT ***
MASS POSITION PLOT PLANE ** X(+AFT) - Z(+UP)

MASS NO	HORIZ AXIS	VERTICAL AXIS	MASS NO	HORIZ AXIS	VERTICAL AXIS	MASS NO	HORIZ AXIS	VERTICAL AXIS	MASS NO	HORIZ AXIS	VERTICAL AXIS
3	-11.64	6.39	5	11.16	6.09	29	3.35	22.50	30	3.45	29.99
31	3.64	45.06									

0.8000 02+

 0.7000 02+

 0.6000 02+

 0.5000 02+

 0.4000 02+

 0.3000 02+

 0.2000 02+

 0.1000 02+

 0.0

*31

*30

*29

*3

*5

0.0

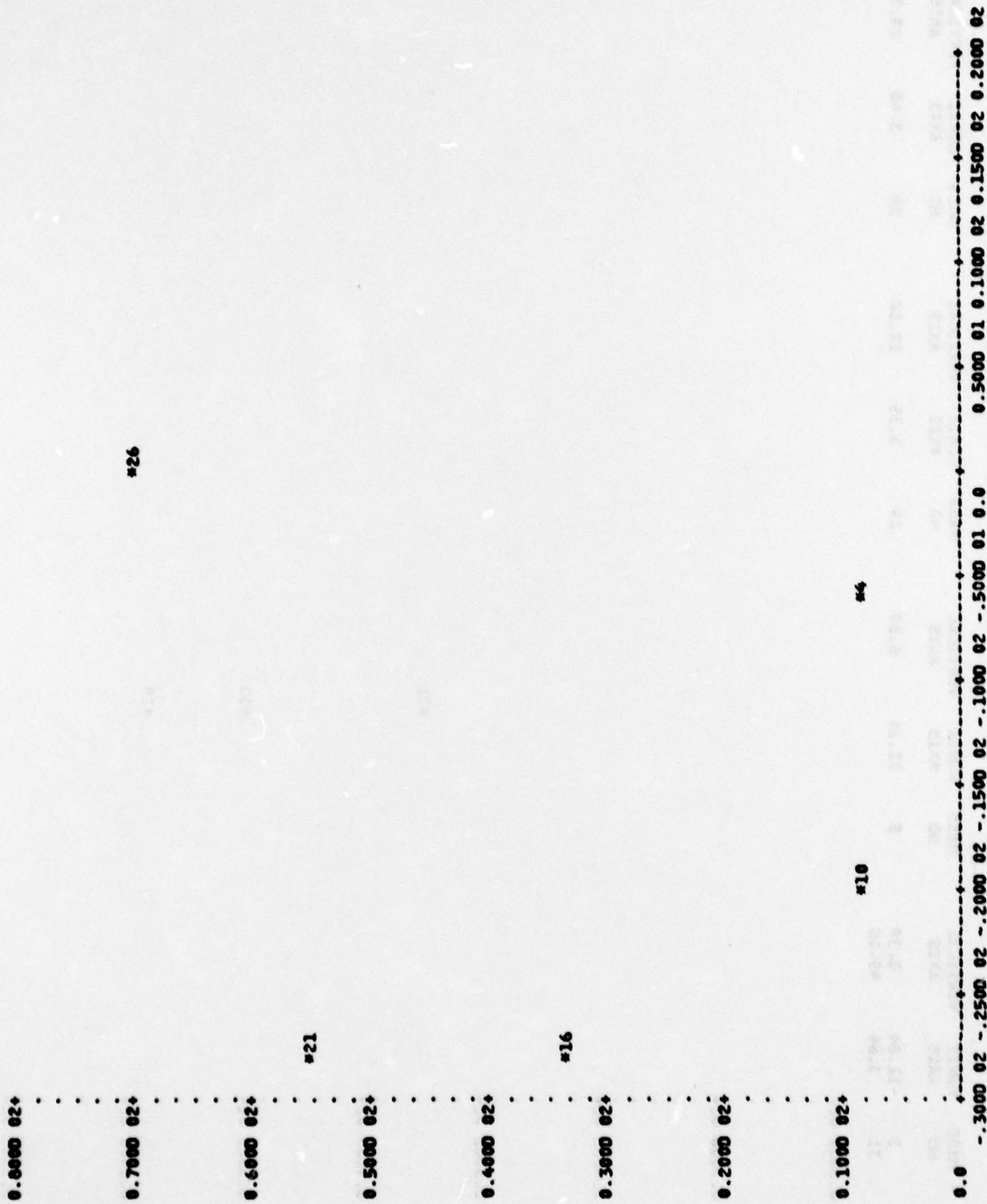
 -0.1500 02 -0.1000 02 -0.5000 01 0.0

 0.5000 01 0.1000 02 0.1500 02 0.2000 02 0.2500 02 0.3000 02 0.3500 02

NOTE *** A MODIFIED RIGHT HAND GROUND COORDINATE SYSTEM HAS BEEN USED FOR THIS PLOT ***

MASS POSITION PLOT PLANE ** Y(+RIGHT) - Z(+UP)

MASS NO	HORIZ AXIS	VERTICAL AXIS	MASS NO	HORIZ AXIS	VERTICAL AXIS	MASS NO	HORIZ AXIS	VERTICAL AXIS	MASS NO	HORIZ AXIS	VERTICAL AXIS
4	-6.00	7.66	10	-19.99	7.00	16	-27.91	32.61	21	-28.05	54.82
26	0.0	70.65									



TIME = 0.054

MASS POSITION PLOT PLANE ** X(+AFT) - Z(+UP) ***

NOTE *** A MODIFIED RIGHT HAND GROUND COORDINATE SYSTEM HAS BEEN USED FOR THIS PLOT ***

MASS NO	HORIZ AXIS	VERTICAL AXIS	MASS NO	HORIZ AXIS	VERTICAL AXIS	MASS NO	HORIZ AXIS	VERTICAL AXIS	MASS NO	HORIZ AXIS	VERTICAL AXIS
9	-14.66	7.03	11	0.33	7.75	29	0.35	22.12	30	7.24	23.03
31	4.62	37.05									

0.0000 02+

0.7000 02+

0.6000 02+

0.5000 02+

0.4000 02+

0.3000 02+

0.2000 02+

0.1000 02+

0.0

#31

#29

#30

#11

0.0 -0.1500 02 -0.1000 02 -0.5000 01 0.0 0.5000 01 0.1000 02 0.1500 02 0.2000 02 0.2500 02 0.3000 02 0.3500 02

**SUMMARY OF INTERNAL BEAM YIELDING AND RUPTURE
BEAM DIRECTION FOR
RUPTURE**

TIME	I	J	M	N	YIELD	RUPTURE
0.0	55	29	30	5	1	1
0.006070	54	29	30	0	0	0
0.016960	32	19	24	0	0	0
0.017310	33	20	25	0	0	0
0.018260	34	21	26	0	0	0
0.019360	35	22	27	0	0	0
0.026100	28	12	18	0	0	0
0.026860	27	11	17	0	0	0
0.027620	25	9	15	0	0	0
0.027650	26	10	16	0	0	0
0.028260	24	8	14	0	0	0
0.029190	23	7	13	0	0	0
0.032440	36	23	28	0	0	2

B-36

LINE-0104

SUMMARY OF ENERGY DISTRIBUTION

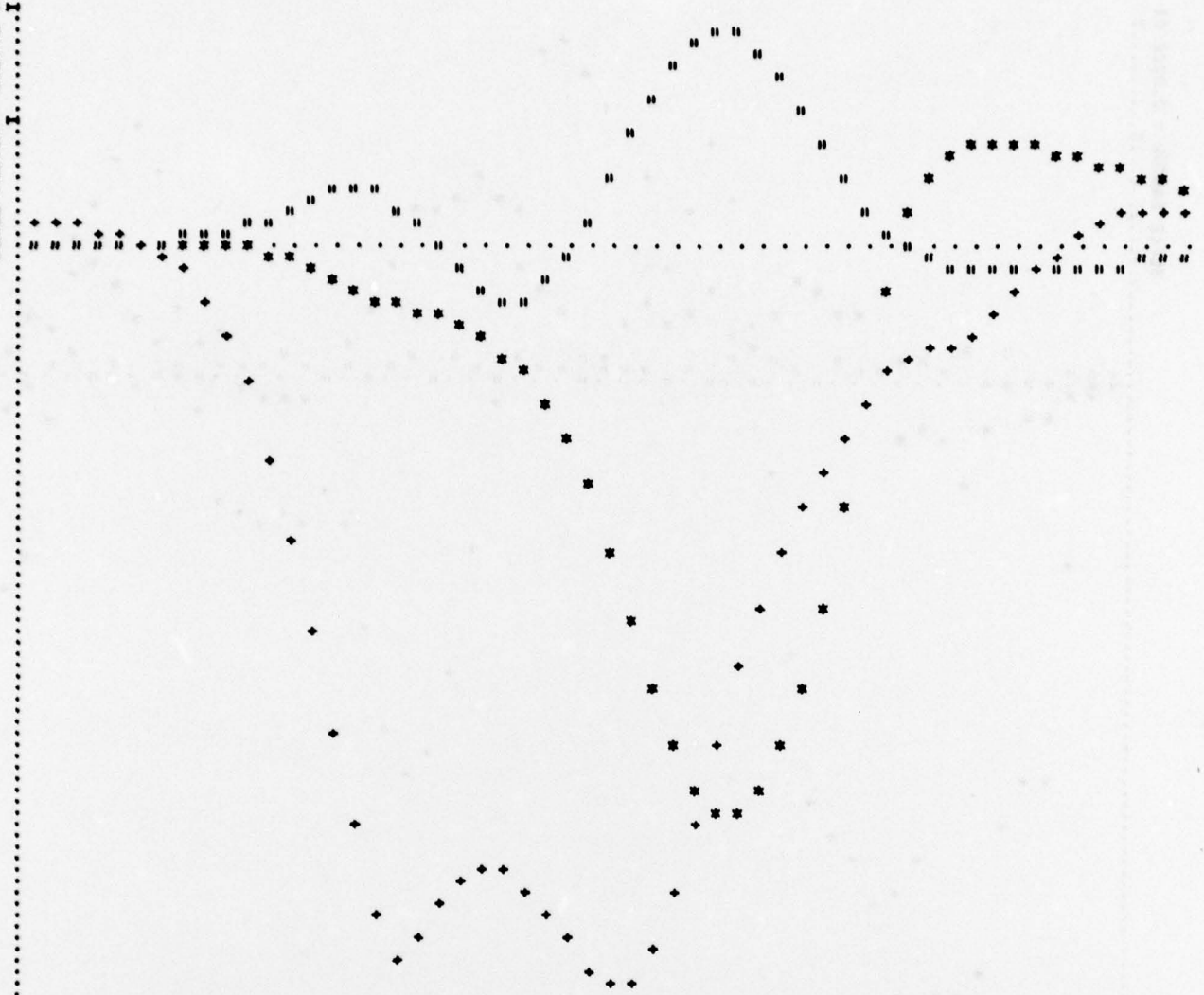
TIME	PERCENT MAXIMUM ENERGY DEVIATION	PERCENT TOTAL SYSTEM ENERGY	PERCENT OF CURRENT TOTAL		PERCENT OF POTENTIAL ENERGY		PERCENT OF STRAIN ENERGY		PERCENT OF DAMPING ENERGY		PERCENT OF CURRENT TOTAL		PERCENT OF CURRENT TOTAL		PERCENT OF CURRENT TOTAL	
			KINETIC ENERGY	TOTAL	POTENTIAL ENERGY	TOTAL	STRAIN ENERGY	TOTAL	DAMPING ENERGY	TOTAL	CRUSHING ENERGY	TOTAL	FRICTION ENERGY	TOTAL	PERCENT OF CURRENT TOTAL	
.0	0.0	100.00	7.669E 04	82.67	1.607E 04	17.33	0.0	0.0	0.0	0.0	0.0	0.0	0.0	0.0	0.0	0.0
.00100	0.253424	100.02	7.495E 04	80.79	1.589E 04	17.13	1.257E 02	0.14	9.968E 00	0.01	1.797E 03	0.0	1.94	0.0	0.0	0.0
.00200	0.368142	100.04	6.998E 04	75.41	1.572E 04	16.94	3.005E 02	0.32	4.003E 01	0.04	6.757E 03	0.0	7.28	0.0	0.0	0.0
.00300	0.279686	100.04	6.413E 04	69.11	1.555E 04	16.76	7.714E 02	0.83	7.714E 02	0.08	1.227E 04	0.0	13.22	0.0	0.0	0.0
.00400	0.281395	100.04	5.911E 04	63.70	1.540E 04	16.59	1.049E 03	1.13	1.115E 02	0.12	1.713E 04	0.0	18.46	0.0	0.0	0.0
.00500	0.511445	100.03	5.464E 04	58.89	1.525E 04	16.43	1.944E 03	2.09	1.487E 02	0.16	2.081E 04	0.0	22.43	0.0	0.0	0.0
.00600	0.640265	100.03	5.075E 04	54.70	1.511E 04	16.28	2.959E 03	3.19	1.938E 02	0.21	2.378E 04	0.0	25.63	0.0	0.0	0.0
.00700	0.677775	100.03	4.728E 04	50.95	1.498E 04	16.14	4.378E 03	4.72	2.365E 02	0.25	2.592E 04	0.0	27.93	0.0	0.0	0.0
.00800	0.747329	100.03	4.436E 04	47.83	1.486E 04	16.01	5.656E 03	6.09	2.716E 02	0.29	2.763E 04	0.0	29.77	0.0	0.0	0.0
.00900	0.833982	100.03	4.203E 04	45.29	1.474E 04	15.89	7.029E 03	7.58	3.000E 02	0.32	2.869E 04	0.0	30.92	0.0	0.0	0.0
.01000	0.959331	100.03	4.035E 04	43.49	1.464E 04	15.78	8.178E 03	8.81	3.208E 02	0.35	2.930E 04	0.0	31.58	0.0	0.0	0.0
.01100	0.881527	100.03	3.913E 04	42.17	1.454E 04	15.67	9.187E 03	9.90	3.422E 02	0.37	2.959E 04	0.0	31.89	0.0	0.0	0.0
.01200	0.833560	100.04	3.813E 04	40.00	1.446E 04	15.58	1.013E 04	10.92	3.726E 02	0.40	2.970E 04	0.0	32.01	0.0	0.0	0.0
.01300	0.833560	100.04	3.712E 04	38.49	1.438E 04	15.49	1.121E 04	12.08	4.201E 02	0.45	2.968E 04	0.0	31.98	0.0	0.0	0.0
.01400	0.830895	100.04	3.572E 04	36.19	1.430E 04	15.41	1.274E 04	13.72	4.956E 02	0.53	2.955E 04	0.0	31.84	0.0	0.0	0.0
.01500	0.808676	100.05	3.359E 04	32.82	1.423E 04	15.34	1.502E 04	16.18	5.923E 02	0.64	2.938E 04	0.0	31.65	0.0	0.0	0.0
.01600	0.799835	100.06	3.046E 04	28.70	1.417E 04	15.27	1.826E 04	19.67	7.098E 02	0.76	2.922E 04	0.0	31.48	0.0	0.0	0.0
.01700	0.744671	100.07	2.664E 04	24.52	1.411E 04	15.21	2.211E 04	23.82	8.245E 02	0.89	2.913E 04	0.0	31.39	0.0	0.0	0.0
.01800	0.686459	100.07	2.276E 04	20.51	1.406E 04	15.15	2.596E 04	27.96	9.260E 02	1.00	2.912E 04	0.0	31.37	0.0	0.0	0.0
.01900	0.686459	100.07	1.904E 04	16.99	1.401E 04	15.09	2.970E 04	31.99	1.001E 03	1.08	2.908E 04	0.0	31.33	0.0	0.0	0.0
.02000	0.717363	100.07	1.577E 04	14.14	1.396E 04	15.04	3.308E 04	35.63	1.043E 03	1.12	2.898E 04	0.0	31.22	0.0	0.0	0.0
.02100	0.647712	100.08	1.312E 04	11.94	1.392E 04	14.99	3.582E 04	38.58	1.074E 03	1.16	2.891E 04	0.0	31.14	0.0	0.0	0.0
.02200	0.673577	100.08	1.109E 04	10.26	1.387E 04	14.94	3.789E 04	40.80	1.108E 03	1.19	2.889E 04	0.0	31.12	0.0	0.0	0.0
.02300	0.670591	100.09	9.529E 03	8.95	1.382E 04	14.89	3.943E 04	42.47	1.150E 03	1.24	2.890E 04	0.0	31.13	0.0	0.0	0.0
.02400	0.709935	100.09	8.309E 03	8.10	1.374E 04	14.79	4.064E 04	43.77	1.191E 03	1.28	2.892E 04	0.0	31.15	0.0	0.0	0.0
.02500	0.830267	100.09	7.525E 03	7.55	1.374E 04	14.75	4.181E 04	45.02	1.295E 03	1.33	2.897E 04	0.0	31.21	0.0	0.0	0.0
.02600	0.934466	100.10	7.009E 03	7.14	1.369E 04	14.70	4.204E 04	45.27	1.359E 03	1.39	2.905E 04	0.0	31.28	0.0	0.0	0.0
.02700	0.922010	100.10	6.626E 03	6.82	1.365E 04	14.66	4.210E 04	45.34	1.424E 03	1.46	2.918E 04	0.0	31.42	0.0	0.0	0.0
.02800	0.918876	100.10	6.336E 03	6.34	1.362E 04	14.63	4.213E 04	45.36	1.493E 03	1.53	2.938E 04	0.0	31.64	0.0	0.0	0.0
.02900	0.961489	100.11	5.895E 03	5.72	1.359E 04	14.60	4.213E 04	45.36	1.567E 03	1.61	2.977E 04	0.0	32.06	0.0	0.0	0.0
.03000	1.017785	100.11	5.315E 03	5.48	1.356E 04	14.58	4.213E 04	45.43	1.645E 03	1.69	3.023E 04	0.0	32.56	0.0	0.0	0.0
.03100	1.050775	100.11	5.087E 03	5.48	1.354E 04	14.58	4.207E 04	45.30	1.645E 03	1.77	3.052E 04	0.0	32.87	0.0	0.0	0.0
.03200	1.076124	100.11	5.290E 03	5.70	1.353E 04	14.57	4.175E 04	44.96	1.735E 03	1.87	3.055E 04	0.0	32.90	0.0	0.0	0.0
.03300	1.094804	100.11	6.030E 03	6.49	1.353E 04	14.57	4.109E 04	44.25	1.839E 03	1.98	3.037E 04	0.0	32.71	0.0	0.0	0.0
.03400	1.101397	100.11	7.332E 03	7.79	1.353E 04	14.57	4.000E 04	43.07	1.963E 03	2.11	3.014E 04	0.0	32.46	0.0	0.0	0.0
.03500	1.113096	100.12	8.817E 03	9.49	1.354E 04	14.58	3.845E 04	41.40	2.101E 03	2.26	2.996E 04	0.0	32.26	0.0	0.0	0.0
.03600	1.115771	100.12	1.058E 04	11.39	1.355E 04	14.59	3.659E 04	39.42	2.240E 03	2.42	2.990E 04	0.0	32.20	0.0	0.0	0.0
.03700	1.126314	100.13	1.237E 04	13.21	1.356E 04	14.60	3.475E 04	37.42	2.404E 03	2.59	2.989E 04	0.0	32.18	0.0	0.0	0.0
.03800	1.143649	100.13	1.368E 04	14.52	1.358E 04	14.62	3.339E 04	35.95	2.566E 03	2.76	2.987E 04	0.0	32.16	0.0	0.0	0.0
.03900	1.151624	100.14	1.378E 04	14.95	1.360E 04	14.64	3.288E 04	35.40	2.718E 03	2.93	2.981E 04	0.0	32.09	0.0	0.0	0.0
.04000	1.168576	100.14	1.362E 04	14.67	1.361E 04	14.66	3.304E 04	35.57	2.842E 03	3.06	2.977E 04	0.0	32.05	0.0	0.0	0.0
.04100	1.217560	100.15	1.334E 04	14.36	1.363E 04	14.68	3.324E 04	35.78	2.939E 03	3.16	2.975E 04	0.0	32.02	0.0	0.0	0.0
.04200	1.237304	100.15	1.315E 04	14.16	1.365E 04	14.70	3.334E 04	35.88	3.024E 03	3.25	2.973E 04	0.0	32.01	0.0	0.0	0.0
.04300	1.258885	100.16	1.222E 04	13.90	1.368E 04	14.72	3.368E 04	36.04	3.097E 03	3.33	2.973E 04	0.0	32.00	0.0	0.0	0.0
.04400	2.452375	100.17	1.251E 04	13.46	1.370E 04	14.74	3.382E 04	36.40	3.165E 03	3.41	2.973E 04	0.0	32.00	0.0	0.0	0.0
.04500	3.917643	100.18	1.227E 04	13.20	1.372E 04	14.76	3.398E 04	36.57	3.231E 03	3.48	2.973E 04	0.0	31.99	0.0	0.0	0.0
.04600	4.318353	100.19	1.235E 04	13.29	1.374E 04	14.78	3.383E 04	36.40	3.299E 03	3.55	2.973E 04	0.0	31.99	0.0	0.0	0.0
.04700	5.195271	100.21	1.146E 04	13.40	1.375E 04	14.80	3.363E 04	36.18	3.360E 03	3.64	2.973E 04	0.0	31.98	0.0	0.0	0.0
.04800	5.426345	100.22	1.254E 04	13.49	1.377E 04	14.82	3.346E 04	35.99	3.458E 03	3.72	2.973E 04	0.0	31.98	0.0	0.0	0.0

-04900	5.568901	107.23	1.226E 04	13.19	1.379E 04	14.84	3.365E 04	36.19	3.539E 03	3.81	2.973E 04	31.98	0.0
-05000	5.996435	107.23	1.173E 04	12.61	1.301E 04	14.86	3.409E 04	36.66	3.619E 03	3.89	2.973E 04	31.98	0.0
-05100	6.181212	100.24	1.141E 04	12.28	1.303E 04	14.87	3.433E 04	36.92	3.680E 03	3.96	2.973E 04	31.97	0.0
-05200	6.342592	100.25	1.154E 04	12.41	1.385E 04	14.89	3.415E 04	36.72	3.728E 03	4.01	2.973E 04	31.97	0.0
-05300	6.348572	100.25	1.183E 04	12.72	1.387E 04	14.91	3.378E 04	36.32	3.787E 03	4.07	2.973E 04	31.97	0.0
-05400	6.358683	100.26	1.202E 04	12.92	1.389E 04	14.93	3.351E 04	36.03	3.859E 03	4.15	2.973E 04	31.97	0.0

MASS 30 FILTERED ACCELERATION(G'S)

TIME(SEC)	XACCF	YACCF	ZACCF
0.0	-1.310E-02	0.0	9.999E-01
0.001	-1.311E-02	-5.990E-04	9.947E-01
0.002	-1.313E-02	3.588E-05	9.741E-01
0.003	-1.369E-02	6.603E-04	7.193E-01
0.004	-1.694E-02	6.017E-03	3.690E-01
0.005	-2.690E-02	2.240E-02	-1.373E-01
0.006	-4.502E-02	5.700E-02	-7.892E-01
0.007	-7.205E-02	1.185E-01	-1.585E 00
0.008	-1.284E-01	2.462E-01	-3.046E 00
0.009	-2.315E-01	3.663E-01	-5.170E 00
0.010	-3.952E-01	7.995E-01	-7.958E 00
0.011	-6.607E-01	1.866E 00	-1.193E 01
0.012	-1.050E 00	1.859E 00	-1.669E 01
0.013	-1.559E 00	2.414E 00	-2.180E 01
0.014	-2.126E 00	2.832E 00	-2.707E 01
0.015	-2.666E 00	2.985E 00	-3.235E 01
0.016	-3.159E 00	2.742E 00	-3.755E 01
0.017	-3.478E 00	1.991E 00	-3.968E 01
0.018	-3.697E 00	9.064E-01	-3.880E 01
0.019	-4.064E 00	-3.380E-01	-3.701E 01
0.020	-4.604E 00	-1.625E 00	-3.547E 01
0.021	-5.287E 00	-2.735E 00	-3.472E 01
0.022	-6.189E 00	-3.364E 00	-3.488E 01
0.023	-7.405E 00	-3.274E 00	-3.562E 01
0.024	-8.979E 00	-2.400E 00	-3.725E 01
0.025	-1.096E 00	-6.331E-01	-3.883E 01
0.026	-1.355E 00	1.245E 00	-4.023E 01
0.027	-1.693E 00	3.573E 00	-4.114E 01
0.028	-2.089E 00	5.906E 00	-4.084E 01
0.029	-2.480E 00	8.056E 00	-3.905E 01
0.030	-2.805E 00	9.863E 00	-3.598E 01
0.031	-3.035E 00	1.117E 01	-3.214E 01
0.032	-3.151E 00	1.177E 01	-2.792E 01
0.033	-3.141E 00	1.158E 01	-2.381E 01
0.034	-3.015E 00	1.075E 01	-2.025E 01
0.035	-2.785E 00	9.405E 00	-1.735E 01
0.036	-2.451E 00	7.672E 00	-1.491E 01
0.037	-2.016E 00	5.712E 00	-1.270E 01
0.038	-1.486E 00	3.729E 00	-1.063E 01
0.039	-8.885E 00	1.928E 00	-8.716E 00
0.040	-2.672E 00	4.415E-01	-7.010E 00
0.041	1.520E 00	-5.089E-01	-6.295E 00
0.042	3.866E 00	-1.054E 00	-6.032E 00
0.043	5.094E 00	-1.350E 00	-5.670E 00
0.044	5.641E 00	-1.491E 00	-5.007E 00
0.045	5.771E 00	-1.535E 00	-4.043E 00
0.046	5.652E 00	-1.519E 00	-2.882E 00
0.047	5.390E 00	-1.467E 00	-1.663E 00
0.048	5.053E 00	-1.397E 00	-5.180E-01
0.049	4.686E 00	-1.319E 00	4.517E-01
0.050	4.317E 00	-1.240E 00	1.185E 00
0.051	3.960E 00	-1.164E 00	1.663E 00
0.052	3.624E 00	-1.093E 00	1.898E 00
0.053	3.308E 00	-1.027E 00	1.930E 00
0.054	3.012E 00	-9.655E-01	1.809E 00

SCALE FACTOR = 6.299E 00



BEAM 55 I,M = 29, 5 J,M = 30, 1 AXIAL AND SHEAR FORCES(LB)

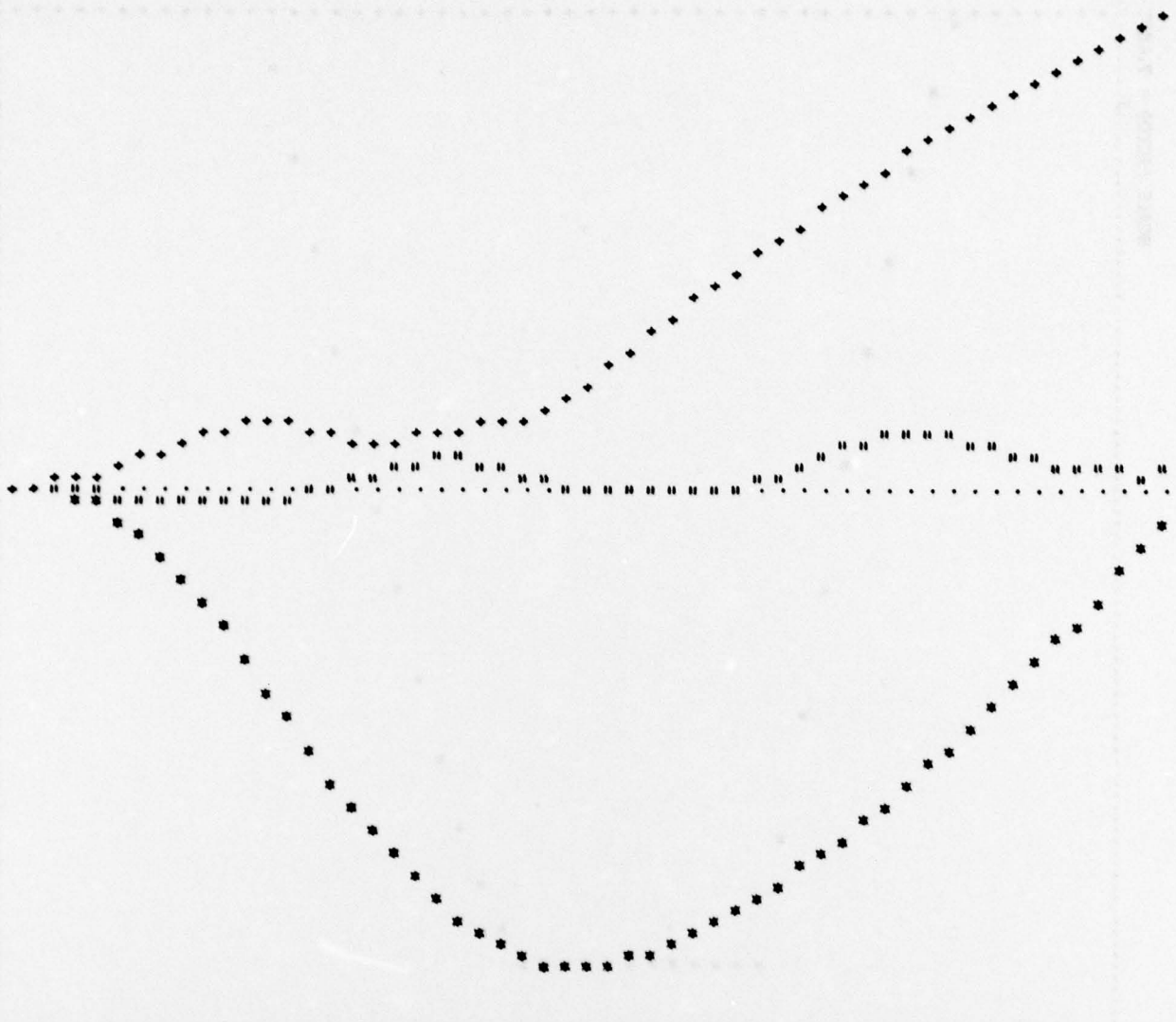
TIME(SEC)	FX	FY	FZ
0.0	0.0	0.0	0.0
0.001	-4.533E-02	0.0	0.0
0.002	-2.554E-01	0.0	0.0
0.003	-6.141E-01	0.0	0.0
0.004	-1.190E 00	0.0	0.0
0.005	-1.945E 00	0.0	0.0
0.006	-2.920E 00	0.0	0.0
0.007	-6.202E 01	0.0	0.0
0.008	-5.206E 02	0.0	0.0
0.009	-1.045E 03	0.0	0.0
0.010	-1.657E 03	0.0	0.0
0.011	-2.330E 03	0.0	0.0
0.012	-3.066E 03	0.0	0.0
0.013	-3.896E 03	0.0	0.0
0.014	-4.746E 03	0.0	0.0
0.015	-5.630E 03	0.0	0.0
0.016	-6.455E 03	0.0	0.0
0.017	-6.455E 03	0.0	0.0
0.018	-6.455E 03	0.0	0.0
0.019	-6.455E 03	0.0	0.0
0.020	-6.455E 03	0.0	0.0
0.021	-6.455E 03	0.0	0.0
0.022	-6.455E 03	0.0	0.0
0.023	-6.455E 03	0.0	0.0
0.024	-6.455E 03	0.0	0.0
0.025	-6.455E 03	0.0	0.0
0.026	-6.455E 03	0.0	0.0
0.027	-6.422E 03	0.0	0.0
0.028	-6.236E 03	0.0	0.0
0.029	-5.924E 03	0.0	0.0
0.030	-5.524E 03	0.0	0.0
0.031	-5.051E 03	0.0	0.0
0.032	-4.512E 03	0.0	0.0
0.033	-3.952E 03	0.0	0.0
0.034	-3.415E 03	0.0	0.0
0.035	-2.859E 03	0.0	0.0
0.036	-2.270E 03	0.0	0.0
0.037	-1.646E 03	0.0	0.0
0.038	-1.014E 03	0.0	0.0
0.039	-4.110E 02	0.0	0.0
0.040	0.0	0.0	0.0
0.041	0.0	0.0	0.0
0.042	0.0	0.0	0.0
0.043	0.0	0.0	0.0
0.044	0.0	0.0	0.0
0.045	0.0	0.0	0.0
0.046	0.0	0.0	0.0
0.047	0.0	0.0	0.0
0.048	0.0	0.0	0.0
0.049	0.0	0.0	0.0
0.050	0.0	0.0	0.0
0.051	0.0	0.0	0.0
0.052	0.0	0.0	0.0
0.053	0.0	0.0	0.0
0.054	0.0	0.0	0.0

SCALE FACTOR = 7.685E 02

BEAM 55 I,M = 29, 5 J,M = 30, 1 RELATIVE DEFLECTIONS#J-I*(IN)

SCALE FACTOR = 1.242E 00

TIME(SEC)	X	Y	Z
0.0	0.0	0.0	0.0
0.001	-3.766E-03	1.000E-03	1.240E-03
0.002	-4.630E-02	1.550E-02	1.570E-02
0.003	-1.106E-01	5.472E-02	4.894E-02
0.004	-2.345E-01	1.055E-01	1.232E-01
0.005	-3.603E-01	1.453E-01	2.107E-01
0.006	-5.675E-01	1.659E-01	2.933E-01
0.007	-7.834E-01	2.167E-01	3.700E-01
0.008	-1.029E 00	2.332E-01	4.676E-01
0.009	-1.299E 00	2.302E-01	5.459E-01
0.010	-1.600E 00	2.330E-01	6.051E-01
0.011	-1.910E 00	2.130E-01	6.303E-01
0.012	-2.240E 00	1.749E-01	6.467E-01
0.013	-2.582E 00	1.300E-01	6.299E-01
0.014	-2.911E 00	8.444E-02	5.901E-01
0.015	-3.229E 00	3.003E-02	5.371E-01
0.016	-3.530E 00	4.026E-02	4.897E-01
0.017	-3.810E 00	1.160E-01	4.657E-01
0.018	-4.060E 00	1.867E-01	4.817E-01
0.019	-4.305E 00	2.309E-01	5.260E-01
0.020	-4.529E 00	2.698E-01	5.740E-01
0.021	-4.734E 00	2.715E-01	6.149E-01
0.022	-4.900E 00	2.400E-01	6.510E-01
0.023	-5.054E 00	1.825E-01	6.927E-01
0.024	-5.165E 00	1.122E-01	7.503E-01
0.025	-5.230E 00	4.421E-02	8.354E-01
0.026	-5.275E 00	0.090E-03	9.534E-01
0.027	-5.271E 00	-4.249E-02	1.101E 00
0.028	-5.237E 00	-6.701E-02	1.270E 00
0.029	-5.179E 00	-9.072E-02	1.445E 00
0.030	-5.102E 00	-1.106E-01	1.624E 00
0.031	-5.009E 00	-1.174E-01	1.809E 00
0.032	-4.896E 00	-1.045E-01	1.995E 00
0.033	-4.775E 00	-7.596E-02	2.172E 00
0.034	-4.653E 00	-3.303E-02	2.341E 00
0.035	-4.521E 00	2.727E-02	2.501E 00
0.036	-4.375E 00	1.089E-01	2.664E 00
0.037	-4.212E 00	2.063E-01	2.832E 00
0.038	-4.039E 00	3.080E-01	2.999E 00
0.039	-3.865E 00	4.007E-01	3.143E 00
0.040	-3.686E 00	4.773E-01	3.322E 00
0.041	-3.409E 00	5.418E-01	3.474E 00
0.042	-3.286E 00	5.862E-01	3.622E 00
0.043	-3.080E 00	5.953E-01	3.759E 00
0.044	-2.889E 00	5.612E-01	3.892E 00
0.045	-2.676E 00	4.909E-01	4.025E 00
0.046	-2.446E 00	4.036E-01	4.163E 00
0.047	-2.205E 00	3.201E-01	4.302E 00
0.048	-1.962E 00	2.571E-01	4.437E 00
0.049	-1.722E 00	2.126E-01	4.573E 00
0.050	-1.489E 00	1.701E-01	4.707E 00
0.051	-1.241E 00	1.504E-01	4.827E 00
0.052	-9.719E-01	1.312E-01	4.943E 00
0.053	-7.052E-01	1.200E-01	5.055E 00
0.054	-4.534E-01	1.071E-01	5.160E 00



EXTERNAL SPRING I,M = 2.0 COMPRESSION(IN)

SCALE FACTOR = 1.875E-01

TIME(SEC)	X	Y	Z
0.0	0.0	0.0	0.0
0.001	0.0	0.0	0.0
0.002	0.0	0.0	1.126E-01
0.003	0.0	0.0	3.064E-01
0.004	0.0	0.0	6.269E-01
0.005	0.0	0.0	9.212E-01
0.006	0.0	0.0	1.142E 00
0.007	0.0	0.0	1.266E 00
0.008	0.0	0.0	1.361E 00
0.009	0.0	0.0	1.426E 00
0.010	0.0	0.0	1.469E 00
0.011	0.0	0.0	1.495E 00
0.012	0.0	0.0	1.504E 00
0.013	0.0	0.0	1.498E 00
0.014	0.0	0.0	1.478E 00
0.015	0.0	0.0	1.445E 00
0.016	0.0	0.0	1.400E 00
0.017	0.0	0.0	1.355E 00
0.018	0.0	0.0	1.305E 00
0.019	0.0	0.0	1.263E 00
0.020	0.0	0.0	1.235E 00
0.021	0.0	0.0	1.212E 00
0.022	0.0	0.0	1.202E 00
0.023	0.0	0.0	1.216E 00
0.024	0.0	0.0	1.276E 00
0.026	0.0	0.0	1.326E 00
0.027	0.0	0.0	1.390E 00
0.029	0.0	0.0	1.440E 00
0.030	0.0	0.0	1.526E 00
0.031	0.0	0.0	1.565E 00
0.032	0.0	0.0	1.579E 00
0.033	0.0	0.0	1.565E 00
0.034	0.0	0.0	1.542E 00
0.035	0.0	0.0	1.513E 00
0.036	0.0	0.0	1.481E 00
0.037	0.0	0.0	1.440E 00
0.038	0.0	0.0	1.390E 00
0.039	0.0	0.0	1.332E 00
0.040	0.0	0.0	1.262E 00
0.041	0.0	0.0	1.189E 00
0.042	0.0	0.0	1.062E 00
0.043	0.0	0.0	9.445E-01
0.044	0.0	0.0	8.226E-01
0.045	0.0	0.0	7.051E-01
0.046	0.0	0.0	5.950E-01
0.047	0.0	0.0	4.877E-01
0.048	0.0	0.0	3.956E-01
0.049	0.0	0.0	3.177E-01
0.050	0.0	0.0	2.554E-01
0.051	0.0	0.0	1.990E-01
0.052	0.0	0.0	1.495E-01
0.053	0.0	0.0	1.074E-01
0.054	0.0	0.0	6.121E-02

EXTERNAL SPRING I,M = 2, 0 AXIAL LOAD(LB)

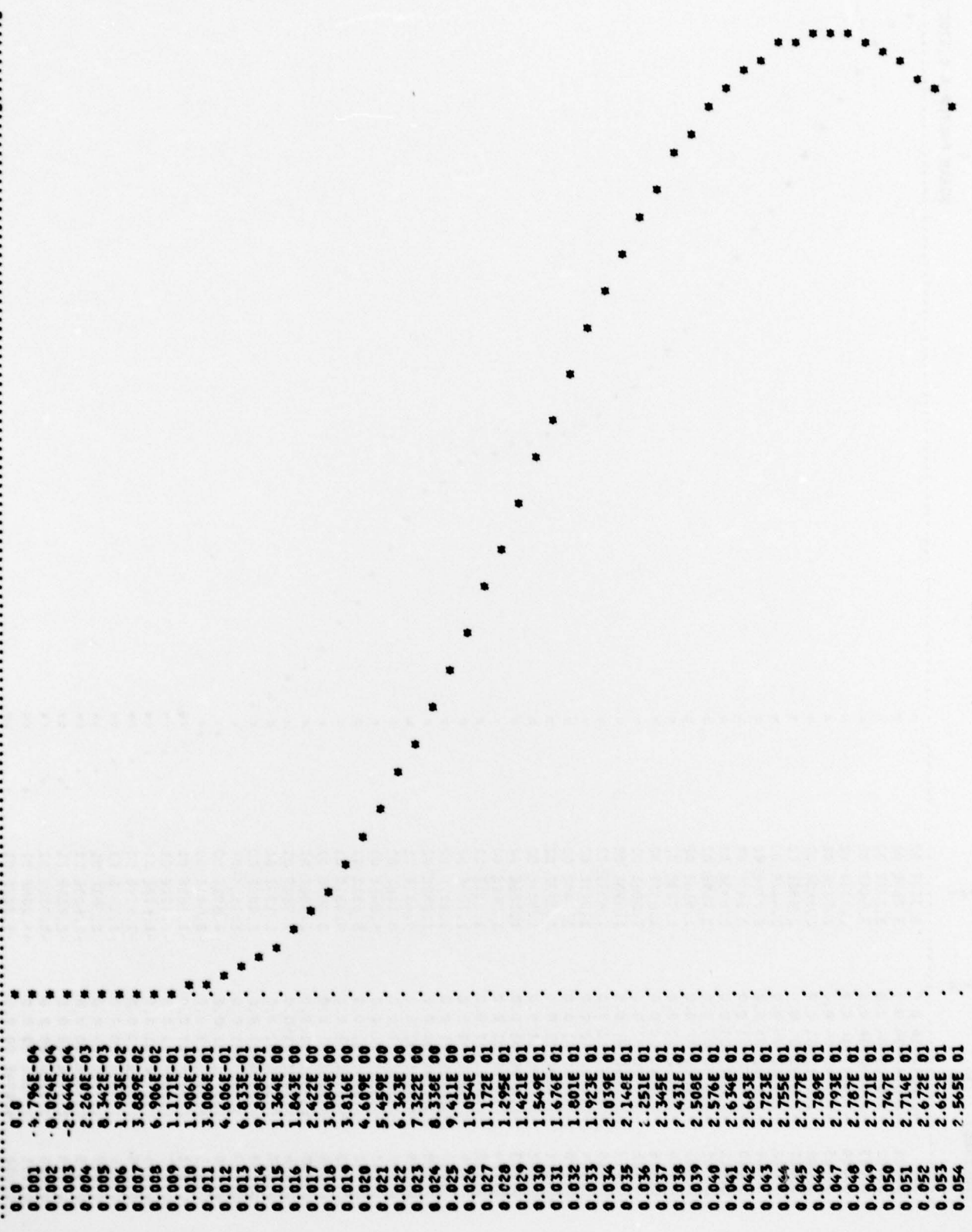
SCALE FACTOR = 2.726E 02
I.....I

TIME(SEC)	X	Y	Z
0.0	0.0	0.0	0.0
0.001	0.0	0.0	0.0
0.002	0.0	0.0	2.290E 03
0.003	0.0	0.0	2.290E 03
0.004	0.0	0.0	2.290E 03
0.005	0.0	0.0	2.290E 03
0.006	0.0	0.0	2.290E 03
0.007	0.0	0.0	2.290E 03
0.008	0.0	0.0	2.290E 03
0.009	0.0	0.0	2.290E 03
0.010	0.0	0.0	2.290E 03
0.011	0.0	0.0	2.290E 03
0.012	0.0	0.0	2.290E 03
0.013	0.0	0.0	2.290E 03
0.014	0.0	0.0	2.113E 03
0.015	0.0	0.0	1.643E 03
0.016	0.0	0.0	6.964E 02
0.017	0.0	0.0	0.0
0.018	0.0	0.0	0.0
0.019	0.0	0.0	0.0
0.020	0.0	0.0	0.0
0.021	0.0	0.0	0.0
0.022	0.0	0.0	0.0
0.023	0.0	0.0	0.0
0.024	0.0	0.0	0.0
0.025	0.0	0.0	0.0
0.026	0.0	0.0	0.0
0.027	0.0	0.0	0.0
0.028	0.0	0.0	0.0
0.029	0.0	0.0	1.407E 03
0.030	0.0	0.0	2.290E 03
0.031	0.0	0.0	2.290E 03
0.032	0.0	0.0	2.288E 03
0.033	0.0	0.0	2.043E 03
0.034	0.0	0.0	1.521E 03
0.035	0.0	0.0	6.520E 02
0.036	0.0	0.0	1.215E 02
0.037	0.0	0.0	0.0
0.038	0.0	0.0	0.0
0.039	0.0	0.0	0.0
0.040	0.0	0.0	0.0
0.041	0.0	0.0	0.0
0.042	0.0	0.0	0.0
0.043	0.0	0.0	0.0
0.044	0.0	0.0	0.0
0.045	0.0	0.0	0.0
0.046	0.0	0.0	0.0
0.047	0.0	0.0	0.0
0.048	0.0	0.0	0.0
0.049	0.0	0.0	0.0
0.050	0.0	0.0	0.0
0.051	0.0	0.0	0.0
0.052	0.0	0.0	0.0
0.053	0.0	0.0	0.0
0.054	0.0	0.0	0.0

DRI MASS 32

SCALE FACTOR = 2.685E 00

TIME(SEC) DRI



VEHICLE C.G. VELOCITY(IN/SEC)

